ISTANBUL TECHNICAL UNIVERSITY ★ GRADUATE SCHOOL OF SCIENCE ENGINEERING AND TECHNOLOGY

IMPACT ANALYSIS OF THE STEPPED CONCENTRIC CRASH TUBES: THE EFFECT OF THE NUMBER OF TUBES

M.Sc. THESIS

Fatih USTA

Department of Aeronautical and Astronautical Engineering

Aeronautical and Astronautical Engineering Programme

MAY 2015

ISTANBUL TECHNICAL UNIVERSITY ★ GRADUATE SCHOOL OF SCIENCE ENGINEERING AND TECHNOLOGY

IMPACT ANALYSIS OF THE STEPPED CONCENTRIC CRASH TUBES: THE EFFECT OF THE NUMBER OF TUBES

M.Sc. THESIS

Fatih USTA
511131114

Department of Aeronautical and Astronautical Engineering

Aeronautical and Astronautical Engineering Programme

Thesis Advisor: Prof. Dr. Halit Süleyman Türkmen

MAY 2015

ISTANBUL TECHNICAL UNIVERSITY ★ GRADUATE SCHOOL OF SCIENCE ENGINEERING AND TECHNOLOGY

KADEMELİ VE EŞ MERKEZLİ ÇARPIŞMA KUTULARININ ANALİZİ: TÜP SAYISININ ETKİSİ

YÜKSEK LİSANS TEZİ

Fatih USTA
511131114

Uçak ve Uzay Mühendisliği Anabilim Dalı

Uçak ve Uzay Mühendisliği Programı

Tez Danışmanı: Prof. Dr. Halit Süleyman Türkmen

MAYIS 2015

Fatih USTA, a **M.Sc**. student of ITU **Graduate School of Science Engineering and Technology** 511131114 successfully defended the thesis entitled **"IMPACT ANALYSIS OF THE STEPPED CONCENTRIC CRASH TUBES: THE EFFECT OF THE NUMBER OF TUBES"**, which she prepared after fulfilling the requirements specified in the associated legislations, before the jury whose signatures are below.

Thesis Advisor :	**Prof. Dr. Halit Süleyman Türkmen** İstanbul Technical University	....
Jury Members :	**Prof. Dr. Zahit Mecitoğlu** İstanbul Technical University	....
	Assoc. Prof. Dr. Zafer Kazancı Turkish Air Force Academy	....

Date of Submission : 4 May 2015
Date of Defense : 26 May 2015

To Eda Kılınçarslan and my family,

FOREWORD

First and foremost I offer my sincerest gratitude to my supervisor, Prof. Dr. Halit Süleyman Türkmen, who has supported me throughout my thesis with his patience and knowledge. Besides my advisor, I would like to thank Zana Eren, Assoc. Prof. Dr. Zafer Kazancı, Prof. Dr. Zahit Mecitoğlu and Dr. Enver Yalçın. Support for this work has been provided by the Scientific and Technological Research Council of Turkey under Project Number 113M395 which is named of '**Numerical and experimental investigation of crushing and crashing behavior of nested crash tubes'**. I am very grateful for the support of TUBITAK and I would like to thank TUBITAK Marmara Research Center due to providing experimental possibilities.

May 2015

Fatih USTA
(Aeronautical Engineer)

TABLE OF CONTENTS

Page

ABBREVIATIONS

ADINA	**:** Automatic Dynamic Incremental Nonlinear Analysis
ANSYS	**:** Analysis System
J	**:** Joule
kg	**:** Kilogram
LS DYNA	: Livermore Software Dynamic
m	**:** Meter
min	**:** Minute
N	**:** Newton
s	**:** Second
SEA	**:** Specific Energy Absorption
SPC	**:** Single Point Constraint
t	**:** Time

LIST OF TABLES

Page

LIST OF FIGURES

Page

IMPACT ANALYSIS OF THE STEPPED CONCENTRIC CRASH TUBES: THE EFFECT OF THE NUMBER OF TUBES

SUMMARY

In this study, stepped concentric crash tubes with circular AL6063 material are investigated using experimental and numerical methods. Crash tubes are used generally in automotive industry to as a passive safety component. In this study, feasibility of crash tubes in different areas are sought. So, it is designed almost ten times smaller than the conventional car crash tubes.

The purpose of this study is to examine the energy absorption characteristics of stepped concentric crash tubes subjected to an axial impact load. The peak forces, internal energy and the total deflection are the selected parameters for the comparison of various crash tubes. The stepped concentric tubes have different lengths and different diameters, while the total mass and volume are kept constant. The area of the impacting object is taken as greater than the internal tube's cross sectional area to prevent passing the impacting object through the tube hole.

First of all, a comprehensive study about articles on crash tubes presented. Almost 127 scientific articles are reviewed and tabulated information according to solution methods, geometry, material properties, impact velocity and impact mass properties. Table is given in Appendices section.

In the next part, one selected model with AL6063 material is fabricated and tested at dynamic and quasi-static velocities. Dynamic tests are done by using INSTRON 8150 Drop Test Machine and quasi-static test is done by using MTS 647 Hydraulic Test Machine. Then, results of experiments compared and validated with results of analysis by using LS-DYNA, an engineering simulation software program.

In the second part, the effects of the number of the tubes and impact velocity are studied at high dynamic velocities by using LS-DYNA software program. To define optimal mesh quality, results of five different mesh sizes of a sample are investigated and chosen the most proper type of them to use in all analyses. After that, four different models are constituted with 3, 6, 9 and 12 stepped concentric tubes, respectively. All samples are analyzed at three different velocities: 50, 60 and 70 m/s and results are compared with one another.

In the third part, stepped concentric crash tubes are modelled with aluminum foam and analyzed at 50 m/s impact velocity. Results of model with foam filled and empty tubes are compared and studied to demonstrate the advantages and disadvantages of foam material. All graphics are established using GRAPHER software program.

KADEMELİ VE EŞ MERKEZLİ ÇARPIŞMA KUTULARININ ANALİZİ: TÜP SAYISININ ETKİSİ

ÖZET

Dünya Sağlık Örgütü'nün verilerine göre her yıl dünya genelinde bir milyonun üzerinde insan trafik kazalarında hayatını kaybetmektedir. 2010 yılına ait verilerde 1.24 milyon insanın hayatını kaybettiği ve 20-30 milyon insanın ölümcül olmayan yaralanmalara maruz kaldığı belirtilmiştir. Bu nedenle yolcu ve sürücülerin güvenliğinin sağlanması ve araçta oluşan hasarın en aza indirilmesi için çok sayıda bilimsel çalışma yapılmıştır. Bu amaçla geliştirilen donanımlardan birisi de otomobillerde tampon ve şase arasına yerleştirilen ezilme kutularıdır.

Ezilme kutuları üzerine yapılan çalışmalarda iki önemli parametre ön plana çıkmaktadır. Bunlar tüplerin enerji emme kapasitesi ve pik kuvvetidir. Ezilme kutuları, çarpışma anında şekil değiştirerek ortaya çıkan kinetik enerjinin bir bölümünün yolcuya ve diğer donanımlara iletilmeden soğurulmasını sağlar. Ayrıca kaza anında oluşan kuvvetlerin ilk anda oluşan kuvvet değeri, diğer kuvvet değerlerinden daha yüksektir. Çarpma anında ortaya çıkan en yüksek kuvvet değeri pik kuvveti olarak adlandırılır. Pik kuvveti ile diğer kuvvetler verileri arasındaki farktan dolayı ivmelenme oluşur ve bu ivmelenme yolcu ile sürücülere zarar verebilmektedir. Zararlı etkinin azaltılması için bu farkın azaltılması gerekir. Ezilme kutularının temel amacı maksimum seviyede enerji emilmesinin yanı sıra pik kuvveti değerlerinin düşürülmesidir.

Enerji emme kapasitesinin yükseltilmesi ve pik kuvvetinin düşürülmesi birbirini olumsuz etkileyen iki prosestir. Yani bir tüpün bir yandan enerji emme kapasitesi artırılmak istenirken, diğer taraftan pik kuvvetleri istenmeyen şekilde artırılabilir. Bu nedenle en ideal ezilme kutularının tasarımı için farklı kesit geometrilerinde, et kalınlıklarda, boylarda ve farklı malzemelerde çok sayıda model geliştirilmiştir. Araştırmalar deneysel, analitik ve sayısal yöntemler kullanılarak yapılmaktadır.

Bu çalışmanın ilk bölümünde ezilme tüpleri ile ilgili kapsamlı bir literatür araştırması yapılmıştır. Ezilme kutuları üzerine yazılan 127 adet bilimsel makaleye ait bilgiler tablolaştırılarak sunulmuştur. Bu çalışmanın amacı ezilme kutuları hakkında çalışma yapmak isteyen araştırmacılara, daha önce yapılmış çalışmaların verilerinin daha kolay incelenebileceği bir kaynak sağlamaktır. Tablonun ilk bölümünde yapılan çalışmalarda kullanılan yöntemler analitik, sayısal ve deneysel olarak sınıflandırılmıştır. İkinci bölümde çarpan kütlenin büyüklüğü ve çarpma hızı bilgileri yer almaktadır. Sonraki bölümde geometri ile ilgili bilgiler yer almaktadır. Kesit geometrileri, et kalınlıkları ve boylarına ait bilgiler tabloda sunulmuştur. Malzeme bilgileri ise bu bölümden sonra gelmektedir. Genellikle alüminyum, çelik ve kompozit malzemeler üzerine yapılan çalışmalar olduğu için bu üç başlıkta sınıflandırma yapılmıştır. Son bölümde ise ezilme tüplerinin konfigürasyon türleri sınıflandırma yapılmıştır. Konfigürasyon tipleri içi boş, köpük dolgulu, tek gözlü ve çok gözlü tüpler olarak sınıflandırılmıştır.

Bu tezin ana konusu kademeli ve eş merkezli iç içe ezilme tüplerinin deneysel ve sayısal yöntemler kullanılarak incelenmesidir. Çalışmanın amacı eksenel darbe yüklerine maruz kalan kademeli eş merkezli ezilme tüplerinin enerji emme karakteristiklerinin değerlendirilmesidir. Pik kuvvetleri, iç enerjiler ve ezilme miktarları incelenen ve çeşitli tüp modelleri için karşılaştırmalarda kullanılan karakteristik özelliklerdir. Testler ve doğrulama analizleri için dairesel kesitli ve AL6063 malzemeli tüpler kullanılmıştır. Diğer analiz çalışmalarında tüpler ve köpük malzeme için alüminyum alaşımı tercih edilmiştir. Numunelerin boyutları otomobillerde kullanılan ezilme tüplerine göre oldukça küçük modellerdir. Bunun nedeni boyutları yeterince küçük ezilme tüplerinin dar bölgelere çok sayıda yerleştirilmeye uygun olması ve uçak ve uzay araçları için de kullanılabilmesi için bir araştırma önerisi olarak ileri sürülmesidir.

Farklı çaplarda ve boylarda iç içe tüpler dıştan içe doğru artan uzunluklarda yerleştirilmiştir. Yerleştirme yapılırken her bir model için en dıştaki tüpün çapı ve en içteki tüpün boyu sabit tutularak farklı tüp sayılarında çeşitli modeller denenmiştir. Numunelerin toplam ağırlıklarının da aynı kalması için kesit kalınlıkları koşulu sağlayacak şekilde her bir model için değiştirilmiştir. Yani farklı numuneler karşılaştırılırken toplam dış hacim ve ağırlıklarının yaklaşık olarak aynı olmasına dikkat edilmiştir.

İlk olarak deneysel çalışmalar ile bu deneysel çalışmaların sayısal yöntemlerle doğrulanması yer almaktadır. Bu çalışma için kademeli eş merkezli iç içe üçlü tüplerden üç adet üretilerek dinamik ve sanki statik hızlarda testleri gerçekleştirilmiştir. Dinamik testler için TÜBİTAK Malzeme Enstitüsü bünyesinde bulunan Instron 8150 Darbe Test Cihazı kullanılmıştır. İki adet numunenin farklı hızlarda dinamik testleri gerçekleştirilmiştir. Üçüncü numune ise İTÜ Uçak ve Uzay Bilimleri Fakültesi Kompozit Yapı Laboratuarı'nda bulunan MTS 647 Hidrolik Test Cihazı kullanılarak 2 mm/dak basma testine tabi tutulmuştur. Deney sonuçları ile numunelerin ezilme öncesi ve sonrası görselleri karşılaştırmalı olarak sunulmuştur. Yapılan testlerin sayısal yöntemlerle doğrulanması için LS-DYNA'da açık zamanlı çözücü ile dinamik analizler ve kapalı zamanlı çözücü ile de sanki statik analizler yapılarak deney sonuçları ile karşılaştırılmıştır. Deneysel ve sayısal yöntemlerin sonuçları birbiriyle uyumlu olduğu gözlemlenmiş ve sonuçlar karşılaştırmalı olarak sunulmuştur.

İkinci bölümde ise LS DYNA yazılımı kullanılarak farklı tüp sayılarında ve farklı hızlarda dinamik analizler yapılmıştır. İlk olarak ideal mesh kalitesinin belirlenmesi amacıyla farklı mesh kalitelerinde beş farklı model tasarlanarak aynı hızlarda ve darbe yüklerinde analizleri yapılmıştır. Mesh boyutları 0.3x0.3, 0.4x0.4, 0.5x0.5, 0.6x0.6 ve 0.7x0.7 mm olarak belirlenmiştir. Mesh boyutları küçültüldükçe sonuçların birbiriyle uyumlu olduğu ancak analizin gerçekleşme süresinin uzadığı tespit edilmiştir. Sonuçları birbirine benzer olan en küçük iki mesh boyutundan analiz süresi daha kısa olanı seçilmiş ve sonraki tüm analizler buna göre yapılmıştır.

Bu bölümde kademeli eş merkezli ve iç içe üçlü, altılı, dokuzlu ve on ikili dört farklı model incelenmiştir. Her model için en geniş tüpün çapı 20 mm ve en uzun tüpün boyu ise 30 mm olarak belirlenmiştir. Et kalınlıkları üçlü tüplerde 1 mm, altılı tüplerde 0.5 mm, dokuzlu tüplerde 0.3 mm ve on ikili tüplerde 0.25 mm olarak belirlenmiştir. Farklı tüp sayılarında tasarımı yapılan dört farklı modelin 50 m/s hız ve 100 gr çarpma yükü etkisinde analiz sonuçları karşılaştırılarak tüp sayısının enerji emme karakteristikleri üzerindeki etkileri incelenmiştir. Tüp sayısı artırıldıkça analizin ezilme süresi uzamakta olduğu ve pik kuvvetleri arasındaki farkların azaldığı gözlemlenmiştir.

Dört model için daha sonra farklı hızlarda dinamik analizler yapılarak bu sefer çarpma hızın enerji emme karakteristiklerine etkileri incelenmiştir. 50, 60 ve 70 m/s hızlarda 12 adet analiz yapılarak sonuçlar karşılaştırılmıştır. Dört model için ayrı ayrı farklı hızlara ait "kuvvet–zaman" ve "iç enerji-zaman" grafikleri GRAPHER programı kullanılarak çizdirilmiştir.

Son bölümde ise, kademeli eş merkezli iç içe tüplerin en iç kısmındaki boşluk, alüminyum köpük malzeme ile doldurularak her bir modelin 50 m/s çarpma hızında analizleri yapılmıştır. Tüpler kabuk olarak modellenirken, köpük malzeme katı model olarak tasarlanmıştır. Her bir modelin kuvvet ve iç enerji değerlerinin zamanla değişimleri aynı grafikler üzerinde çizdirilip karşılaştırılarak köpük dolgulu ezilme tüplerinin içi boş tüplere göre farkları incelenmiştir.

Yapılan deneysel ve sayısal çalışmalar ile tablolama çalışmasına ait sonuçlar tezin sonuçlar bölümünde aktarılmıştır. Bu konuda yapılması öngörülen çalışmalar sonuçlar bölümünün ardından listelenmiştir.

1. INTRODUCTION

Impact phenomenon can be encountered in many field such as automobile accident, debris impact on spacecraft vehicle, impact on a protection shield, etc. Because of having various types of this phenomenon, researchers have tried several ways to take precaution and reduce its harmful effects on drivers, passengers and vehicles.

In space, vehicles might be subjected to impact of meteoroids and debris particles or the loads acting during landing. Design of spacecraft shield gains more importance for protection of spacecraft's structural integrity and crews' health. Researchers generally focus on hypervelocity impact phenomenon due to being more common encountered problem.

Over one million people are killed and 20-50 million people are injured during traffic accidents per a year. According to WHO, 1.24 million people are killed in 2010 [1]. For this reason, raising safety level of a car is an important scientific research subject. Crash tubes are used to reduce the harm of the accidents on passengers and equipped generally in front of the cars. They have an important role to reduce harmful effects of accidents. Numerous studies have been done to enhance the crashworthiness characteristics of crash tubes at dynamic and quasi-static velocities.

The main targets of crash tube design are peak load should be lower and amount of energy absorption should be higher at the same time despite being adverse processes. Researchers aim to obtain its better crashworthiness characteristic.

1.1 Literature Review

There are several studies based on experiences of different geometrical parameters such as thickness and cross section of the crash box. Yamashita et al. [2] investigated the different types of polygonal crash boxes and the effects of wall thickness and plastic hardening rate of material on the crush behavior. As long as the number of corners of cross-sections increases, the crush strength of tube increases. It is observed apparently at smaller initial wall thicknesses. In addition, strength of circular cross section is higher than square cross section tubes. Palanivelu et al. [3] searched crashworthiness characteristics of different geometrical shapes (cylindrical, square, hexagonal, conical, and hourglass) and different thicknesses (1 and 2 mm) of composite tubes under quasi-static loading conditions. Conical circular tubes gives higher SEA and P_{peak} values than the other standard geometrical profiles. Abramowicz and Jones [4,5] investigated the circular and square steel crash tubes under dynamic and static loading. Salehghaffari et al. [6] showed that wall thickness, ring spacing and ring thickness width have important effects on the reinforced cylindrical crash box and demonstrates externally stiffened circular tubes are more efficient than prismatic circular tubes. Karagiozova and Jones [7] searched dynamics effects of cylindrical shells testing numerically different types of materials to show the influence of the material properties, shell geometry, boundary conditions and loading techniques on buckling and energy absorption. It is shown that the fold length increases with increase of the shell thickness.

Experimental tests and numerical solutions are also important ways of study on crush boxes. There are several studies about comparison of numerical and experimental results. Jensen et al. [8] investigated the transition from progressive to global buckling by investigating AA6060-T6 crash boxes using ABAQUS software program. The impact velocity has important role on the collapse mode. Fyllingen et al. [9] studied the influence of the element type and formulation for modeling aluminum profiles under axial loading using LS-DYNA and ABAQUS software program. According to Kazancı and Bathe [10], the results of numerical analysis using ADINA (based on implicit time integration method) and LS DYNA (based on explicit time integration method) are in agreement with the experimental results at quasi static crush speeds which means that ADINA can be a good alternative because of having shorter solution time. Besides, changing velocity of impact mass affects the crashworthiness characteristics of crash boxes. They are tested many times at various dynamic and quasi-static speeds. Karagiozova et al. [11] studied the inertial effects in axissymetrical cylinders and showed shell elements absorbed higher energy while crash speed is increased and impact mass is reduced.

Steel, aluminum and composite materials are the most common used materials for crash boxes. Ince et al. [12] investigate the energy absorption characteristics of hybrid crash tubes saving of %17.5 for total weight. Mamalis et al. [13] analyzed theoretically failure mechanism of thin walled fiberglass composite circular crash boxes based on experimental results. Langthseth et al. [14] validated the experimental results of Al6060-T4 and T6 alloy crash box by analyzing them at dynamic and static speeds. Kim [15] analyzed the new types of multi-cell profiles with square elements at the corner over conventional square box column to improve energy absorption and weight efficiency. Aktay and Kroplin [16] investigated the quasi-static axial crushing behavior of empty and foam-filled single, bitubular and multi-tube-packed made experimentally and numerically. Foam filling changes the failure mechanism of crash box, but it has lower SAE over the single empty tubes. In addition, squared and hexagonal multicellular tubes increased SAE values over single empty tubes. Olabi et al. [17] analyzed numerically and experimentally the quasi-static lateral compression of nested systems that is different from multi cell profiles.

1.2 Review of Articles on Crash Tubes

In this section, 127 articles on crash tubes are reviewed. These articles are listed in Reference section [2-11,13-15,19 and 21-131]. They are listed according to their published year and important informations are tabulated, shown in Table A1 in the Appendix section. This study can be used by researchers as a source including some general informations and datas of these articles. Table is divided into mainly six parts.

In the first section, software programs: LS-DYNA, ABAQUS, ADINA, PAM-CRASH and ANSYS and solution methods: implicit or explicit are placed. Besides, analytical and experimental studies are figured out afterwards. Second part of table includes datas of impact mass and impact velocity.

In the third section geometrical information like cross section types, thickness and length measurements are listed in the next section. Cross section types are classified as circular, square, rectangular, hexagonal and a generalized row for the other types of cross section.

Then material information are given. In the literature, it can be observed that there there main material types of crash tubes which are aluminum, aluminum alloys, steel, and composite materials. Table presents a row for each material types.

Finally, configuration types are indicated for all articles. They are listed according to empty, foam-filled, multi-cell and singular types.

1.3 Purpose of Thesis

The purpose of this study is to examine the energy absorption characteristics of stepped concentric crash tubes experimentally and numerically subjected to an axial impact load. The stepped concentric tubes considered here have different tube numbers and thickness, but external volume and total mass are kept constant. Effects of the tubes numbers, velocity and foam filled are investigation parameters in this thesis. Also, a comprehensive literature research is presented as a tabulating study at the end.

2. EXPERIMENTAL STUDIES

2.1 Model Specifications

In this study, three stepped and concentric circular crash tubes are tested at dynamic and quasi-static speeds. Tube lengths are 30, 25 and 20 mm, diameters are 12, 16, 20 mm from the inside out and wall thickness of all of them is 1 mm. After cutting process, three samples are located in grooves on a plate and fastened with gluing method, shown in Fig. 2.1.

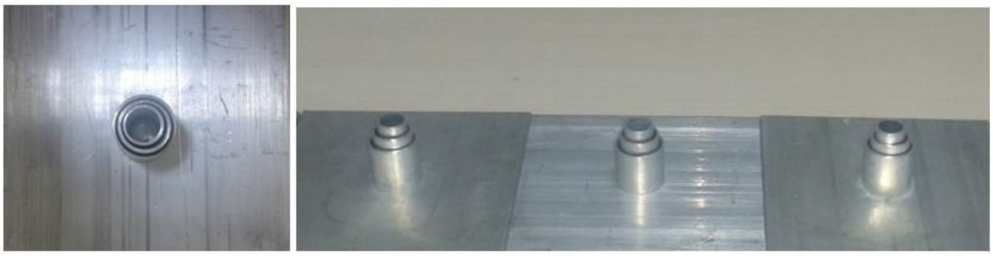

Figure 2.1 : Test specimens.

2.1.1 Material properties

All specimens are made of same material. The material is selected as AA6063, which is a strain rate insensitive material. Young modulus, E is equal to 68.7 GPa and density, ρ is equal to 2700 kg/m^3. Stress-strain curve of AL6063 is shown in Fig. 2.2.

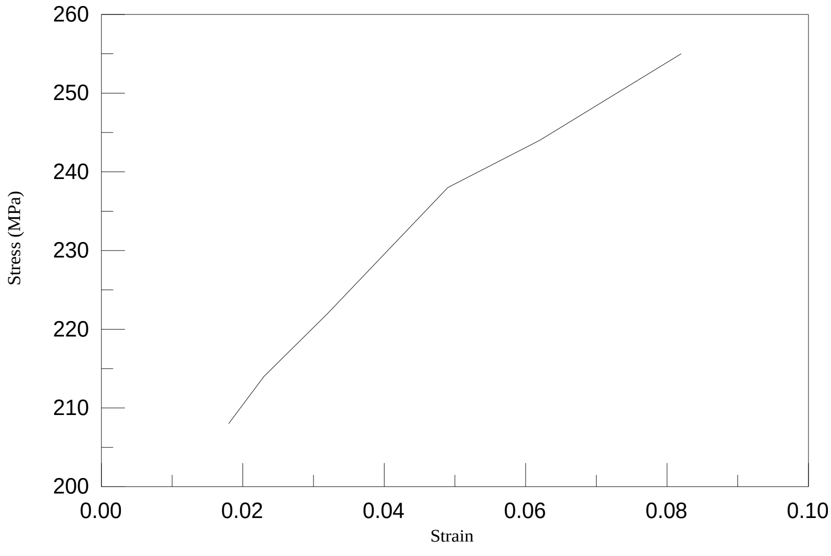

Figure 2.2 : Stress-strain curve of AL6063.

2.2 Quasi Static Test

Static test is done with MTS 647 Hydraulic Test Machine in Composite Structure Laboratory in ITU shown in Fig. 2.3. This machine is used for tension, compression and fatigue tests. Maximum load capacity is 100 kN. For this study, compression test is applied at 2 mm/min speed constantly.

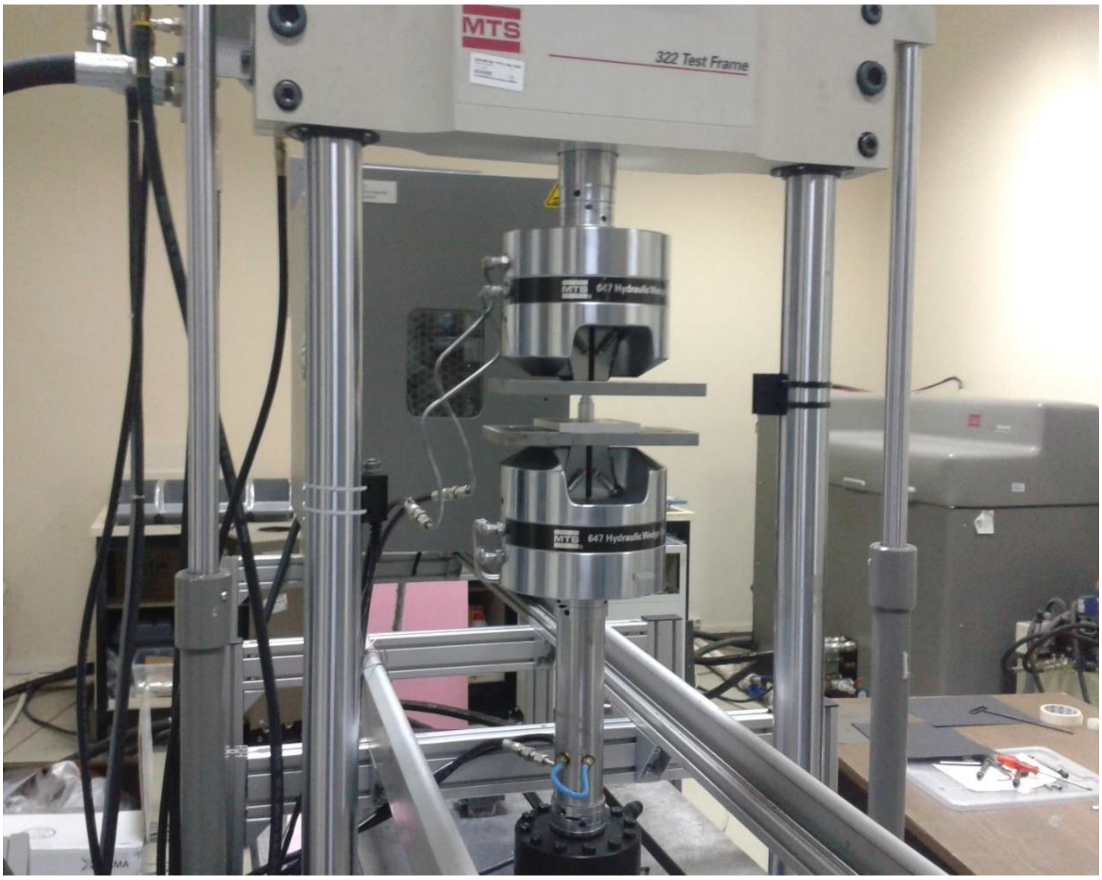

Figure 2.3 : MTS 647 Hydraulic Test Machine.

Appearances of the crushing sample are shown in various time for static test in Fig. 2.4a-h. Tubes fold progressively and interactions come out between tubes that are side by side. Force versus time curve is plotted according to experimental results, in Fig 2.5. The peak forces of all tubes can be viewed on this curve. Quasi-static test takes about 500 second.

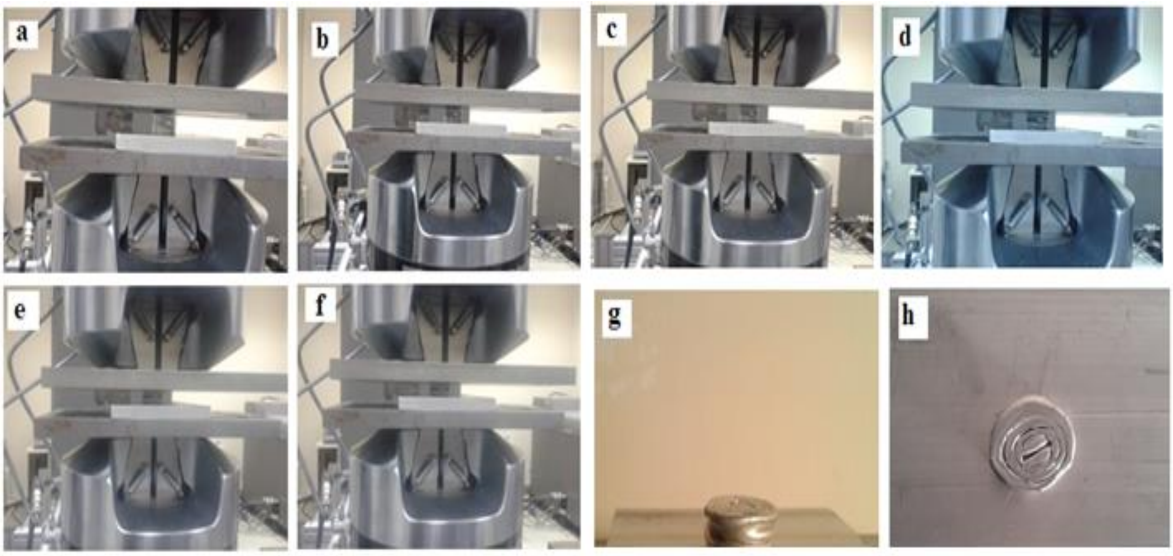

Figure 2.4 : Results of static test.

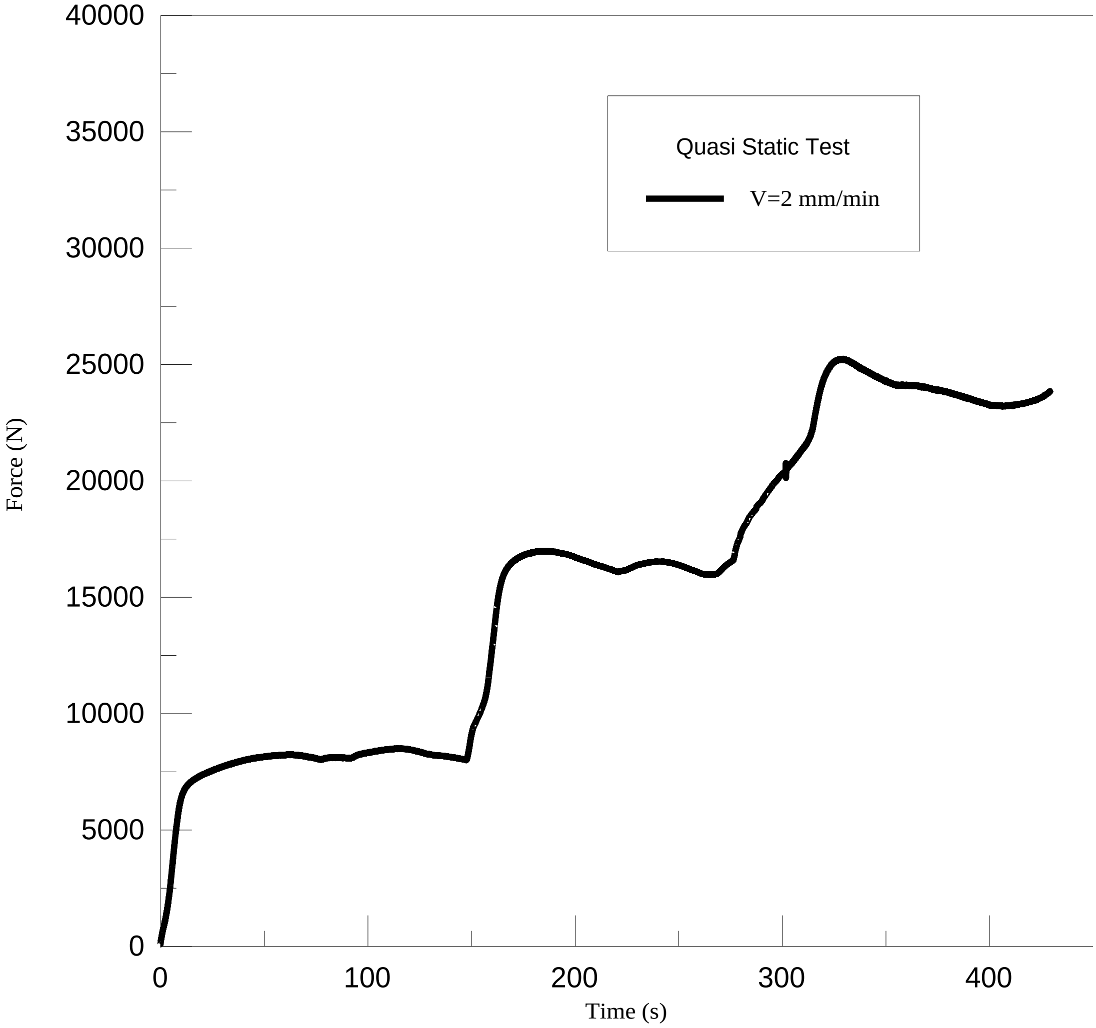

Figure 2.5 : Force vs time for static test.

2.3 Dynamic Tests

Dynamic tests are done by using INSTRON 8150 Impact Test Machine at TUBITAK Marmara Research Center (MAM), in Fig. 2.6. Impact mass capacity of this machine is 1132 kg. Its working principle is based on free fall motion. It can be reached 7 m/s impact velocity with this machine. However, dimensions of test specimens are too low and can be deformed with low energy. Also, the amount of impact mass can not be changed. Therefore, it is dropped too lower height.

Figure 2.6 : INSTRON 8150 Drop Test Machine [18].

2.3.1 Test of specimen A

In Fig. 2.7.a and 2.7.b, front and top view of sample A are demonstrated. The appearance of sample after test is demonstrated in Fig. 2.7.c and 2.7.d. From the figures, it can be observed that tubes folded progressively and interactions come out between tubes which are side by side like static test.

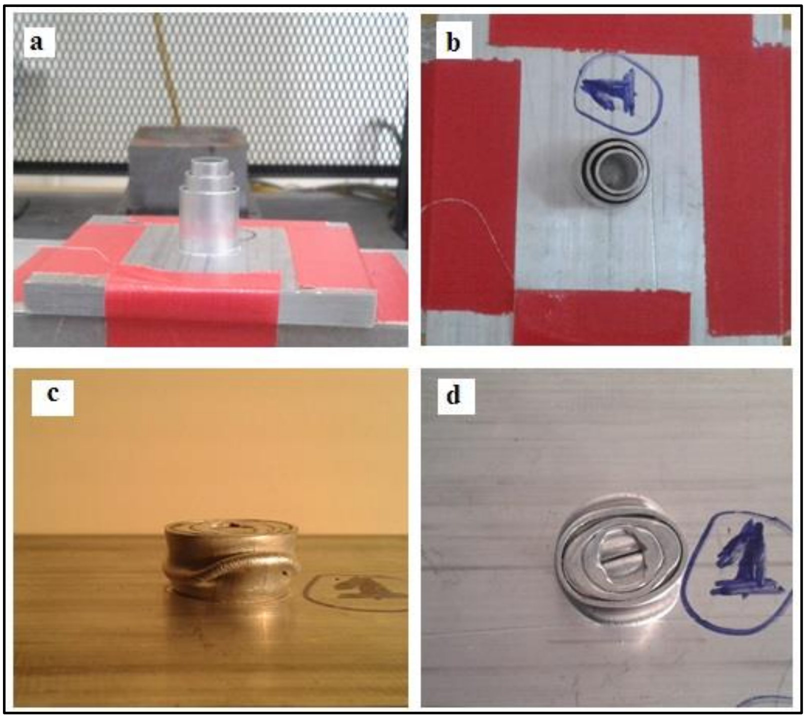

Figure 2.7 : Dynamic test of sample A.

2.3.2 Test of specimen B

In Fig. 2.8a and 2.8b front and top view of sample B is shown. The appearance of sample after test is demonstrated in Fig. 2.8c and 2.8d. Folding mechanism of sample B is similar with specimen A.

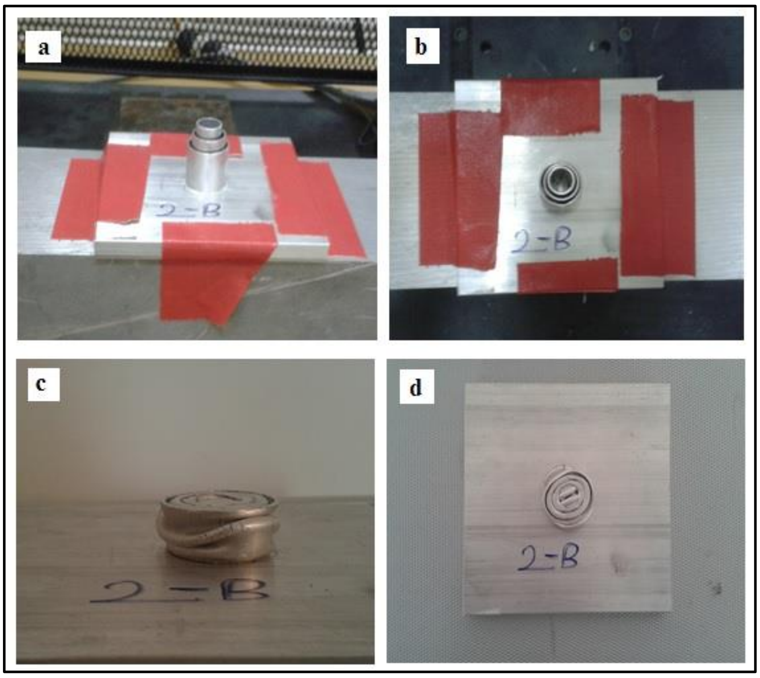

Figure 2.8 : Dynamic test of sample B.

2.3.3 Comparison of dynamic tests

"Force vs. Time" graphic is plotted in Grapher software program for two dynamic tests, in Fig. 2.9. Their peak forces and internal energy change are close each other due to having low difference between impact velocities.

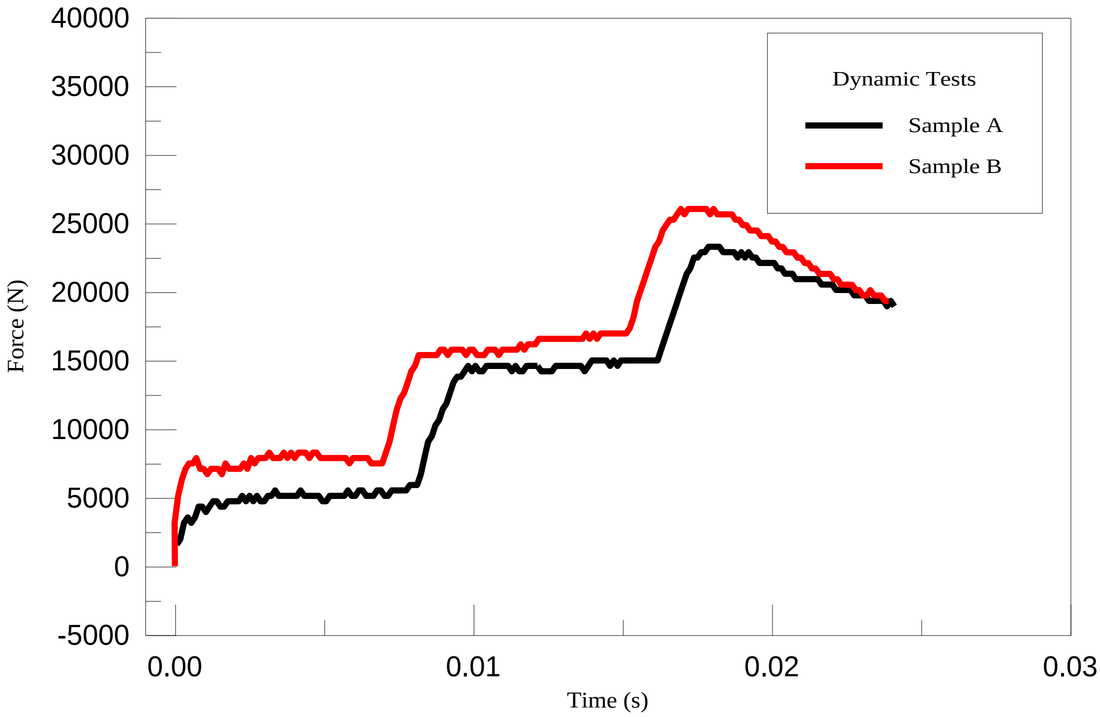

Figure 2.9 : Force versus time for dynamic tests.

2.4 Validation of Dynamic and Static Tests by Using LS DYNA

It is preferred to use mostly the explicit solver of the nonlinear finite element code LS-DYNA. Therefore, dynamic tests are validated by using LS-DYNA software program that is generally selected as an explicit time integration method to study nonlinear dynamic problems. In the next parts, modelling of specimen in LS-DYNA is explained and compared numerical and experimental results.

2.4.1 Finite element modelling

Three concentric circles are drawn under CURVE toolbar in XY plane, then circles are extruded in Z direction by using "extrude" under SURFACE toolbar. Thickness of cross section is defined as 1 mm by using SHELL under SECTION toolbar. The bottom of all tubes is clamped with SPC NODE and a rigid wall is defined 1 mm far from the top of the longest tube.

All tubes are modeled by using Belytschko-Tsay shell elements. After comparing the analysis of triple concentric tubes at different mesh qualities, optimum element size is defined as 0.4x0.4 mm. Element number of tubes is 22712. Defining optimum mesh sizing is explained in Section 3.1.

AUTOMATIC SINGLE SURFACE contacts are identified for each sample, because they have possibility of lapping after deformation. Also, AUTOMATIC SURFACE TO SURFACE contacts are defined between surfaces of tubes. The static and dynamic friction coefficients are chosen as 0.2 and 0.3 respectively for each contact definition [19].

2.4.2 Explicit analysis in LS DYNA

To model dynamic analysis, RIGIDWALL-PLANAR MOVING FORCES is used as an impactor in LS DYNA. An example schematic view for sample 1 and rigid wall is plotted together in Fig. 2.10. Tubes are crashed with an initial velocity in the axial direction. Mass of rigid wall is 1132 kg, and its initial velocity is 0.65 and 0.70 m/s.

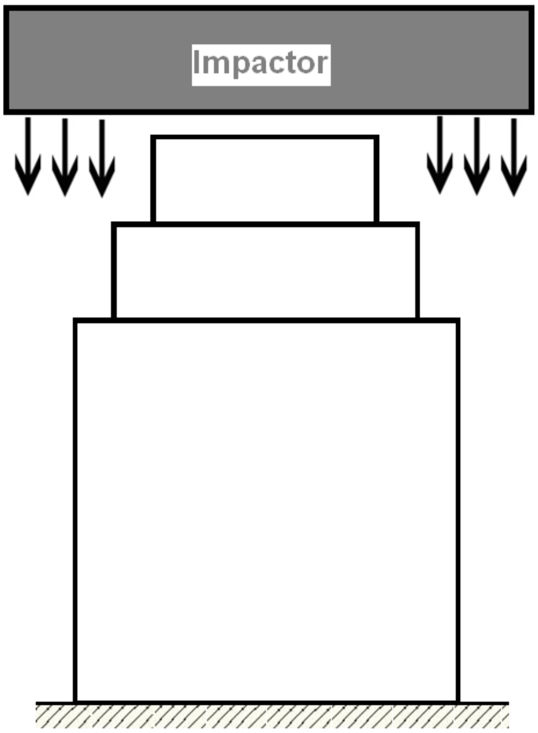

Figure 2.10 : Schematic of geometry with an example model and rigid wall.

2.4.2.1 Comparison of dynamic test results with analysis results

To validate experimental results with numerical solution, “Force vs. Time” curve is drawn in LS-DYNA by selecting SPCFORC under DATABASE toolbar. This module gives reaction forces at boundaries which are defined SPC NODES under BOUNDARY toolbar. “Force vs. Time” curves of experimental and numerical results are plotted in same graphic for each velocity, in Fig 2.11 and Fig 2.12.

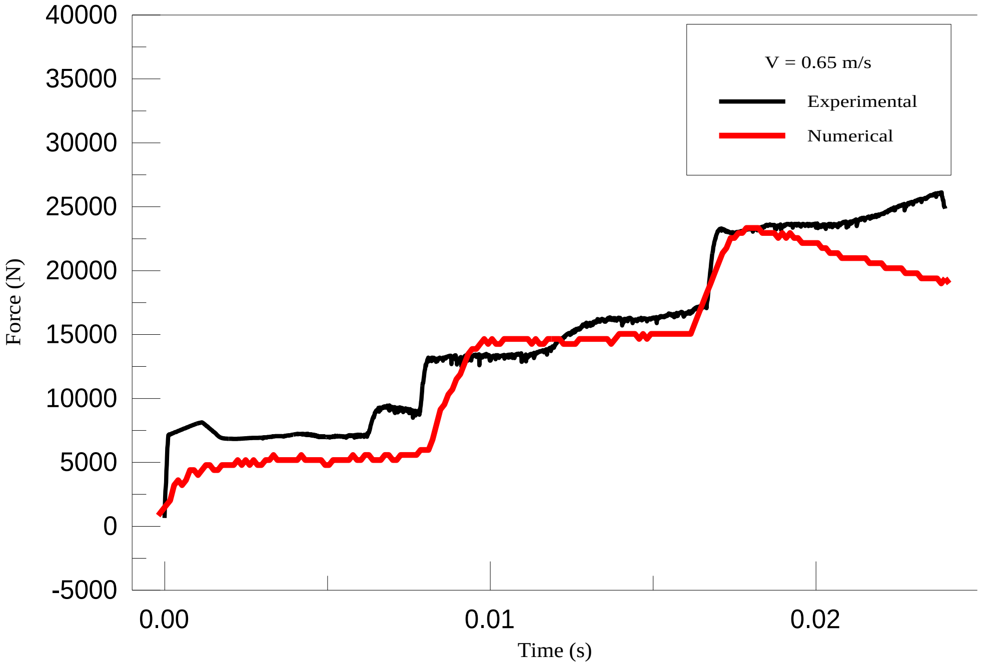

Figure 2.11 : “Force vs. Time” curves of sample A.

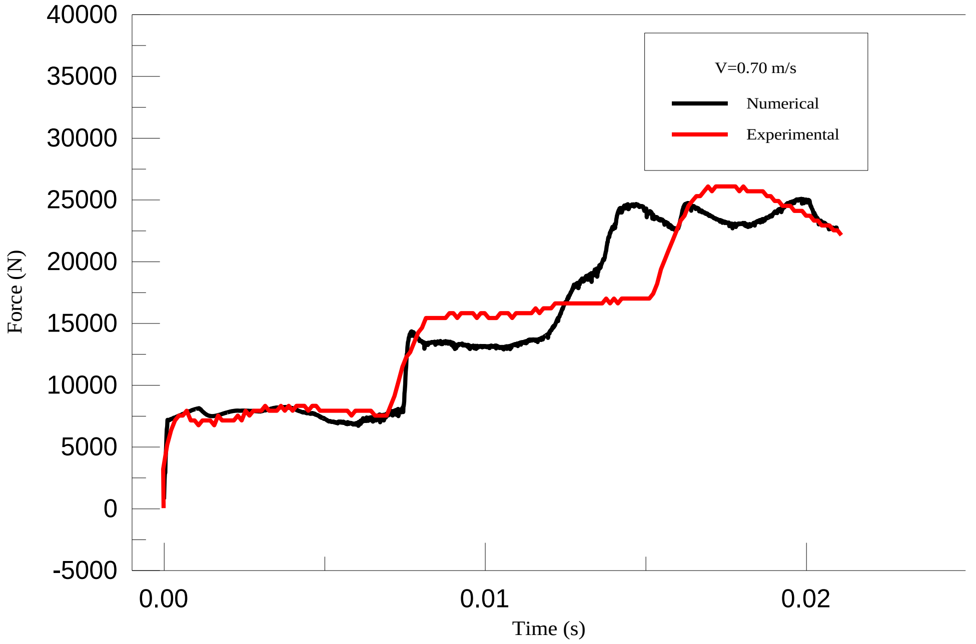

Figure 2.12 : “Force vs Time” curves of sample B.

It can be understood from the figures results of analyses and experiments are compatible each other. In addition, the values of three peak forces and their percantage error are listed in Table 2.1.

Table 2.1 : List of peak forces for dynamic cases

	1st peak force (kN)	Error (%)	2nd peak force (kN)	Error (%)	3rd peak force (kN)	Error (%)
Dynamic Test A	8.69	7	16.18	17	25.60	8
Analysis A	8.08		13.43		23.45	
Dynamic Test B	8.68	6	15.78	9	26.04	5
Analysis B	8.15		14.31		24.69	

2.4.3 Quasi static analysis in LS DYNA by using implict solver

To model static test in LS DYNA, implicit solution method is practical rather than explicit methods. Solution time takes longer by using explicit method contrary to implicit method. A SHELL is modelled in LS DYNA to crush the tubes. It is defined by using PRESCRIBED MOTION RIGID under BOUNDARY toolbar. An example schematic of model for implicit analysis is plotted in Fig. 2.13.

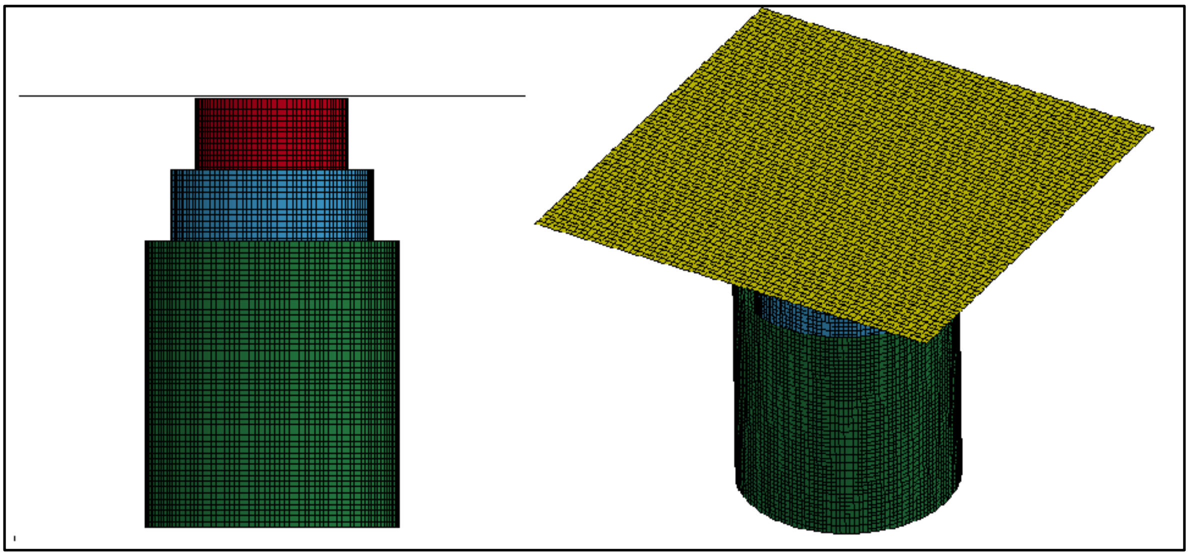

Figure 2.13: FEM for implicit analysis in LS DYNA.

2.4.3.1 Comparison of quasi static test results with analysis results

To validate static test results with numerical solution, “Force vs. Time” curve is drawn in LS-DYNA by selecting SPCFORC under DATABASE toolbar. “Force vs.

Time” curves of experimental and numerical results are plotted in same graphic, in Fig 2.14.

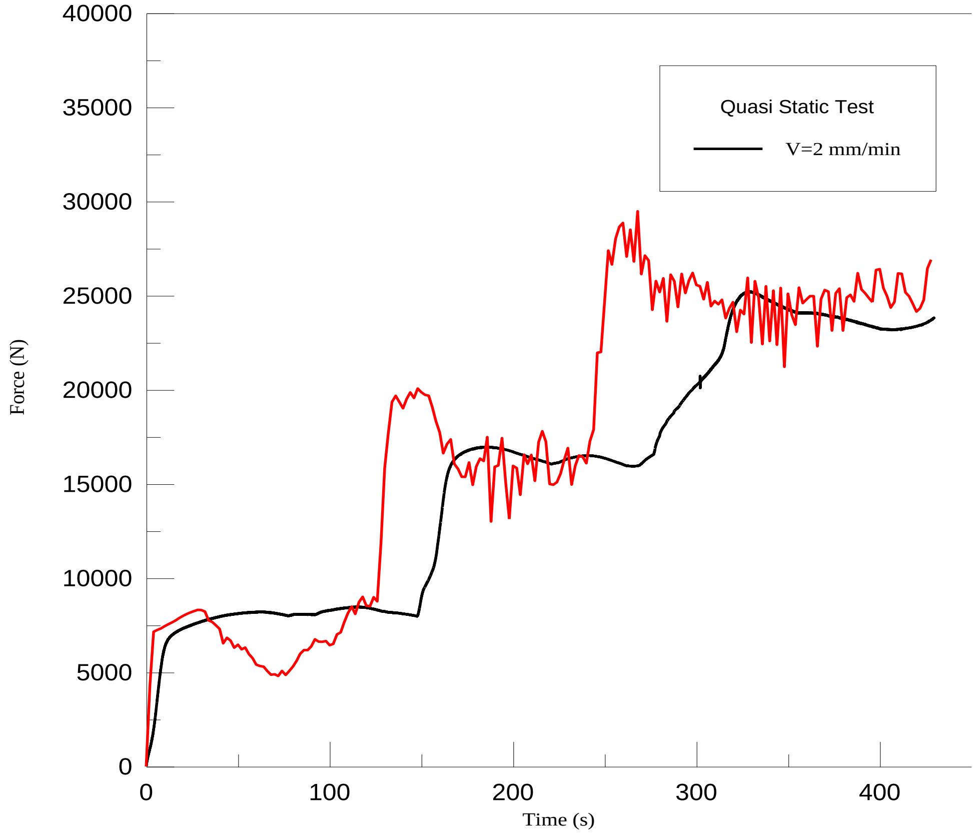

Figure 2.14 : Force vs. time curves of static case.

It can be understood from the Fig. 2.14, results of analyses and experiments are compatible eacother despite of a bit differences. The values of three peak forces and their percantage error are listed in Table 2.2 .

Table 2.2 : List of peak forces for static case.

	1st peak force (kN)	Error (%)	2nd peak force (kN)	Error (%)	3rd peak force (kN)	Error (%)
Static Test	8.09	3	16.80	19	25.94	14
Static Analysis	8.30		20.06		29.47	

3. NUMERICAL STUDIES BY USING LS DYNA

3.1 Defining Optimum Mesh Sizing

3.1.1 Material properties

All specimens are made of same material. The material uses here AL alloy, which is a strain rate insensitive material, has young modulus, E is equal to 78 GPa and density, ρ is equal to 2700 kg/m^3. Material properties are listed in Table 3.1 and stress-strain curve shown in Fig. 3.1 is used to determine the material properties. Tubes are modelled with MAT024 PIECEWISE LINEAR PLASTICITY material model in LS-DYNA.

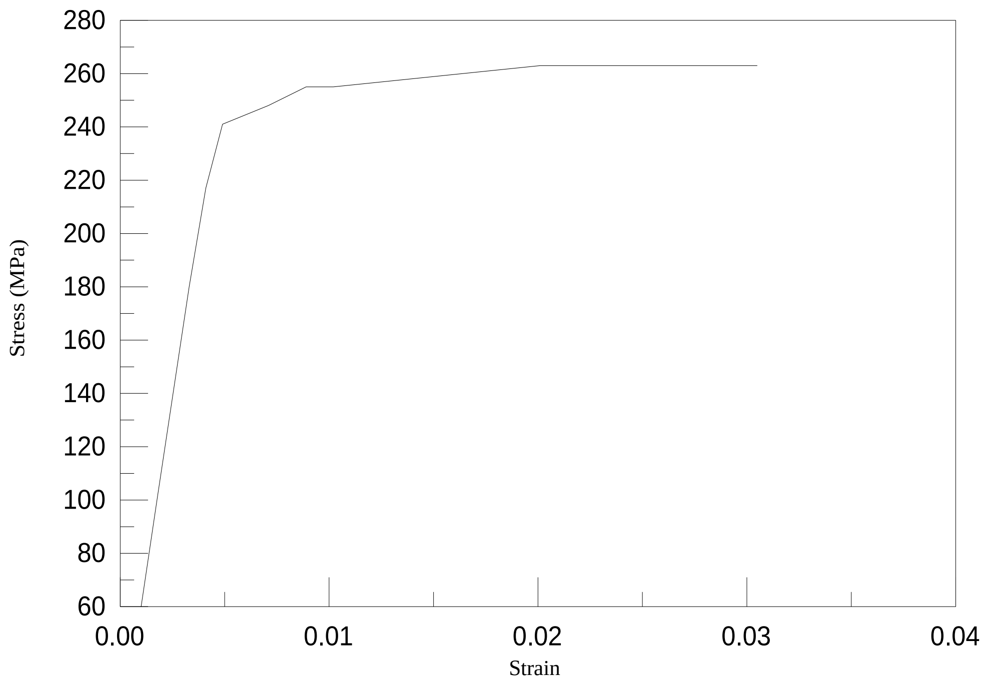

Figure 3.1 : Stress-strain curve of AL6063.

Table 3.1: Material properties.

Density (kg/m^3)	**Young Modulus (GPa)**	**Poison Ratio**	**Yield stress (MPa)**	**Ultimate tensile stress (MPa)**
2700	78	0.33	241	263

3.1.2 Comparison of results

In this section, stepped concentric three tubes are modelled with 5 different mesh qualities. Mesh sizes are 0.3x03, 0.4x0.4, 0.5x0.5, 0.6x0.6 and 0.7x0.7 mm. Impact velocity and mass are defined as 50 m/s and 100 g, respectively. “Force vs. Time” graphics are plotted separately for each analysis result, which are shown in Fig 3.2-3.6. It can be came out that force values in time are so close between two smallest mesh sizes models: 0.3x03 and 0.4x0.4 mm.

However, solution time strings out so much that is not suitable to do more analysis. Accordingly, 0.4x0.4 mm mesh size is chosen for all analysis models.

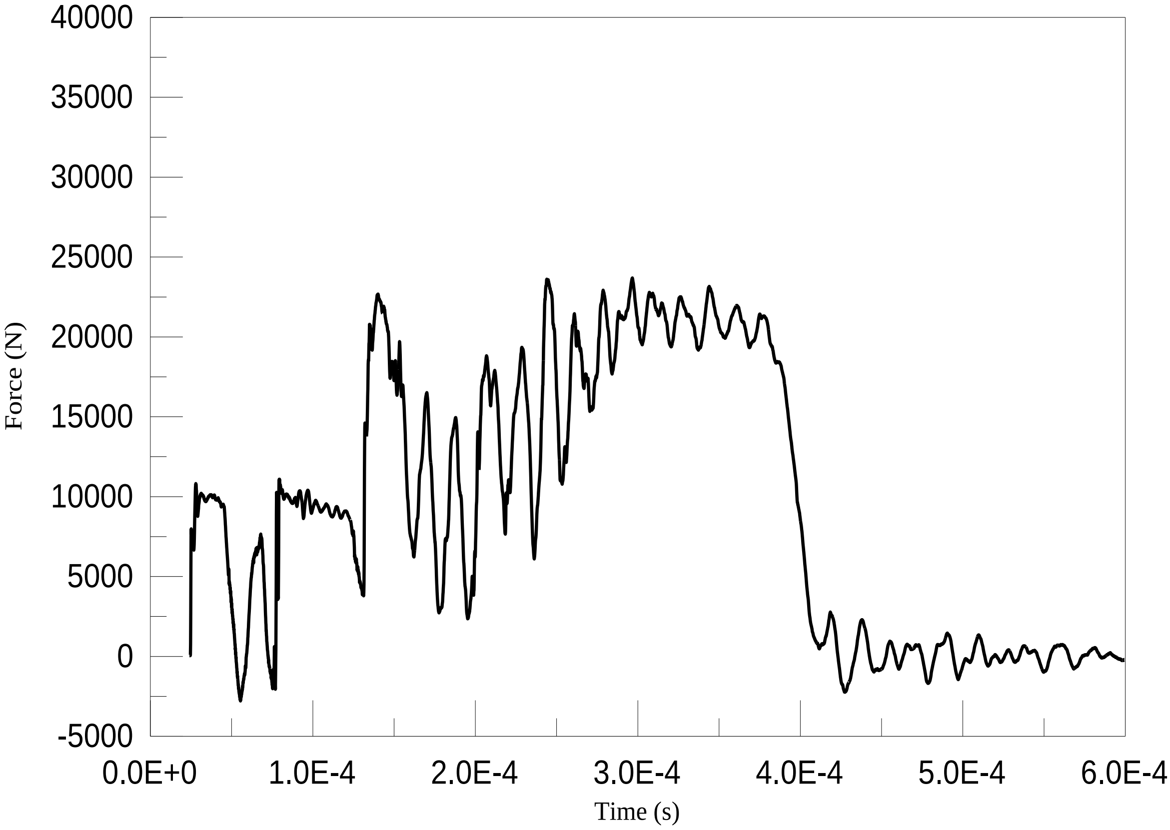

Figure 3.2 : Force versus time of 0.3x0.3 mm mesh sizing.

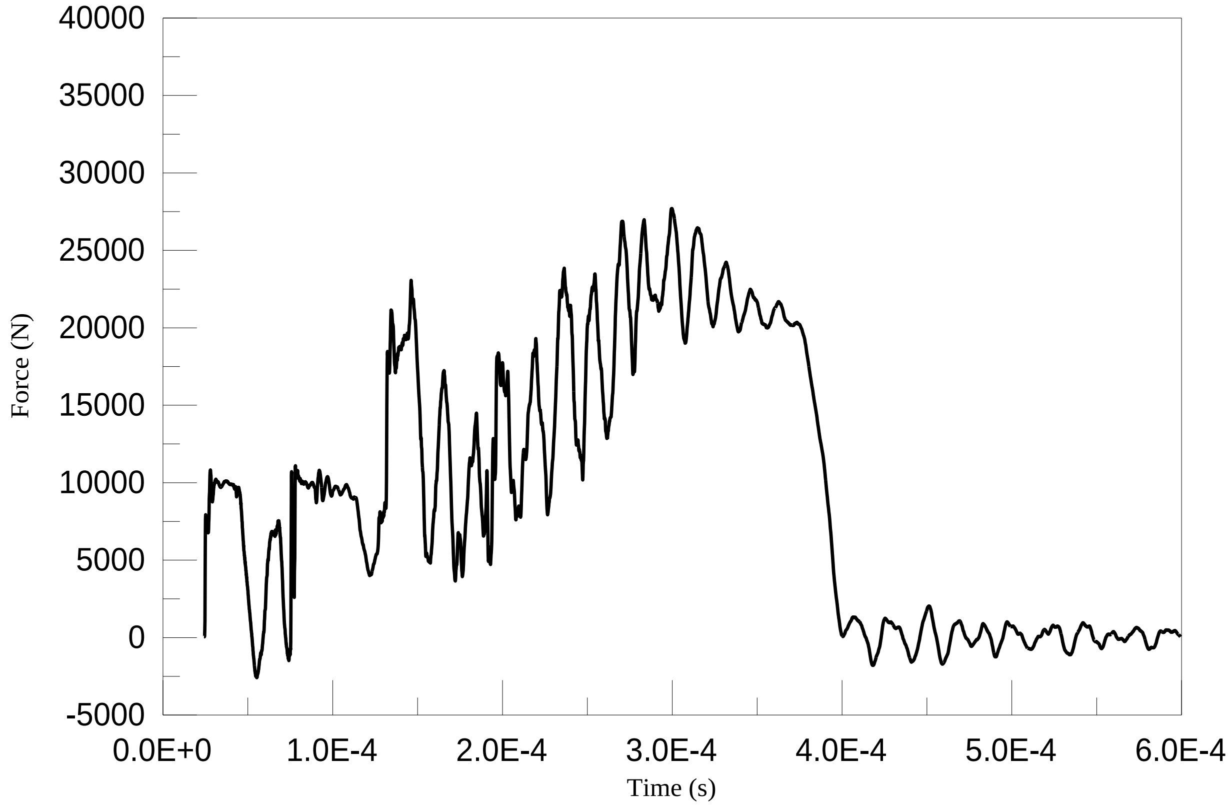

Figure 3.3 : Force versus time of 0.4x0.4 mm mesh sizing.

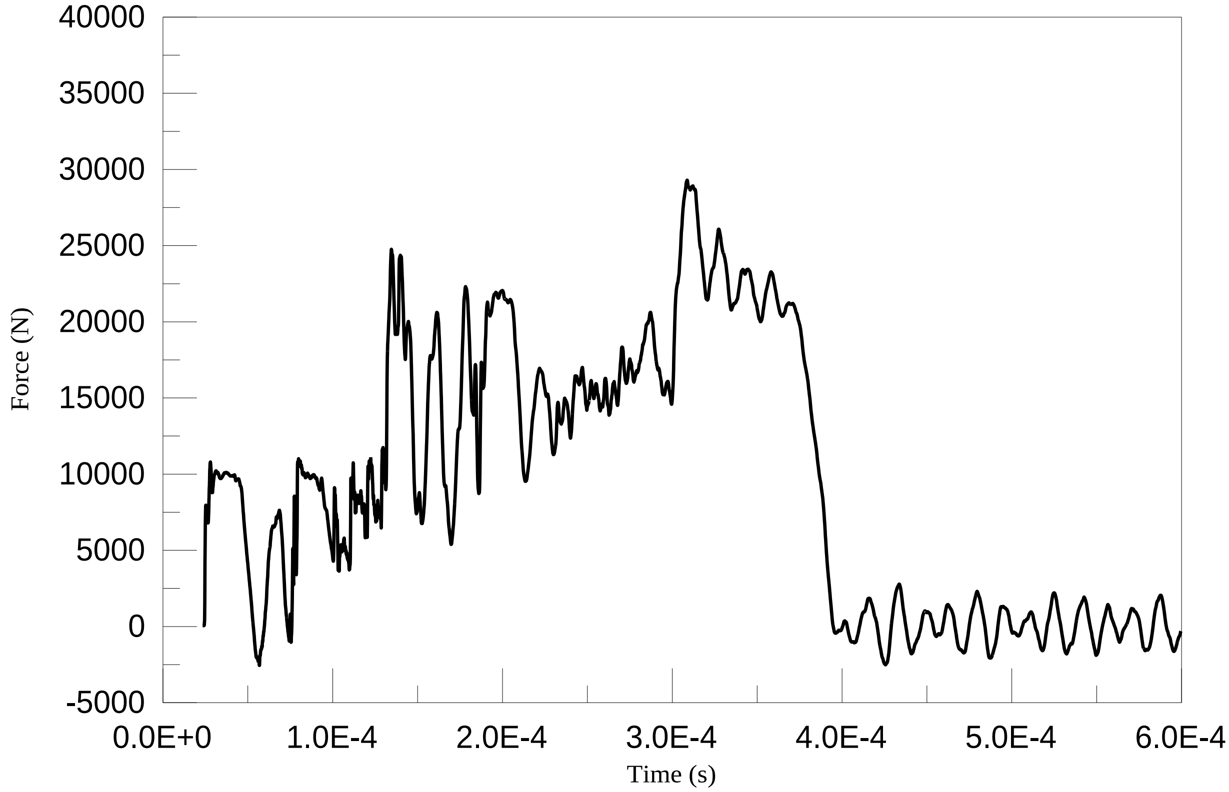

Figure 3.4 : Force versus time for with 0.5x0.5 mm mesh sizing.

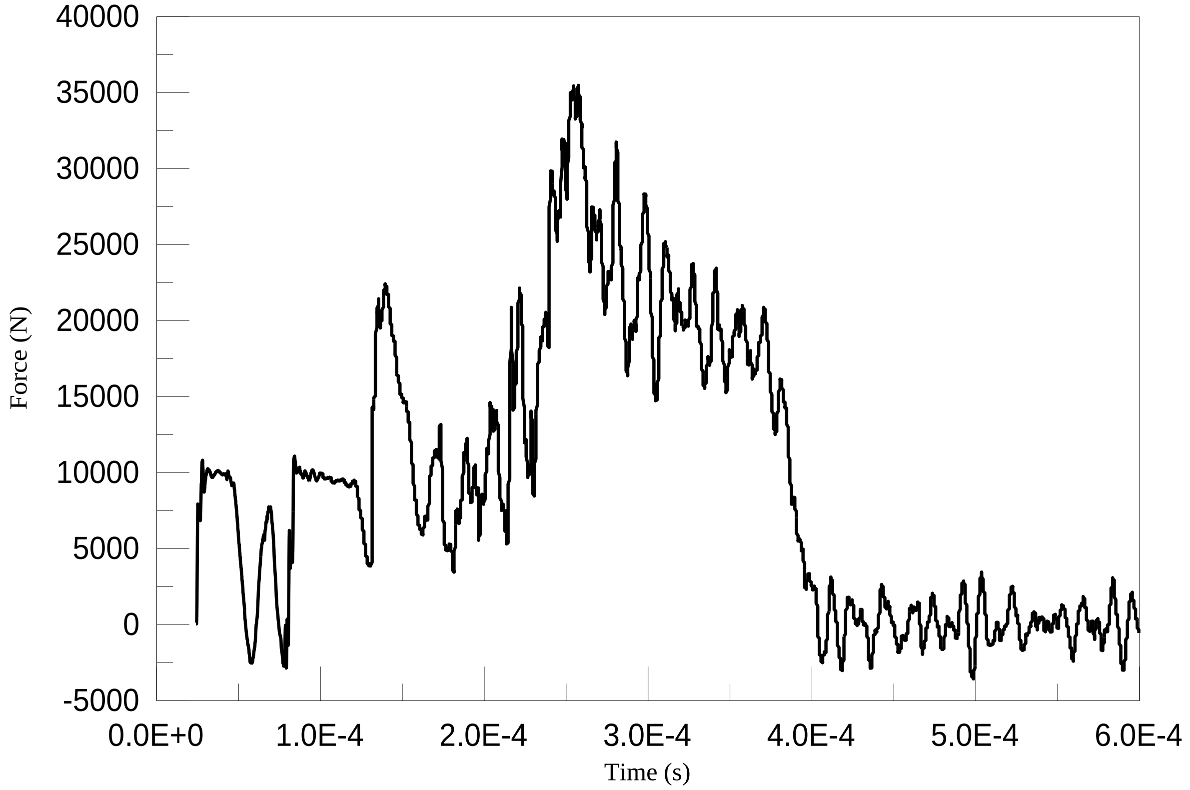

Figure 3.5 : Force versus time of 0.6x0.6 mm mesh sizing.

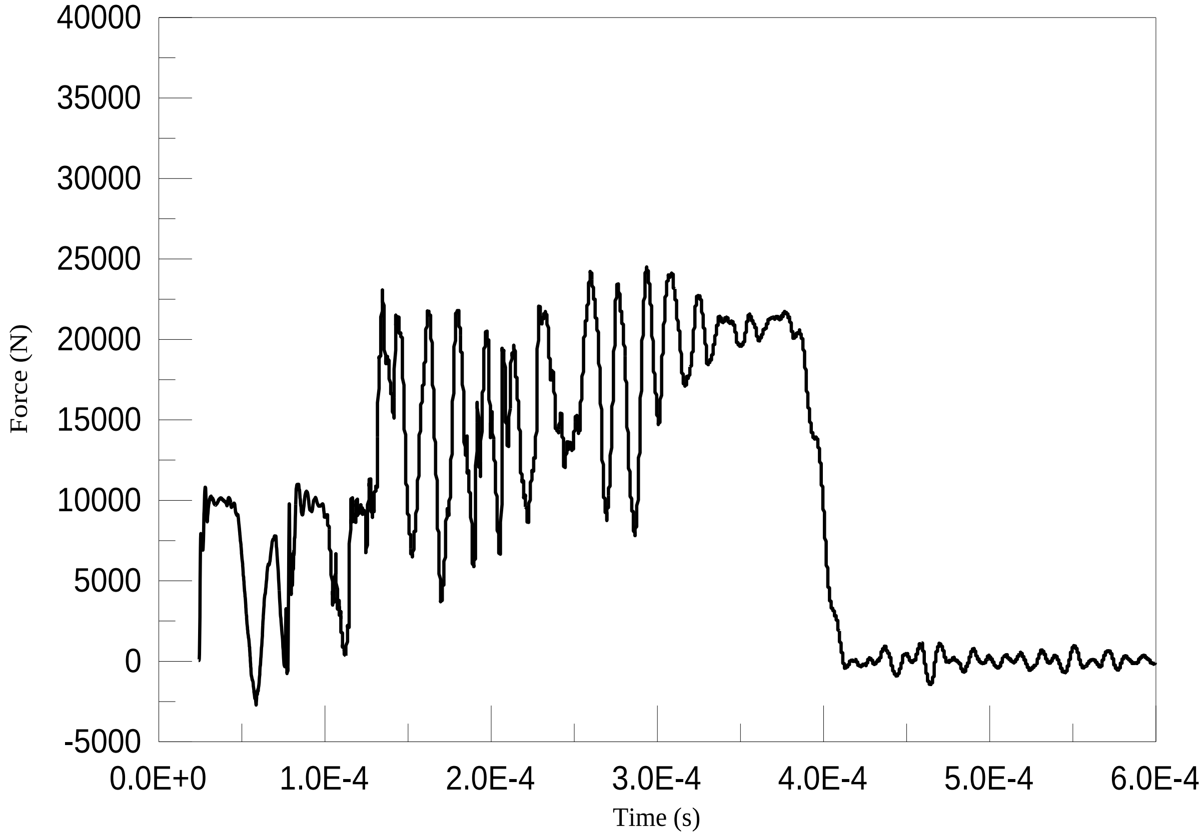

Figure 3.6 : Force versus time of 0.7x0.7 mm mesh sizing.

3.2 Investigation the Effects of Tube Numbers

In this part, the effects of tube numbers are studied at a constant velocity. Four different models are constituted with 3, 6, 9 and 12 stepped concentric tubes and all are named as Sample 1, 2, 3 and 4, respectively.

3.2.1 Specifications of samples

Dimensions of Sample 1 and 2 are listed in Table 3.2, also, Sample 3 and 4 are listed in Table 3.3. Tube no states how many number of tubes are concluded. Mean radius, length and wall thickness are listed for each tube one by one.

Table 3.2 : Dimensions of Sample 1 and 2.

	Sample 1			Sample 2		
Tube no	***r_mean* (mm)**	***L* (mm)**	***t* (mm)**	***r_mean* (mm)**	***L* (mm)**	***t* (mm)**
1	6	30	1	5	30	0.5
2	8	25	1	6	28	0.5
3	10	20	1	7	27	0.5
4				8	25	0.5
5				9	23	0.5
6				10	21	0.5

Table 3.3 : Dimensions of Sample 3 and 4.

	Sample 3			Sample 4		
Tube no	***r_mean* (mm)**	***L* (mm)**	***t* (mm)**	***r_mean* (mm)**	***L* (mm)**	***t* (mm)**
1	6.0	30.0	0.3	4.5	30	0.25
2	6.5	28.5	0.3	5.0	29.5	0.25
3	7.0	28.0	0.3	5.5	29	0.25
4	7.5	27.0	0.3	6.0	28.5	0.25
5	8.0	26.0	0.3	6.5	28	0.25
6	8.5	25.0	0.3	7.0	27	0.25
7	9.0	24.0	0.3	7.5	26	0.25
8	9.5	23.0	0.3	8.0	25	0.25
9	10.0	22.5	0.3	8.5	24	0.25
10				9.0	23	0.25
11				9.5	22	0.25
12				10.0	21	0.25

In Fig. 3.7, front and section views of finite element models are shown from LS-DYNA. Maximum tube lengths and diameters are same for all samples. It can be seen that spaces between tubes reduces when the tube number increases.

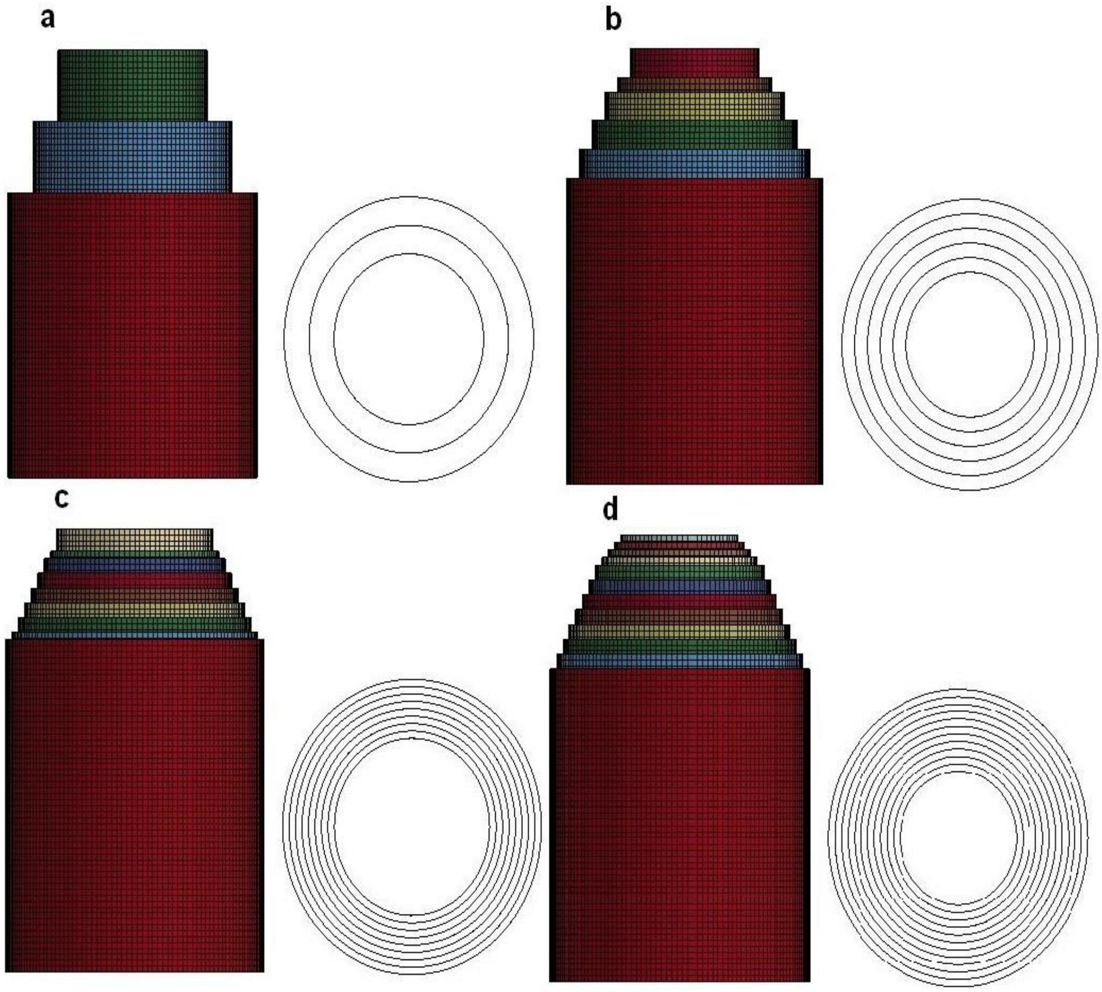

Figure 3.7 : FEM of four samples.

3.2.2 Comparison of results

"Force vs. Time" curve of each sample is plotted separetely, in Fig. 3.8-11. Sample 1 has three noticeable peak forces in Fig.3.8. Also, peak forces of Sample 2 can be seen on Fig. 3.9, but difference between two neighbour forces decrease. In addition, number of peak forces are not same with the tube numbers for Sample 3 and 4. This means some of the peak forces disappear with the increase of the number of tubes. It results from reduction of the wall thickness and space between two side by side tubes.

"Internal Energy vs. Time" curve of four sample are plotted in same figure, Fig. 3.12. According to this figure, total internal energy reduces, while the tube numbers are increased.

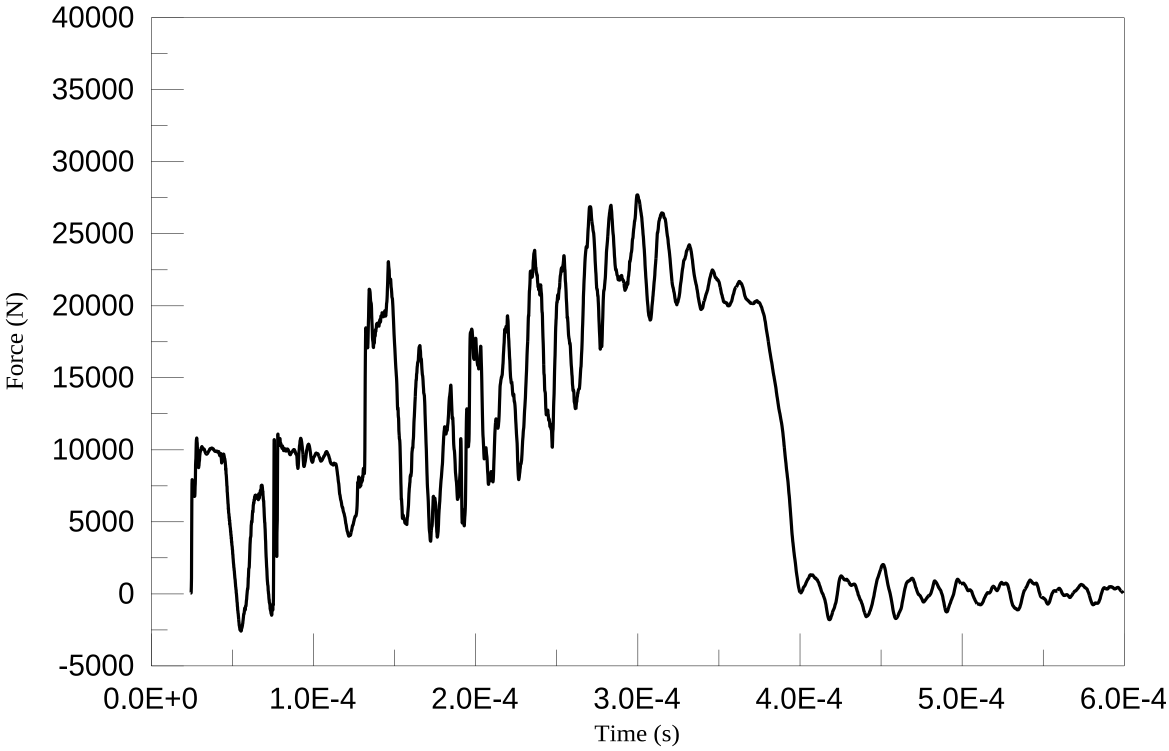

Figure 3.8 : Force versus time for sample 1.

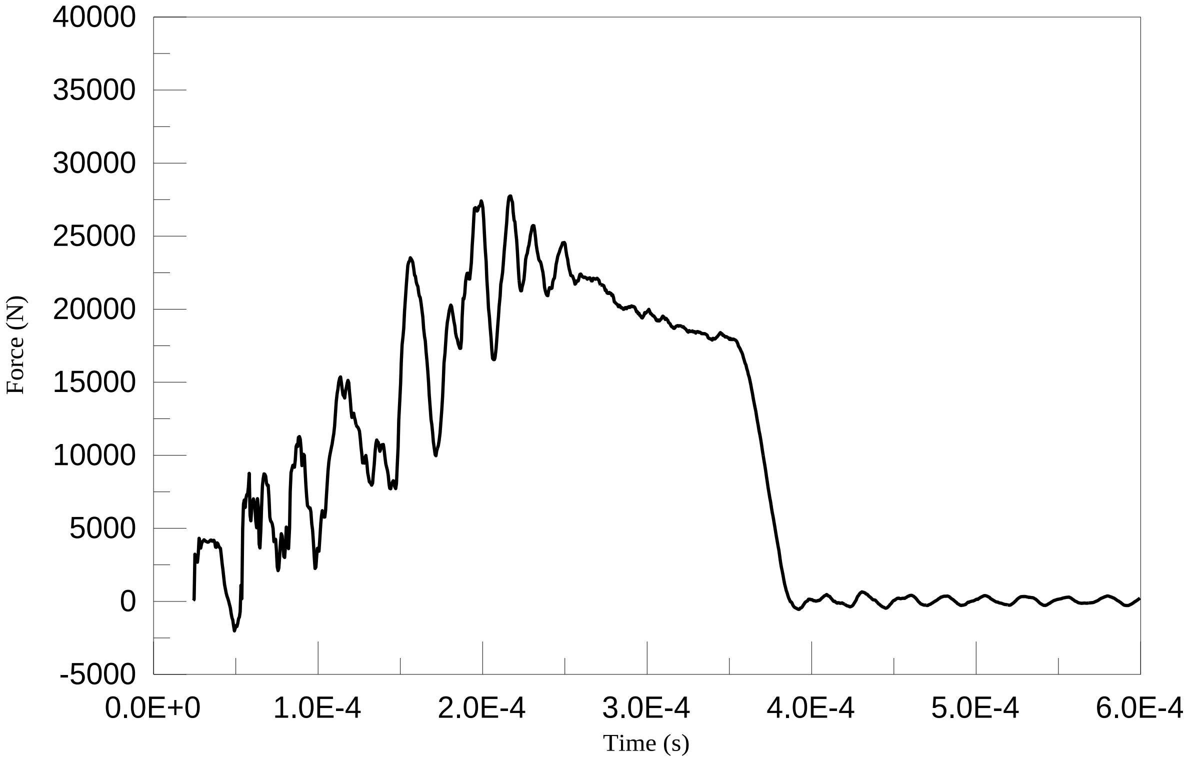

Figure 3.9 : Force versus time for sample 2.

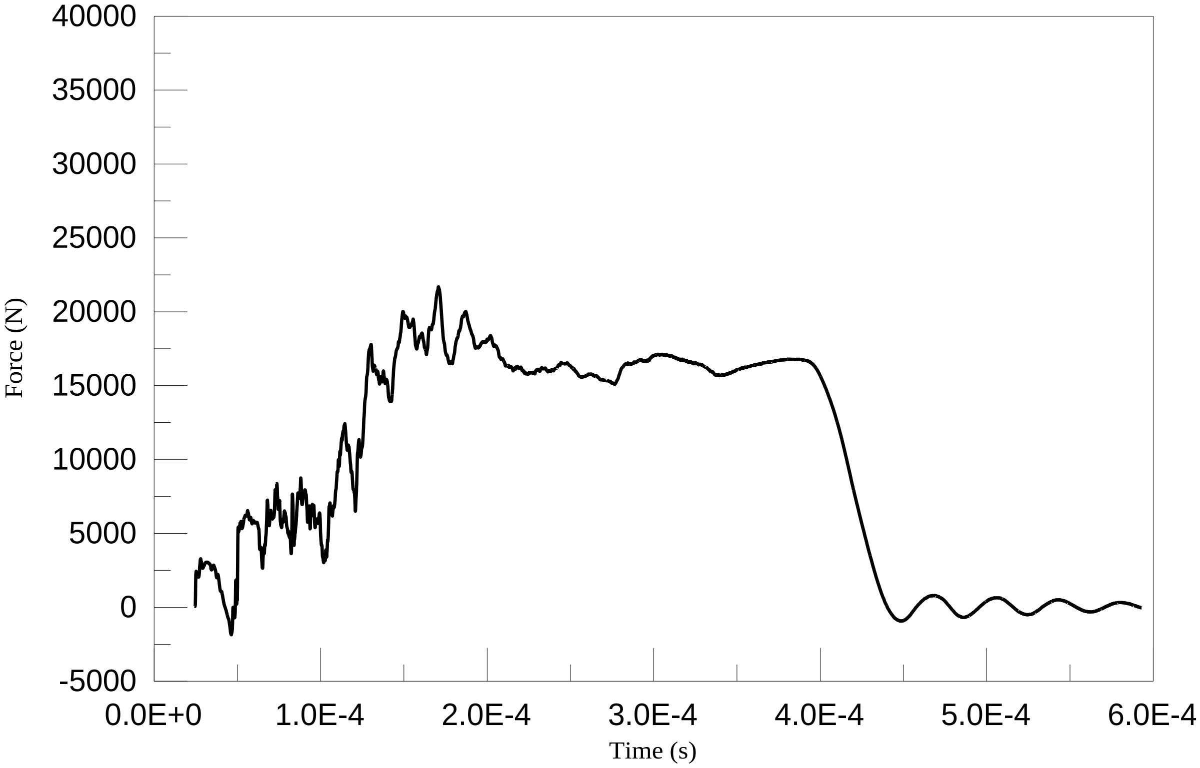

Figure 3.10 : Force versus time for sample 3.

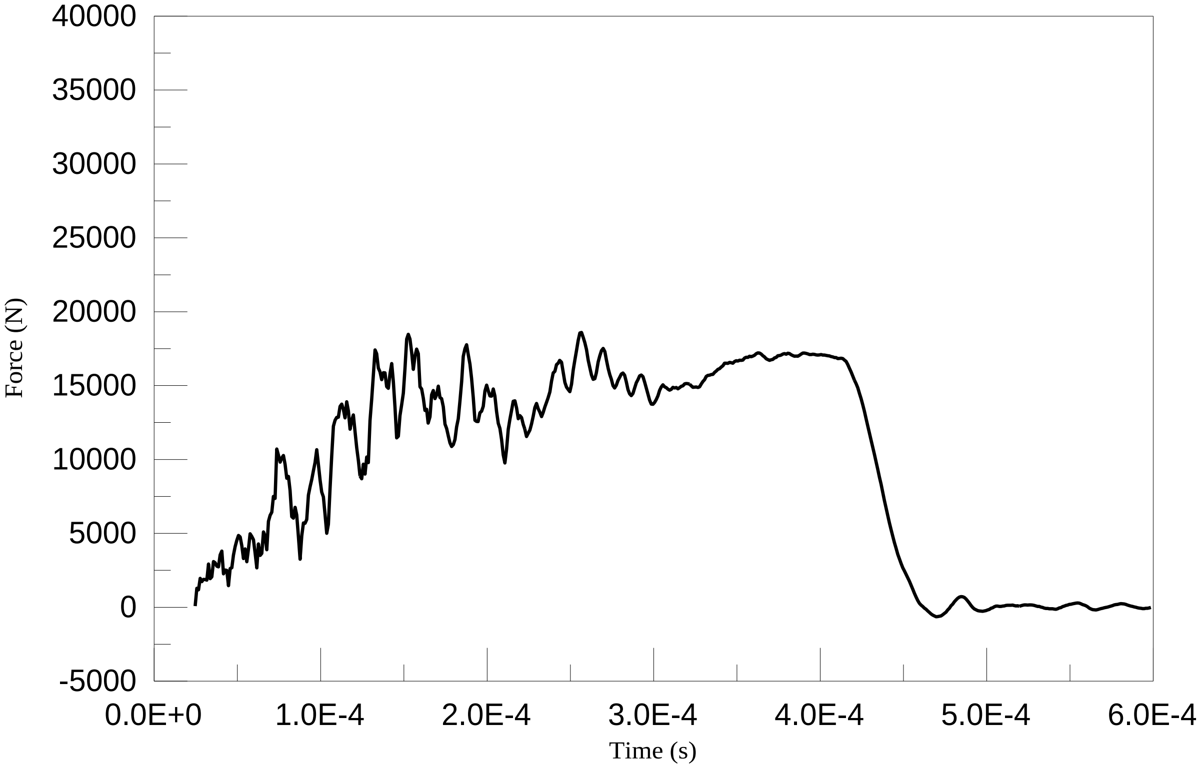

Figure 3.11 : Force versus time for sample 4.

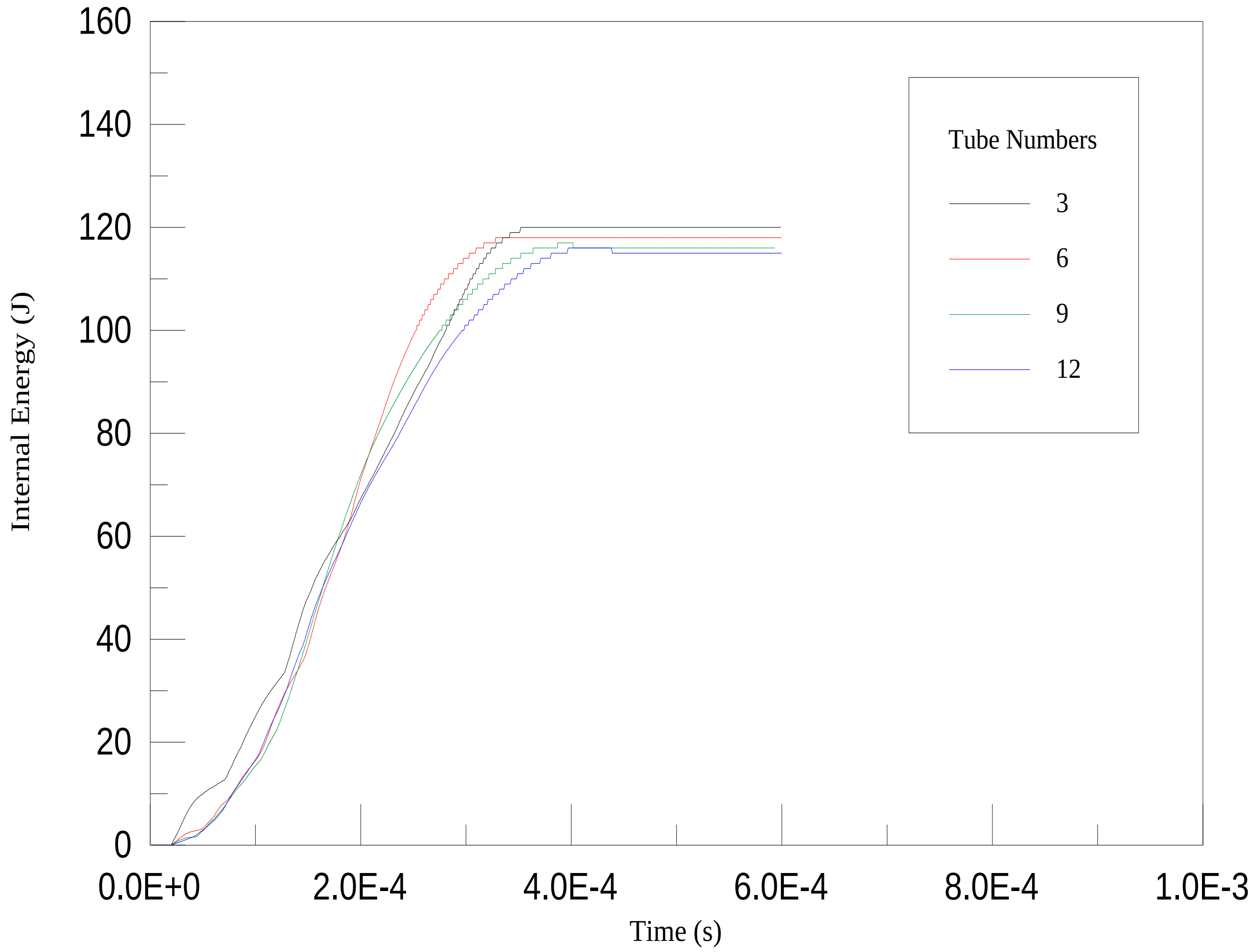

Figure 3.12 : Internal energy vs. time for all samples.

In Fig. 3.13, von Mises stress distribution and lengths of each samples after deformation are demonstrated. Deflection amounts are 10.6, 11.6, 10.7 and 11.2 mm, respectively.

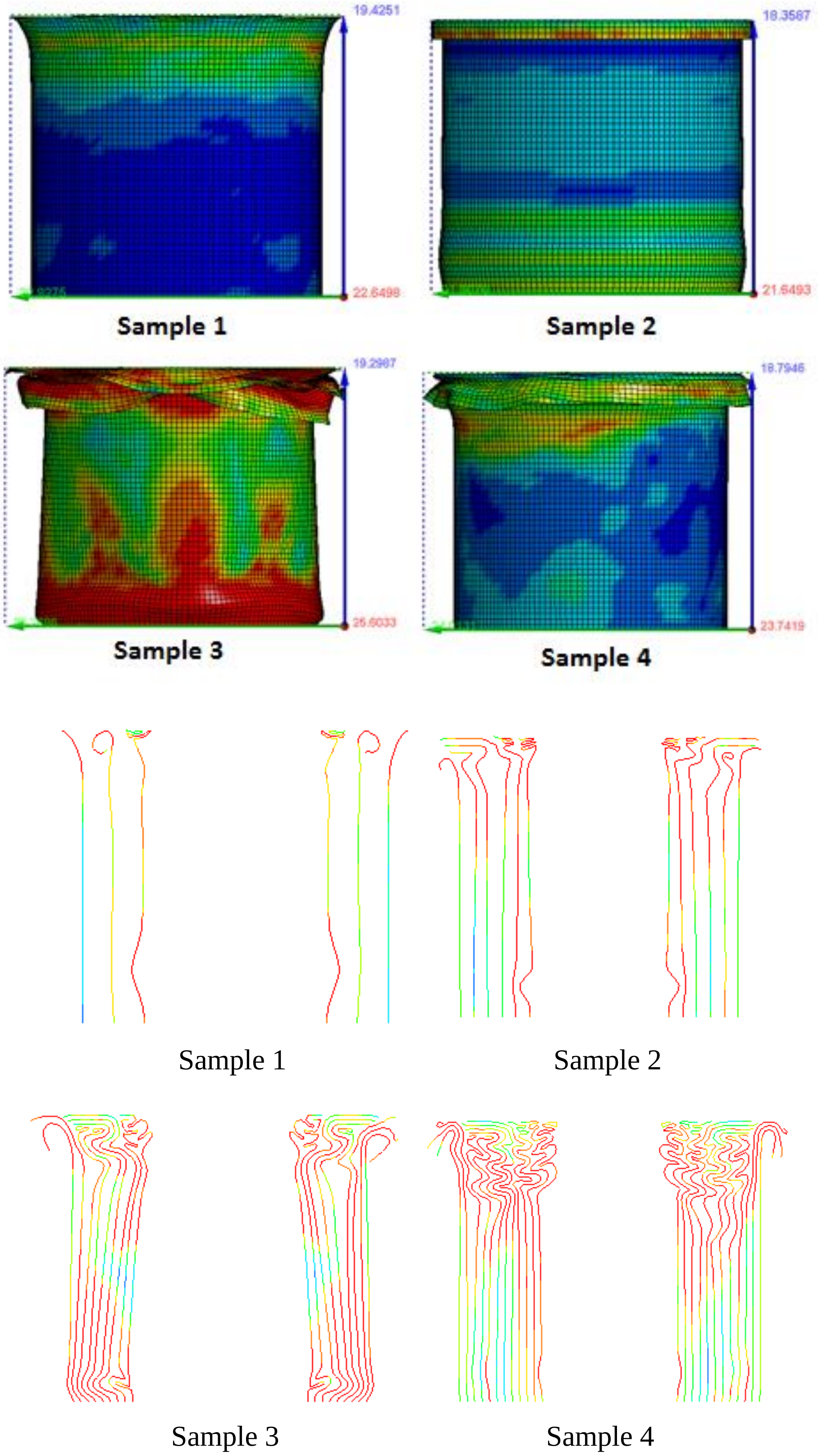

Figure 3.13 : Von Mises stress distribution and final lengths of each samples.

3.3 Behavior of Samples at Different Impact Velocities

In this section, the effects of impact velocity on stepped concentric tubes are investigated. In RIGIDWALL toolbar, impact velocities are selected 50, 60 and 70 m/s and without changing impact masses for each sample. Force, internal energy and total deflection are compared at different velocities.

3.3.1 Velocity effects on peak forces

It is seen from Fig 3.14-17 that solution time at higher velocity takes longer, also, peak forces get higher when velocity increases.

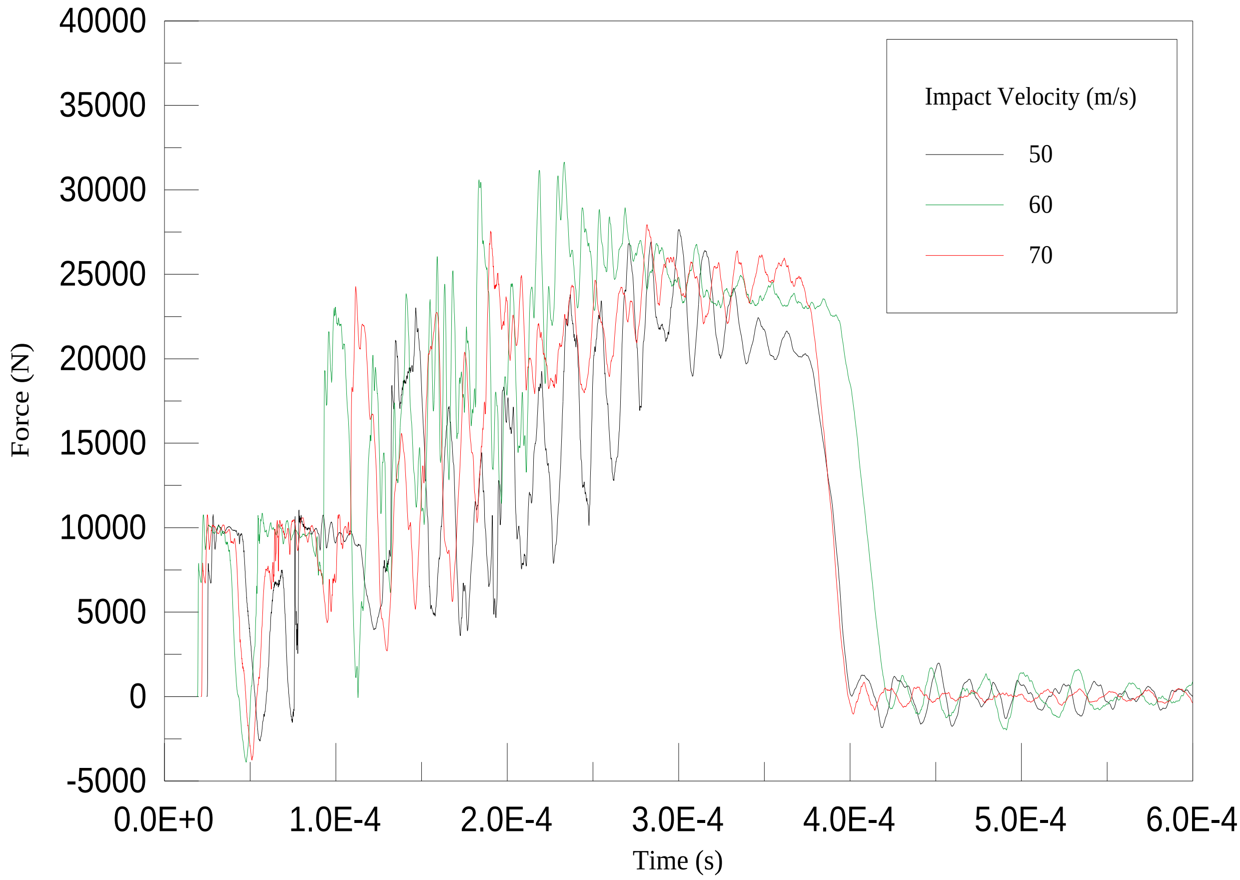

Figure 3.14 : Force versus time for sample 1.

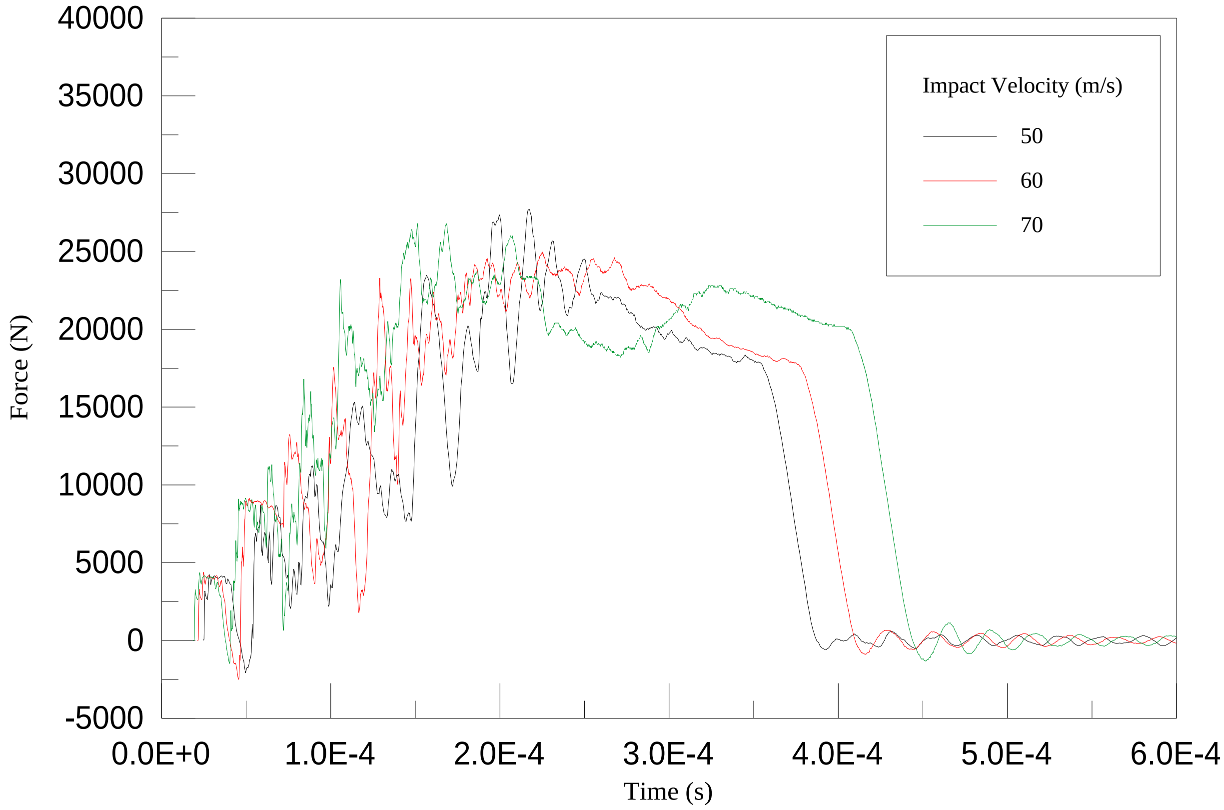

Figure 3.15 : Force versus time for sample 2.

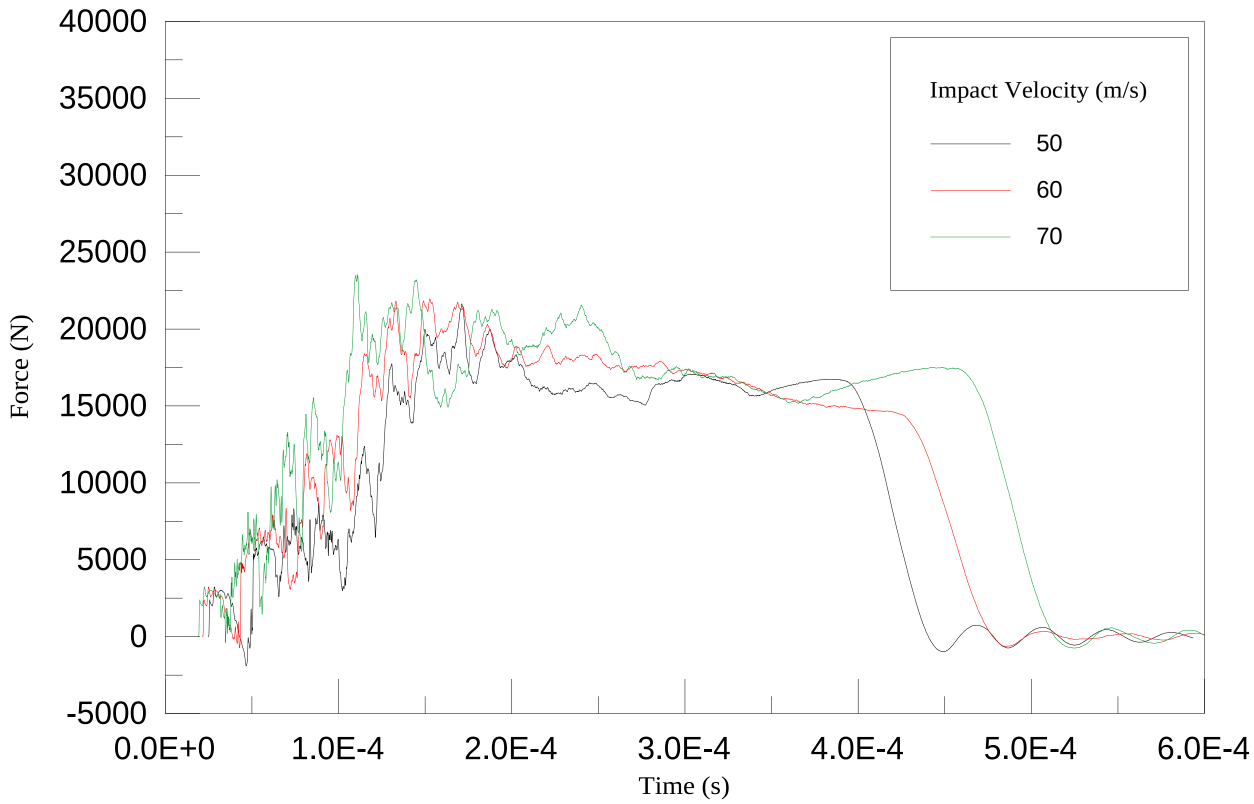

Figure 3.16 : Force versus time for sample 3.

3

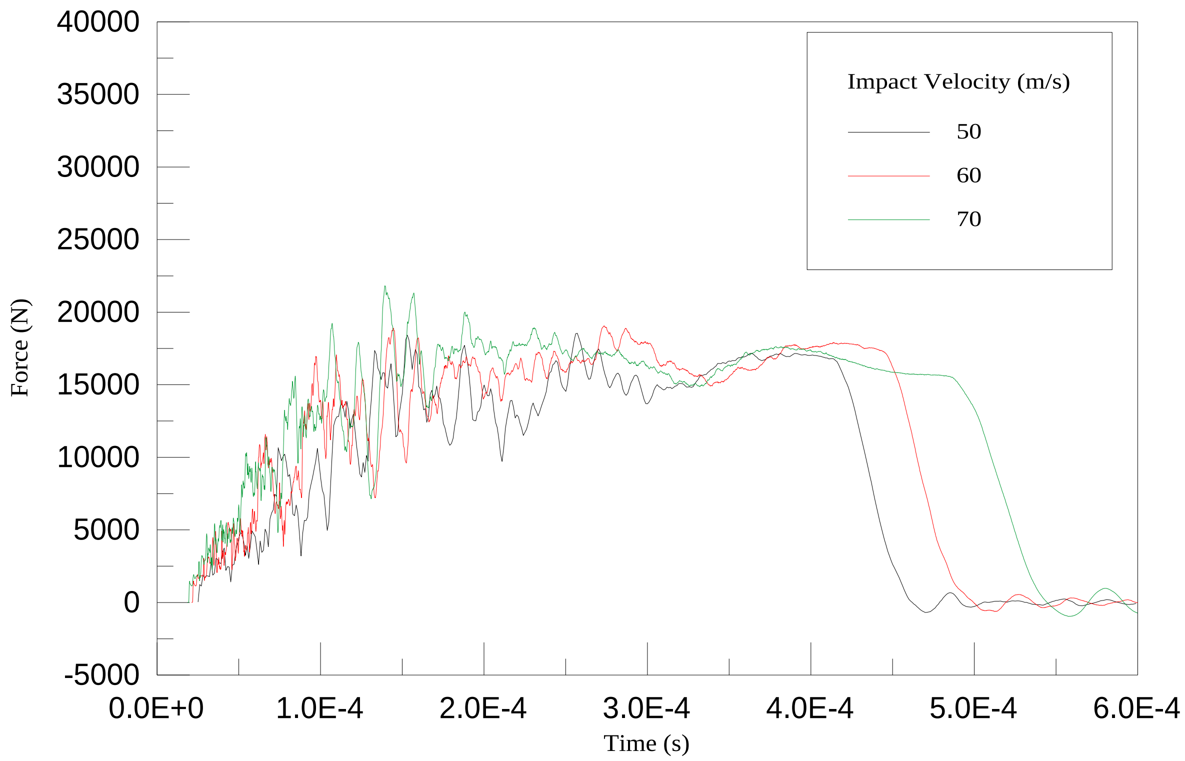

Figure 3.17 : Force versus time for sample 4.

3.3.2 Velocity effects on internal energy and amount of deformation

Naturally, the amount of internal energy increases at higher velocity. For sample 1, internal energy amounts are 120, 168 and 230 J in Fig 3.18, respectively. Besides, total deflections are 10.5749, 12.3167 and 15.0346 mm in Fig. 3.19.

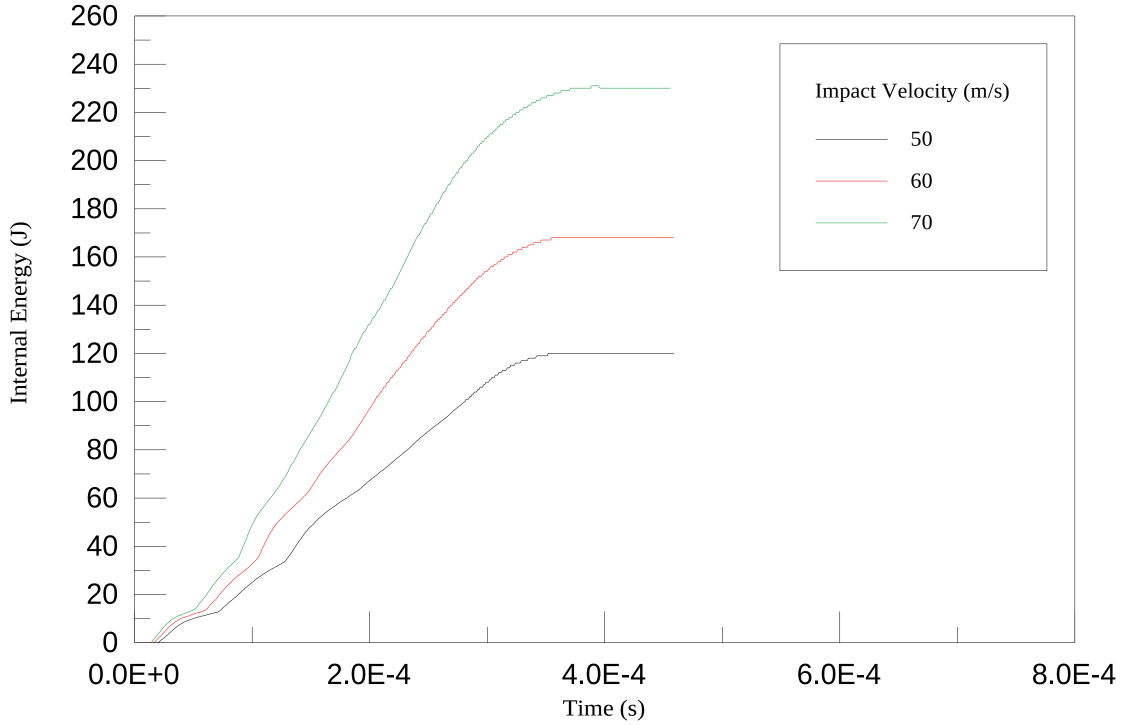

Figure 3.18 : Internal energy vs. time at different velocities for sample 1.

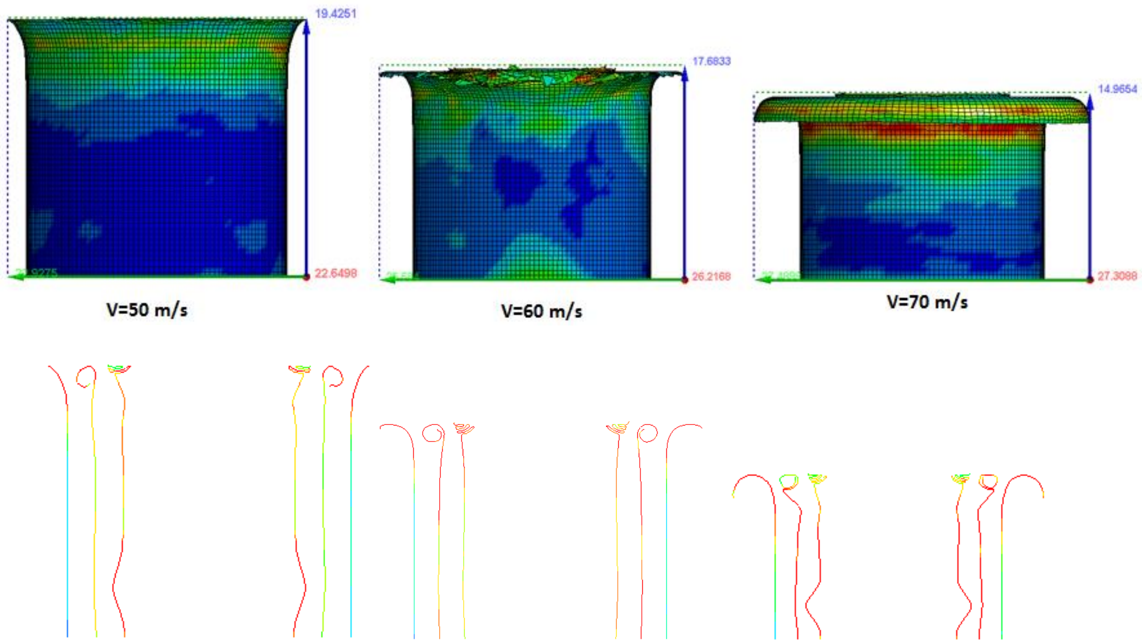

Figure 3.19 : Von Mises stress distribution and final lengths of sample 1.

For sample 2, internal energy amounts are 118, 171 and 279 J in Fig. 3.20, respectively. Besides, total deflections are 11.6, 12.4 and 15.1 mm in Fig. 3.21.

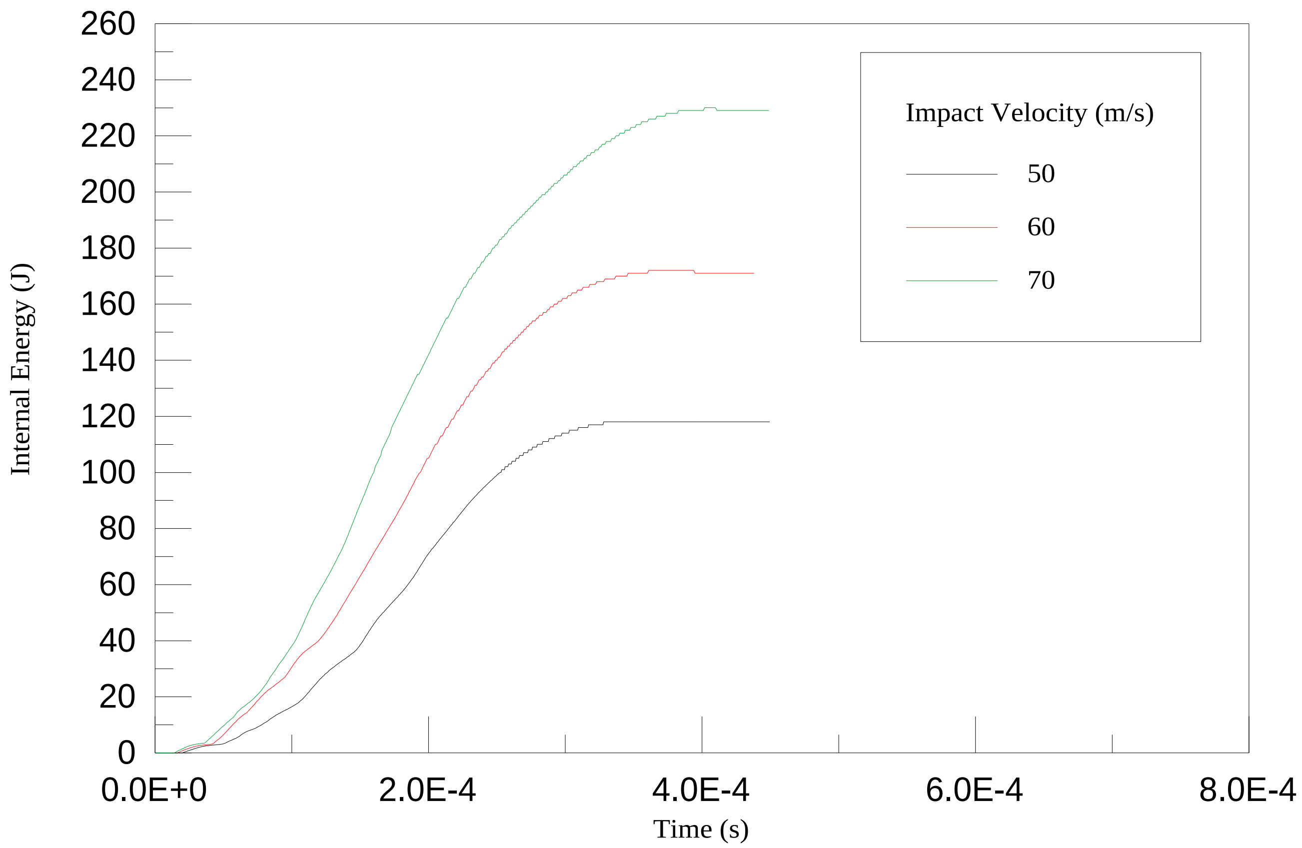

Figure 3.20 : Internal energy vs. time at different velocities for sample 2.

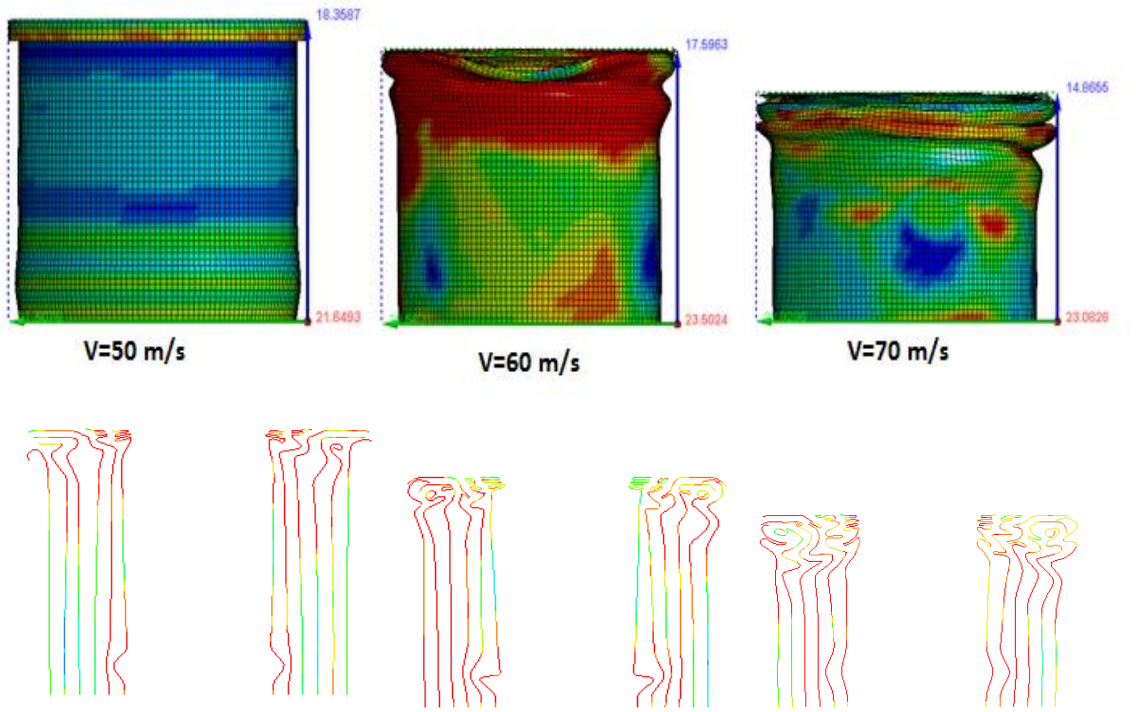

Figure 3.21 : Von Mises stress distribution and final lengths of sample 2.

For sample 3, internal energy amounts are 116, 168 and 226 J in Fig. 3.22, respectively. Besides, total deflections are 10.7, 13.0 and 16.4 mm in Fig. 3.23.

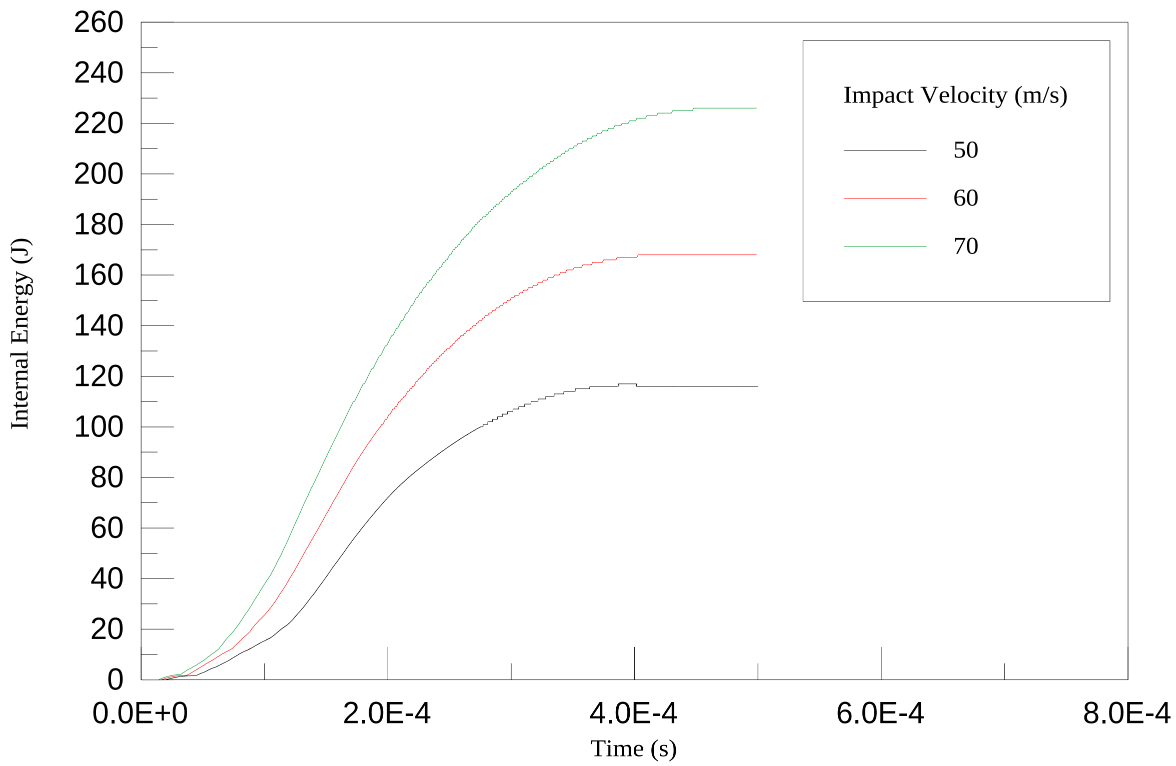

Figure 3.22 : Internal Energy vs. time at different velocities for sample 3.

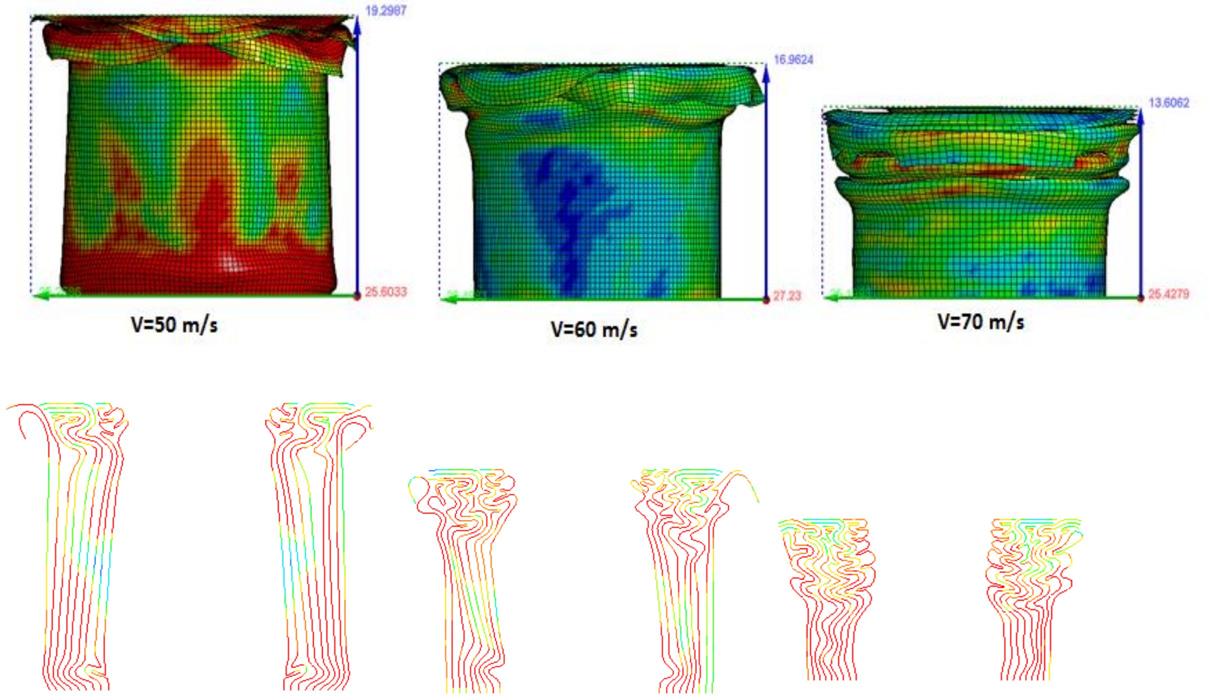

Figure 3.23 : Von Mises stress distribution and final lengths of sample 3.

For sample 4, internal energy amounts are 115, 163 and 224 J in Fig. 3.24, respectively. Besides, total deflections are 11.2054, 14.1296 and 17.4430 mm in Fig. 3.25.

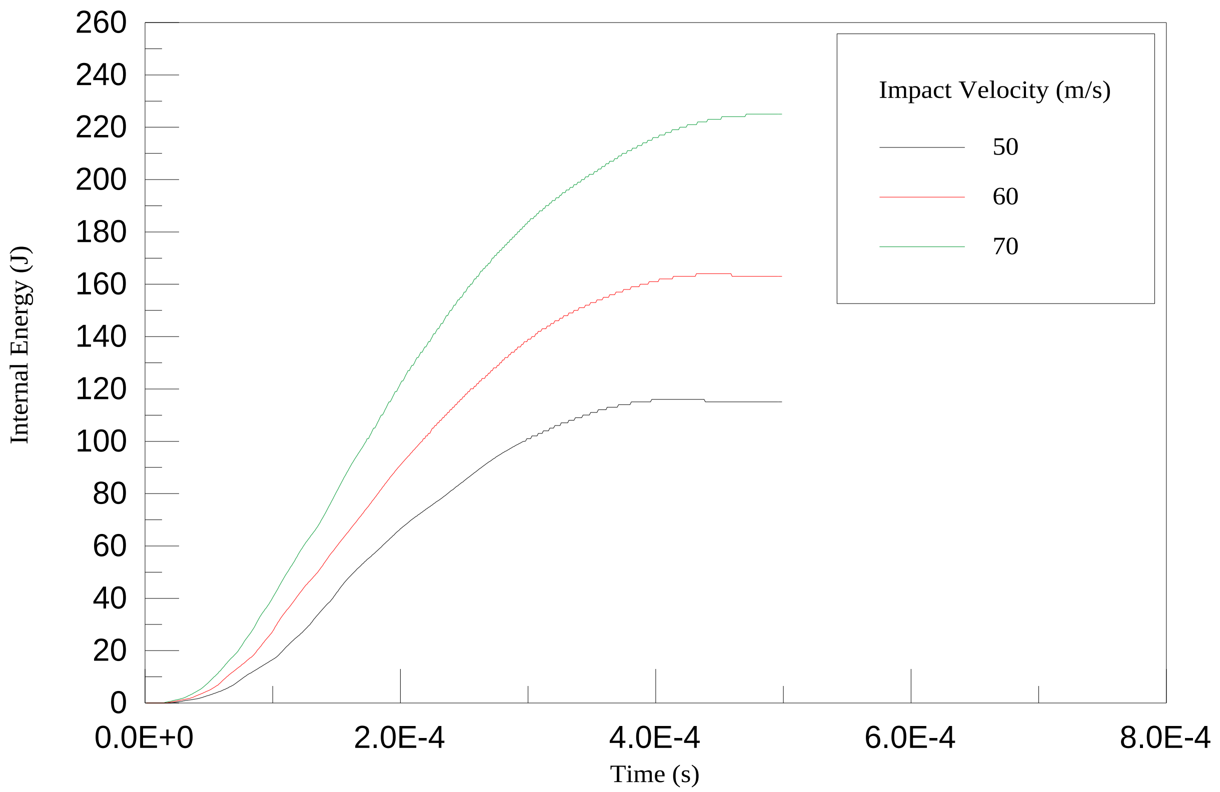

Figure 3.24 : Internal Energy vs. time at different velocities for Sample 4.

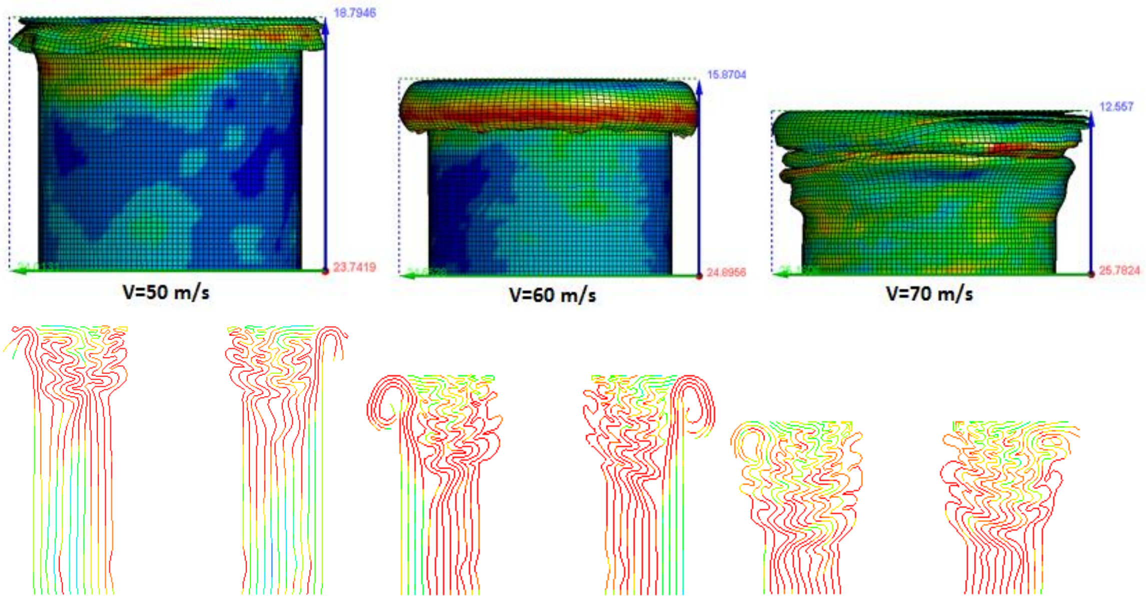

Figure 3.25 : Von Misses stress distribution and final lengths of sample 4.

3.4 Comparison of Foam Filled and Empty Crash Tubes

3.4.1 FEM of foam material in LS DYNA

Material of foam is selected as Aluminum. Stress-strain curve is shown in Fig. 3.26. Young modulus of aluminum foam is equal to 64.8 GPa and density is equal to 270 kg/m^3. Foam material has too low density. Also, its poison ratio is too low which is equal to 0.011 [20]. Therefore, under axially impact loads, longitudinal deformation of tubes is higher than its lateral deformation. Material properities in LS DYNA is defined with 063 CRUSHABLE FOAM under MAT toolbar.

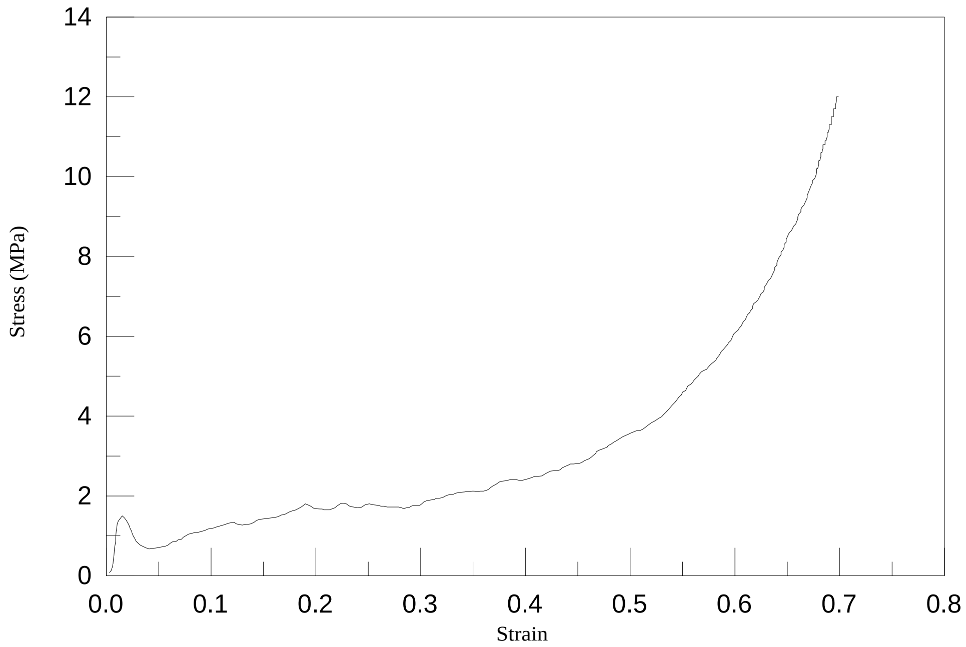

Figure 3.26 : Stress vs. strain curve of foam material made of aluminum.

3.4.2 Analyses and comparison of foam filled tubes with empty tubes

In Fig. 3.27, view of four models with foam material are shown before and after crashing. Results of these analysis are compared with results of empty tubes' analysis. "Force vs. Time" and "Internal Energy vs. Time" curves are drawn for each sample in Fig 3.28-3.35. According to these comparison, it is seen that peak forces of tubes with foam models are higher especially for 3rd peak forces.

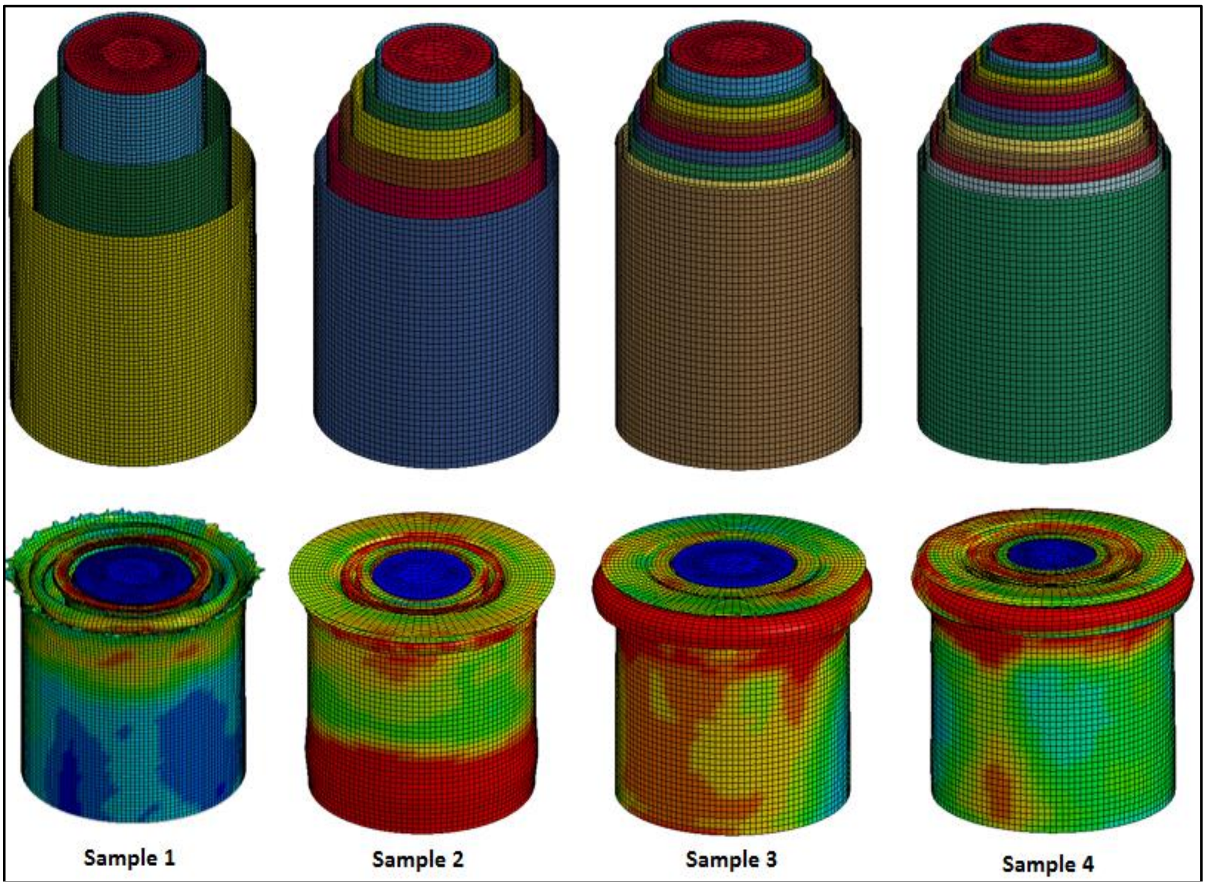

Figure 3.27 : FEM and von Mises stress distribution of foam filled tubes.

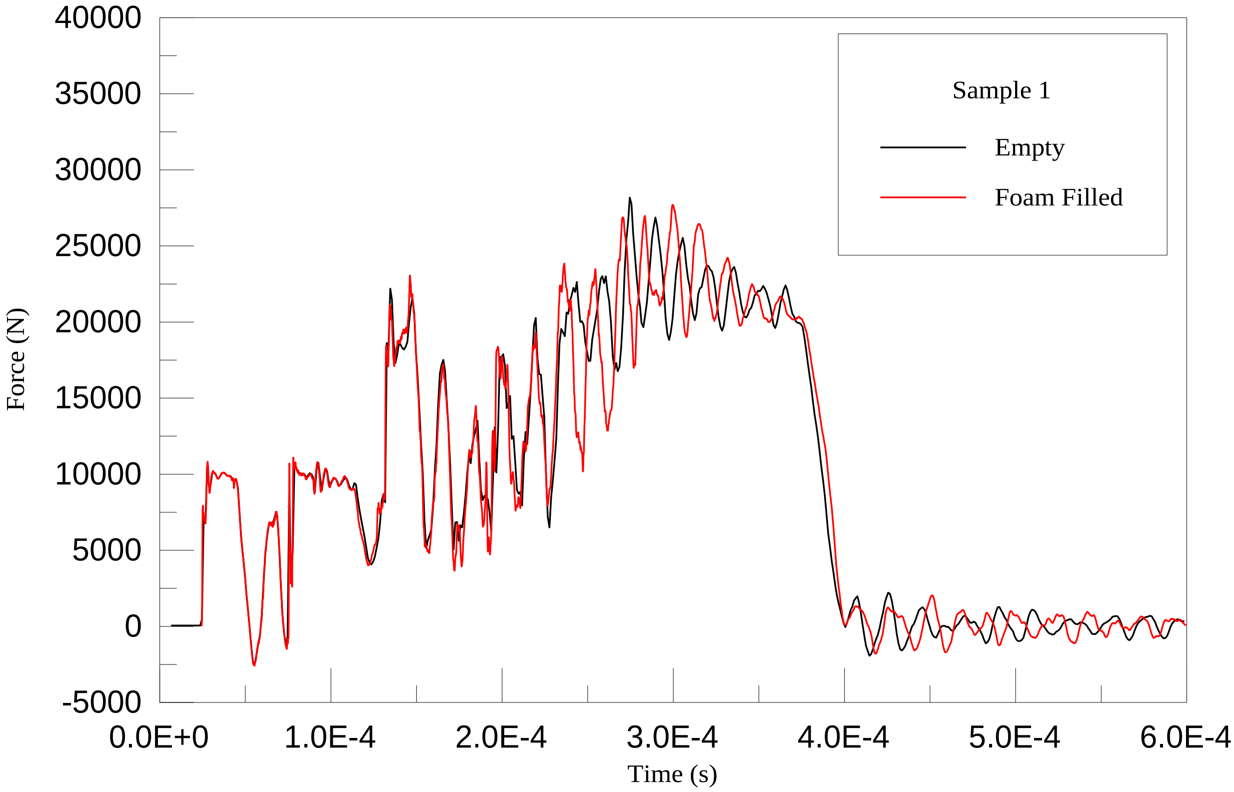

Figure 3.28 : Force vs. time curves of sample 1.

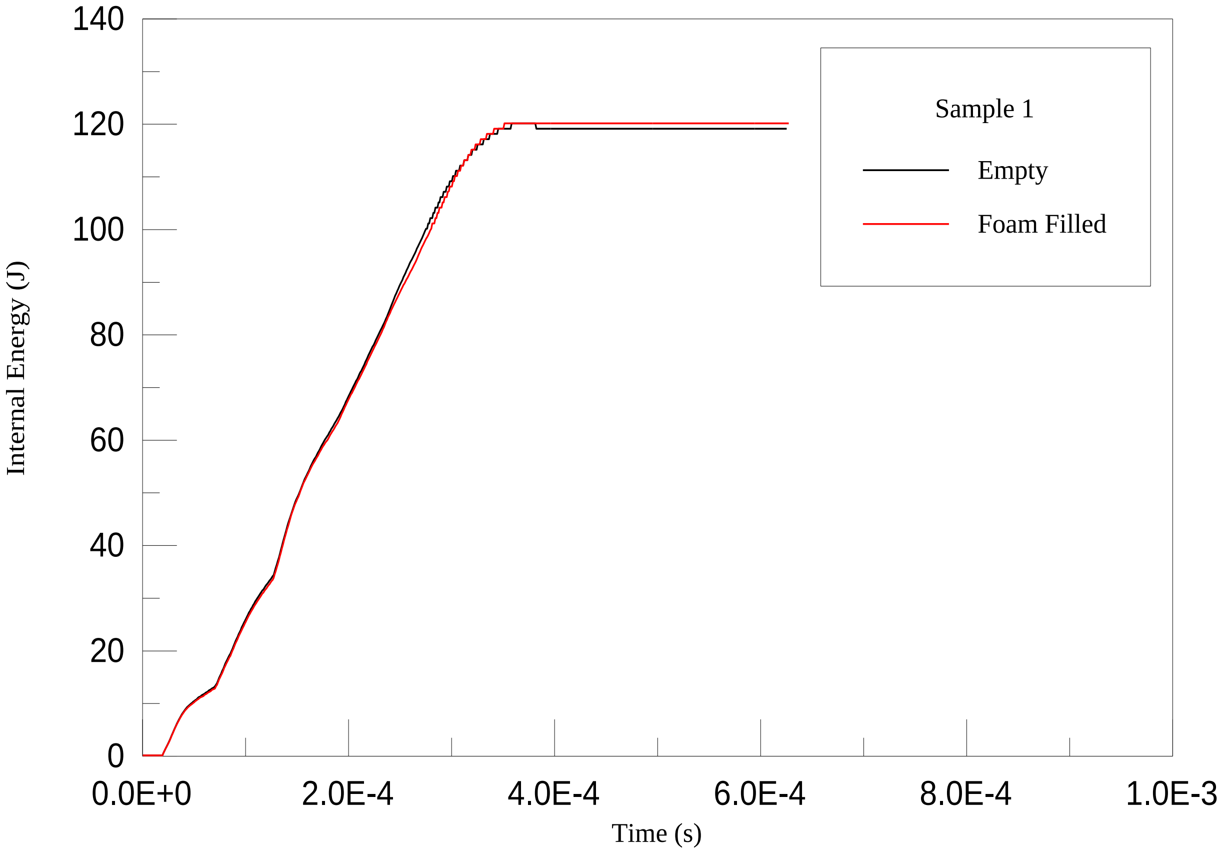

Figure 3.29 : Internal energy vs. time curves of sample 1.

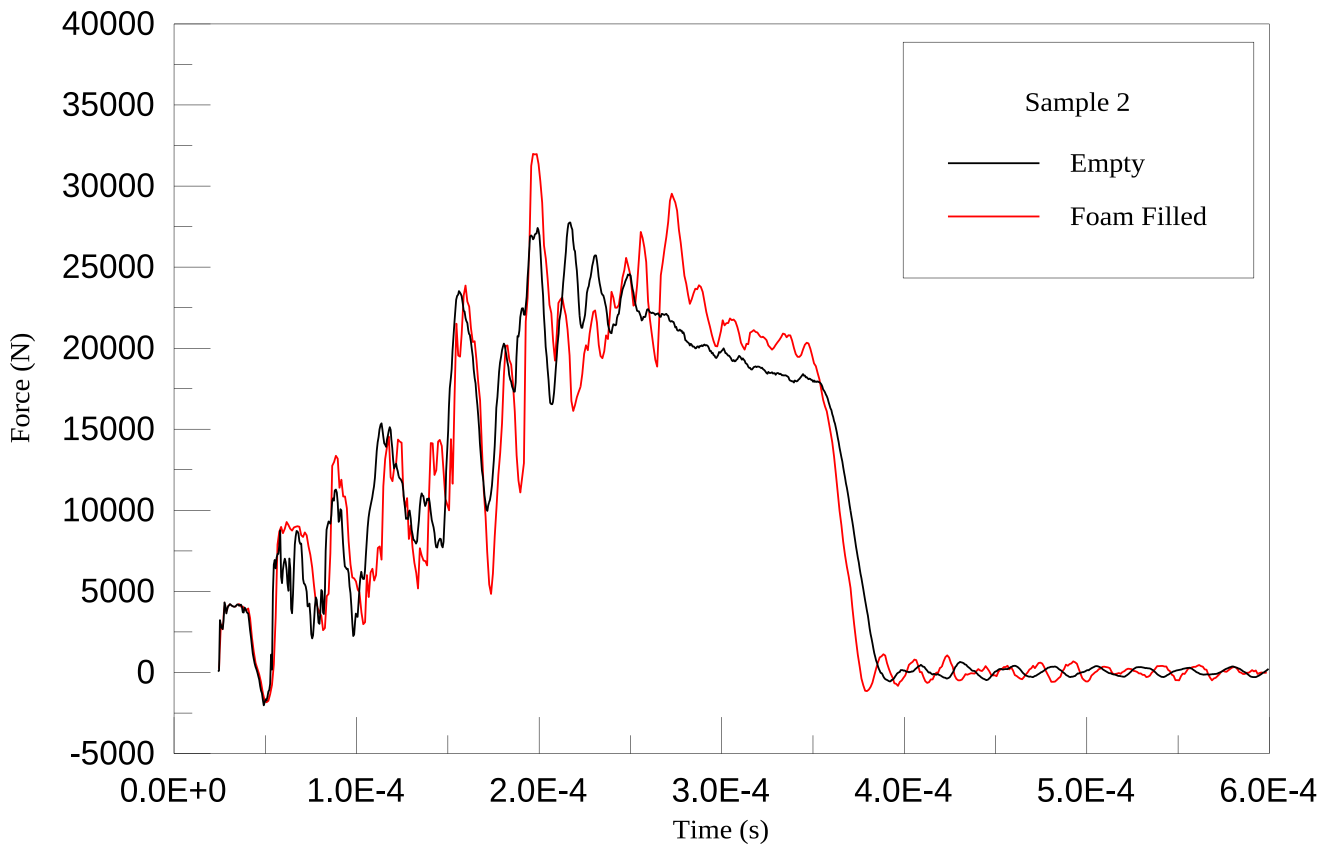

Figure 3.30 : Force vs. time curves of sample 2.

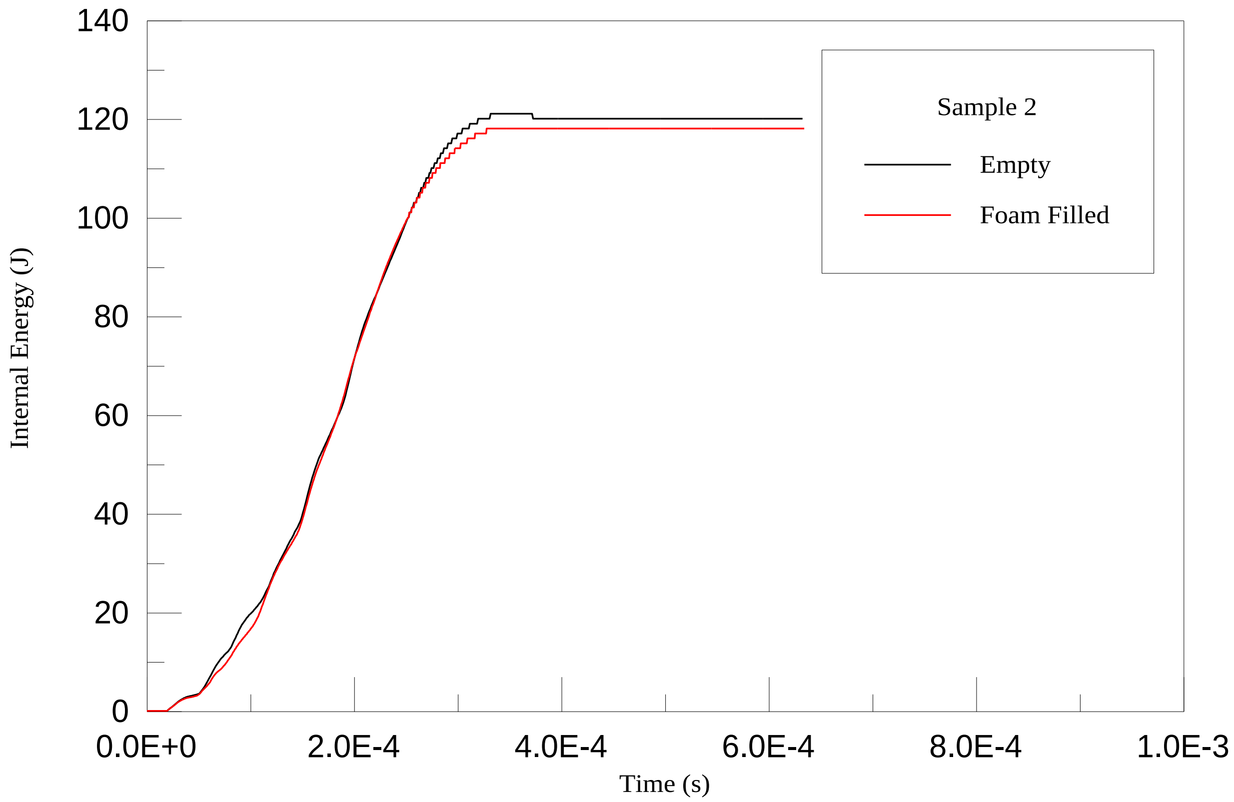

Figure 3.31 : Internal energy vs. time curves of sample 2.

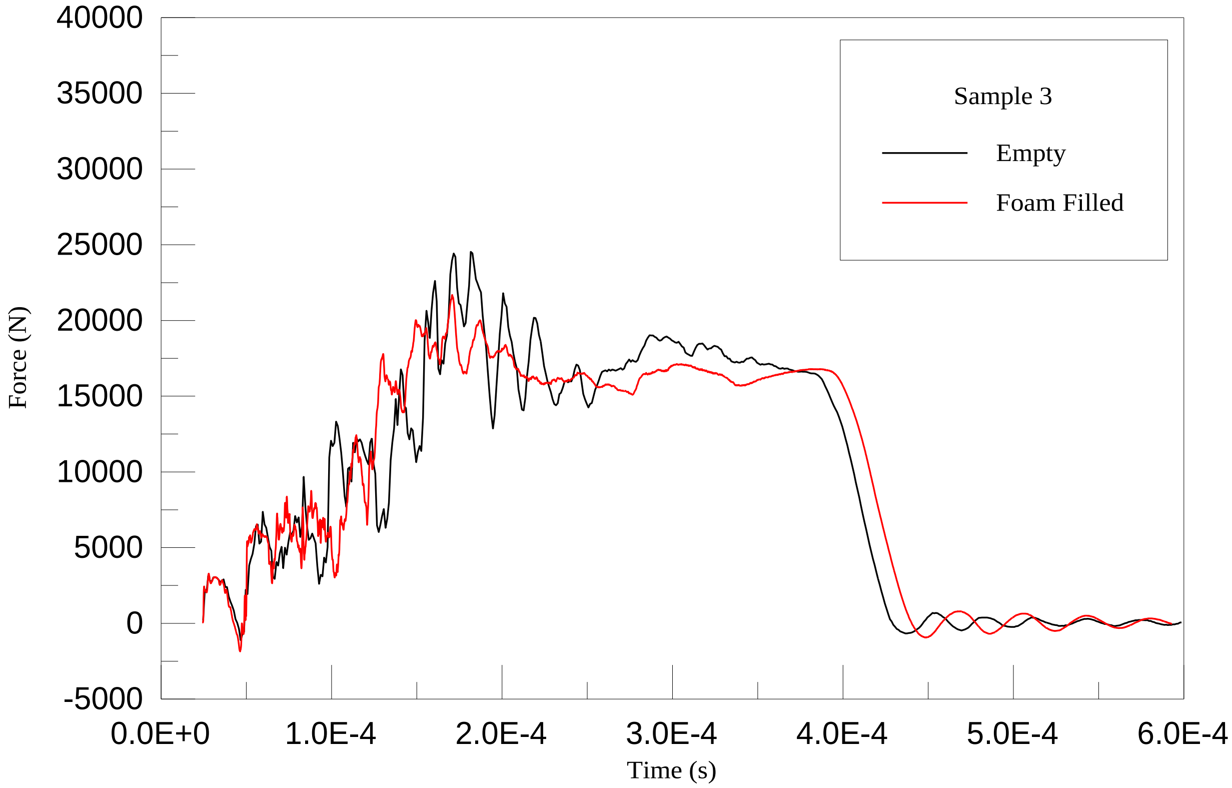

Figure 3.32 : Force vs. time curves of sample 3.

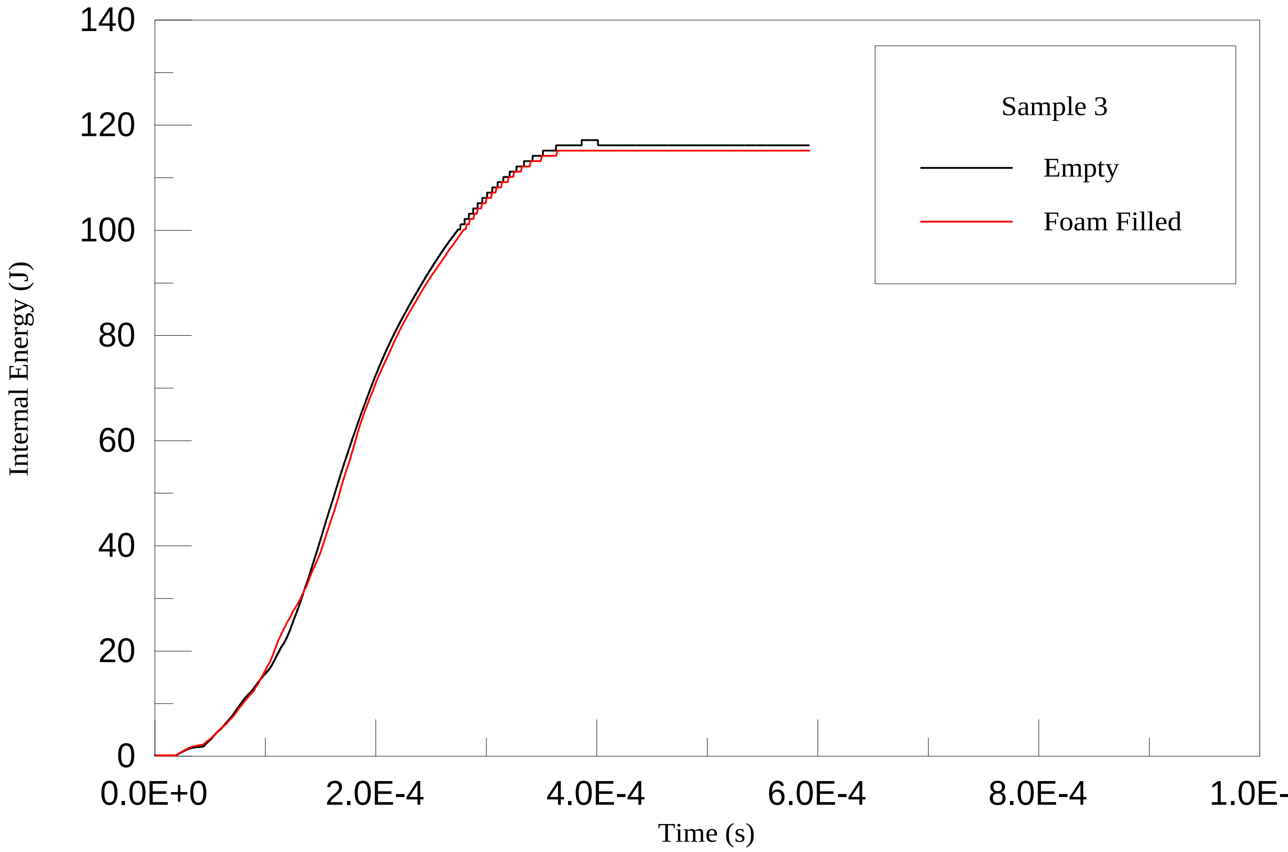

Figure 3.33 : Internal energy vs. time curves of sample 3.

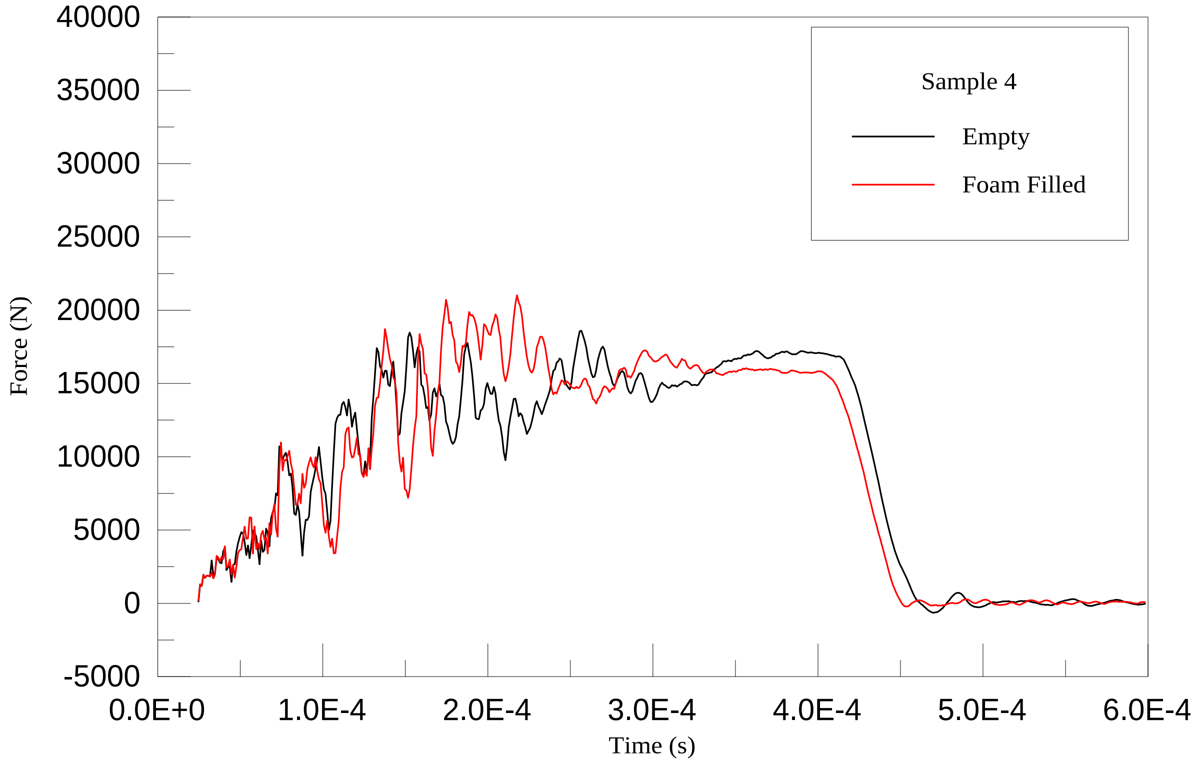

Figure 3.34 : Force vs. time curves of sample 4.

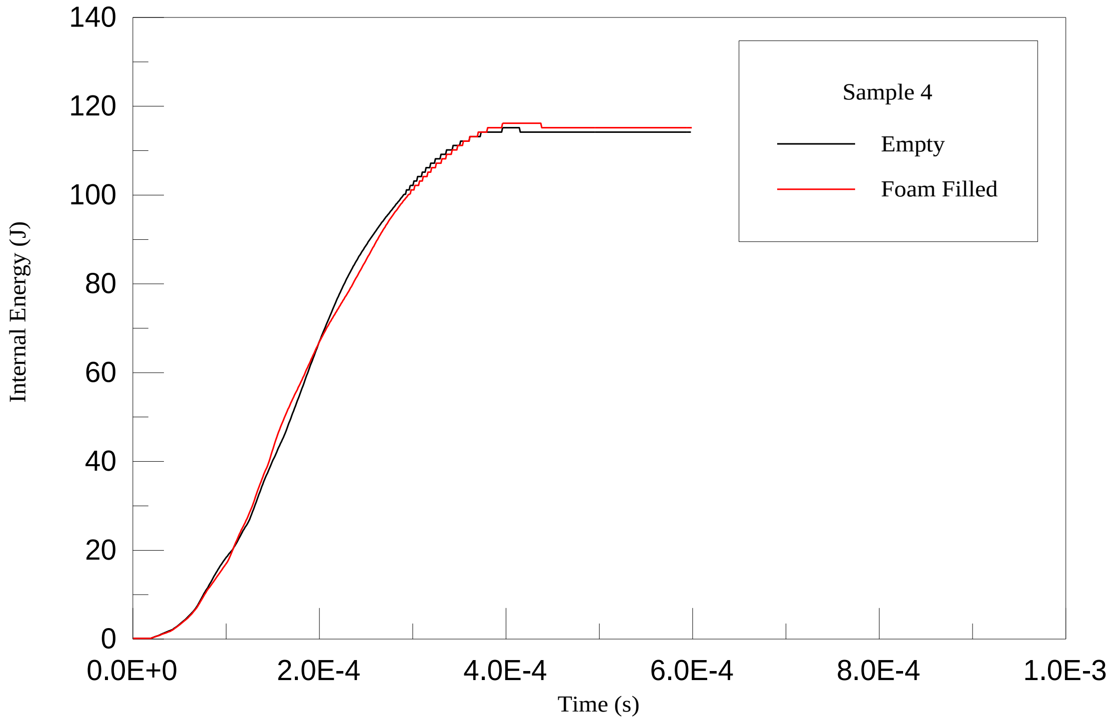

Figure 3.35 : Internal energy vs. time curves of sample 4.

4. CONCLUSION

In this thesis, stepped concentric crash tubes made of aluminum alloy are analyzed under axial loads and investigated the effect of the number of tubes in LS DYNA software program. Total mass and volume of all samples are restricted to observe efficiency of crashworthiness properties such as peak crushing force and energy absorption capability.

As the number of concentric tubes is increased, it is observed a smooth transition of the peak forces during the impact. Beside this, increasing the number of tubes results in reducing the maximum peak force. Also, it brings about a reduction of the initial peak force due to lower wall thickness of the tubes. It can reduce the inertial effects because of peak forces on vehicles and people. These results show that increasing the number of stepped concentric tubes improves crashworthiness properties in terms of peak forces. Furthermore, minimizing the size of concentric tubes can prevent or reduce the probability of penetration of impact objects. Analyzing models at different impact velocities gives similar results. In addition to these, crash tubes with aluminum foam have higher the peak forces in comparison with empty tubes.

4.1 Future Works

There might be implemented three future works. First study is comparison of the solution time at quasi-static speed by using LS-DYNA and ADINA. Second one is an experimental study on foam filled crash tubes and validation of experimental results by using numerical methods. Final future work is considered as an experimental study on small-sized crash tubes in sandwich plates as an energy absorber.

REFERENCES

[1] **World Health Organisation** (2013). WHO global status report on road safety 2013: supporting a decade of action.

[2] **Yamashita, M., Gotoh M., and Sawairi Y.** (2003). Axial crush of hollow cylindrical structures with various polygonal cross-sections: Numerical simulation and experiment. Journal of Materials Processing Technology. **140**(1): p. 59-64.

[3] **Palanivelu, S., Paepegem, W. V., Degrieck, J., Vantomme, J., Kakogiannis.,** et al. (2011). Crushing and energy absorption performance of different geometrical shapes of small-scale glass/polyester composite tubes under quasi-static loading conditions. Composite Structures, **93**(2): p. 992-1007.

[4] **Abramowicz, W. and Jones, N.** (1986). Dynamic progressive buckling of circular and square tubes. International Journal of Impact Engineering, **4**(4): p. 243-270.

[5] **Abramowicz, W. and Jones, N.** (1997). Transition from initial global bending to progressive buckling of tubes loaded statically and dynamically. International Journal of Impact Engineering, **19**(5): p. 415-437.

[6] **Salehghaffari, S., Rais-Rohani, M. and Najafi, A.** (2011). Analysis and optimization of externally stiffened crush tubes. Thin-walled structures, **49**(3): p. 397-408.

[7] **Karagiozova, D. and Jones, N.** (2001). Dynamic effects on buckling and energy absorption of cylindrical shells under axial impact. Thin-Walled Structures, **39**(7): p. 583-610.

[8] **Jensen, Ø., Hopperstad, O. and Langseth, M.** (2005). Transition from progressive to global buckling of aluminium extrusions–a numerical study. International Journal of Crashworthiness, 2005. **10**(6): p. 609-620.

[9] **Fyllingen, Ø., Hopperstad, O. S., Hanssen A. G. and Langseth M.** (2010). Modelling of tubes subjected to axial crushing. Thin-walled structures, **48**(2): p. 134-142.

[10] **Kazancı, Z. and Bathe, K. J.** (2012). Crushing and crashing of tubes with implicit time integration. International Journal of Impact Engineering, 2012. **42**: p. 80-88.

[11] **Karagiozova, D., Alves, M. and Jones, N.** (2000). Inertia effects in axisymmetrically deformed cylindrical shells under axial impact. International Journal of Impact Engineering, **24**(10): p. 1083-1115.

[12] **Ince, F., Türkmen, H.S., Mecitoglu, Z., Uludag, N., Durgun, I., Altınok, E.,** et al. (2011). A numerical and experimental study on the impact behavior of box structures. Procedia Engineering, **10**: p. 1736-1741.

[13] **Mamalis, A., Manolakos, D. E., Demosthenous, G. A. and Ioannidis M. B.** (1996). Analysis of failure mechanisms observed in axial collapse of thin-walled circular fibreglass composite tubes. Thin-Walled Structures, **24**(4): p. 335-352.

[14] **Langseth, M., Hopperstad, O. and Berstad, T.** (1999). Crashworthiness of aluminium extrusions: validation of numerical simulation, effect of mass ratio and impact velocity. International Journal of Impact Engineering, **22**(9): p. 829-854.

[15] **Kim, H. S.** (2002). New extruded multi-cell aluminum profile for maximum crash energy absorption and weight efficiency. Thin-Walled Structures, **40**(4): p. 311-327.

[16] **Aktay, L., Kröplin, B. H., Toksoy, A. K. and Güden, M.** (2008). Finite element and coupled finite element/smooth particle hydrodynamics modeling of the quasi-static crushing of empty and foam-filled single, bitubular and constraint hexagonal-and square-packed aluminum tubes. Materials & design, 2008. **29**(5): p. 952-962.

[17] **Olabi, A. G., Morris, E. and Hashmi, M.** (2007). Metallic tube type energy absorbers: a synopsis. Thin-walled structures, **45**(7): p. 706-726.

[18] **Url-1** <*http://me.mam.tubitak.gov.tr/tr/laboratuvarlar/darbe-test-laboratuvari*>, date retrieved 29.04.2015.

[19] **Fang, J., Gao, Y., Sun, G., Zhang, Y. and Li, Q.** (2014). Parametric analysis and multiobjective optimization for functionally graded foam-filled thin-wall tube under lateral impact. Computational Materials Science, **90**: p. 265-275.

[20] **Bi, J., Fang, H., Wang, Q. and Ren, X.** (2010). Modeling and optimization of foam-filled thin-walled columns for crashworthiness designs. Finite Elements in Analysis and Design, **46**(9): p. 698-709.

[21] **Reid, S.** (1993). Plastic deformation mechanisms in axially compressed metal tubes used as impact energy absorbers. International Journal of Mechanical Sciences, 1993. **35**(12): p. 1035-1052.

[22] **Miyazaki, M., Endo, H. and Negishi. H.** (1999). Dynamic axial plastic buckling of square tube. Journal of Materials Processing Technology, **85**(1): p. 213-216.

[23] **Mamalis, A., Manolakos, D. and Viegelahn. G.** (1989). The axial crushing of thin PVC tubes and frusta of square cross-section. International Journal of Impact Engineering, **8**(3): p. 241-264.

[24] **Markiewicz, E., Ducrocq, P. and Drazetic, P.** (1998). An inverse approach to determine the constitutive model parameters from axial crushing of thin-walled square tubes. International Journal of Impact Engineering

[25] **Hanssen, A., Hopperstad, O. and Langseth, M.** (2000). Bending of square aluminium extrusions with aluminium foam filler. Acta Mechanica, **142**(1-4): p. 13-31.

[26] **Jimenez, M., Miravete, A., Larrode, E. and Revuelta, D.** (2000). Effect of trigger geometry on energy absorption in composite profiles. Composite Structures, **48**(1): p. 107-111.

[27] **Chen, W. and Nardhi, D.** (2000). Experimental study of crush behaviour of sheet aluminium foam-filled sections. International Journal of Crashworthiness, **5**(4): p. 447-468.

[28] **Hanssen, A.G., Langseth, M. and Hopperstad, O.S.** (2000). Static and dynamic crushing of square aluminium extrusions with aluminium foam filler. International Journal of Impact Engineering, **24**(4): p. 347-383.

[29] **Chen, W.** (2001). Experimental and numerical study on bending collapse of aluminum foam-filled hat profiles. International Journal of Solids and Structures, **38**(44): p. 7919-7944.

[30] **Huh, H. and Kang, W.** (2002). Crash-worthiness assessment of thin-walled structures with the high-strength steel sheet. International journal of vehicle design, **30**(1): p. 1-21.

[31] **Chiandussi, G. and Avalle, M.** (2002). Maximisation of the crushing performance of a tubular device by shape optimisation. Computers & structures, **80**(27): p. 2425-2432.

[32] **Kim, H. S., Chen, W. and Wierzbicki, T.** (2002). Weight and crash optimization of foam-filled three-dimensional “S” frame. Computational mechanics, **28**(5): p. 417-424.

[33] **Mamalis, A., Manolakos, D. E., Ioannidis, M. B. and Papapostolou D. P.** (2004). Crashworthy characteristics of axially statically compressed thin-walled square CFRP composite tubes: experimental. Composite Structures, **63**(3): p. 347-360.

[34] **Karagiozova, D. and Jones, N.** (2004). Dynamic buckling of elastic–plastic square tubes under axial impact—II: structural response. International Journal of Impact Engineering, **30**(2): p. 167-192.

[35] **Børvik, T., Hopperstad, O. S., Reyes, A., Langseth, M., Solomosb, G.,** et al. (2003). Empty and foam-filled circular aluminium tubes subjected to axial and oblique quasistatic loading. International journal of crashworthiness, **8**(5): p. 481-494.

[36] **Reyes, A., Langseth, M. and Hopperstad, O.** (2003). Square aluminum tubes subjected to oblique loading. International Journal of Impact Engineering, **28**(10): p. 1077-1106.

[37] **Schneider, F. and Jones, N.** (2004). Impact of thin-walled high-strength steel structural sections. Proceedings of the Institution of Mechanical Engineers, Part D: Journal of Automobile Engineering, **218**(2): p. 131-158.

[38] **Jensen, Ø., Langseth, M. and Hopperstad, O.** (2004). Experimental investigations on the behaviour of short to long square aluminium tubes subjected to axial loading. International Journal of Impact Engineering, **30**(8): p. 973-1003.

[39] **Mamalis, A., Manolakos, D. E., Ioannidis, M. B. and Papapostolou D. P.** (2005). On the response of thin-walled CFRP composite tubular components subjected to static and dynamic axial compressive loading: experimental. Composite structures, **69**(4): p. 407-420.

[40] **Reyes, A., Hopperstad, O. and Langseth, M.** (2004). Aluminum foam-filled extrusions subjected to oblique loading: experimental and numerical study. International journal of solids and structures, **41**(5): p. 1645-1675.

[41] **Nagel, G. M. and Thambiratnam, D. P.** (2006). Dynamic simulation and energy absorption of tapered thin-walled tubes under oblique impact loading. International Journal of Impact Engineering, **32**(10): p. 1595-1620.

[42] **Alkateb, M., Mahdi E., Hamouda A. M. S. and Hamdan M. M.** (2004). On the energy absorption capability of axially crushed composite elliptical cones. Composite structures, **66**(1): p. 495-501.

[43] **Meguid, S., Stranart, J. and Heyerman, J.** (2004). On the layered micromechanical three-dimensional finite element modelling of foam-filled columns. Finite elements in analysis and design, **40**(9): p. 1035-1057.

[44] **Hörmann, M. and Wacker. M.** (2005). Simulation of the crash performance of crash boxes based on advanced thermoplastic composite. in Proceedings of the 5th European LS-DYNA Users Conference.

[45] **Nagel, G. and Thambiratnam, D.** (2005). Computer simulation and energy absorption of tapered thin-walled rectangular tubes. Thin-Walled Structures, **43**(8): p. 1225-1242.

[46] **Mahdi, E., Hamouda, A. S. M., Mokhtar, A. S. and Majid, D. L**. (2005). Many aspects to improve damage tolerance of collapsible composite energy absorber devices. Composite structures, **67**(2): p. 175-187.

[47] **Song, H. W., Fan, Z. J., Yu, G., Wang Q. J. and Tobota, A.** (2005). Partition energy absorption of axially crushed aluminum foam-filled hat sections. International Journal of Solids and Structures, **42**(9): p. 2575-2600.

[48] **Toksoy, A. and Güden, M.** (2005). The strengthening effect of polystyrene foam filling in aluminum thin-walled cylindrical tubes. Thin-walled structures, **43**(2): p. 333-350.

[49] **DiPaolo, B. and Tom, J.** (2006). A study on an axial crush configuration response of thin-wall, steel box components: The quasi-static experiments. International journal of solids and structures, **43**(25): p. 7752-7775.

[50] **Qiao, J., Chen, J. and Che, H.** (2006). Crashworthiness assessment of square aluminum extrusions considering the damage evolution. Thin-walled structures, **44**(6): p. 692-700.

[51] **Durrenberger, L., Even, D., Molinari, A. and Rusinek, A.** (2006). Influence of the strain path on crash properties of a crash-box structure by experimental and numerical approaches. in Journal de Physique IV (Proceedings). EDP sciences.

[52] **Güden, M. and Kavi, H.** (2006). Quasi-static axial compression behavior of constraint hexagonal and square-packed empty and aluminum foam-

filled aluminum multi-tubes. Thin-walled structures, 2006. **44**(7): p. 739-750.

[53] **Aktay, L., Toksoy, A. and Güden, M.** (2006). Quasi-static axial crushing of extruded polystyrene foam-filled thin-walled aluminum tubes: experimental and numerical analysis. Materials & design, **27**(7): p. 556-565.

[54] **Zhang, X., Cheng, G. and Zhang, H.** (2006). Theoretical prediction and numerical simulation of multi-cell square thin-walled structures. Thin-Walled Structures, **44**(11): p. 1185-1191.

[55] **Shakeri, M., Salehghaffari, S. and Mirzaeifar, R.** (2007). Expansion of circular tubes by rigid tubes as impact energy absorbers: experimental and theoretical investigation. International Journal of Crashworthiness, **12**(5): p. 493-501.

[56] **Zarei, H., Kröger, M. and Albertsen, H.** (2008). An experimental and numerical crashworthiness investigation of thermoplastic composite crash boxes. Composite structures, **85**(3): p. 245-257.

[57] **Liu, Y. and Day, M. (**2007). Development of simplified finite element models for straight thin-walled tubes with octagonal cross section. International Journal of Crashworthiness, **12**(5): p. 503-508.

[58] **Guden, M., Yuksel, S., Taşdemirci, A. and Tanoğlu, M.** (2007). Effect of aluminum closed-cell foam filling on the quasi-static axial crush performance of glass fiber reinforced polyester composite and aluminum/composite hybrid tubes. Composite structures, **81**(4): p. 480-490.

[59] **Zhang, X., Chenga, G.,Youb, Z. and Zhanga, H.** (2007). Energy absorption of axially compressed thin-walled square tubes with patterns. Thin-Walled Structures, **45**(9): p. 737-746.

[60] **Hou, S., Li, Q., Long, S., Yanga, X. and Li, W.** (2008). Multiobjective optimization of multi-cell sections for the crashworthiness design. International Journal of Impact Engineering, **35**(11): p. 1355-1367.

[61] **Zarei, H. and Kröger, M.** (2008). Bending behavior of empty and foam-filled beams: Structural optimization. International Journal of Impact Engineering, **35**(6): p. 521-529.

[62] **Rusinek, A., Zaera, R., Forquina, P. and Klepaczko, J. R.** (2008). Effect of plastic deformation and boundary conditions combined with elastic wave propagation on the collapse site of a crash box. Thin-Walled Structures, **46**(10): p. 1143-1163.

[63] **Zarei, H. and Kröger, M.** (2008). Optimization of the foam-filled aluminum tubes for crush box application. Thin-Walled Structures, **46**(2): p. 214-221.

[64] **Sheriff, N. M., Gupta, N. K., Velmurugan, R. and Shanmugapriyan, N.** (2008). Optimization of thin conical frusta for impact energy absorption. Thin-Walled Structures, **46**(6): p. 653-666.

[65] **Zhang, X., Cheng, G., Wang, B. and Zhang, H.** (2008). Optimum design for energy absorption of bitubal hexagonal columns with honeycomb core. International Journal of Crashworthiness, **13**(1): p. 99-107.

[66] **Zarei, H. and Kröger, M.** (2008). Optimum honeycomb filled crash absorber design. Materials & Design, **29**(1): p. 193-204.

[67] **Mirfendereski, L., Salimi, M. and Ziaei-Rad, S.** (2008). Parametric study and numerical analysis of empty and foam-filled thin-walled tubes under static and dynamic loadings. International Journal of Mechanical Sciences, **50**(6): p. 1042-1057.

[68] **Peroni, L., Avalle, M. and Belingardi, G.** (2009). Comparison of the energy absorption capability of crash boxes assembled by spot-weld and continuous joining techniques. International journal of impact engineering, **36**(3): p. 498-511.

[69] **Hou, S., Li, Q., Long, S., Yang, X. and Li, W.** (2009). Crashworthiness design for foam filled thin-wall structures. Materials & design, **30**(6): p. 2024-2032.

[70] **Zhang, X. and Huh, H.** (2009). Energy absorption of longitudinally grooved square tubes under axial compression. Thin-Walled Structures, **47**(12): p. 1469-1477.

[71] **Ghasemnejad, H., Blackman, B. R. K., Hadavinia, H. and Sudall. B.** (2009). Experimental studies on fracture characterisation and energy absorption of GFRP composite box structures. Composite structures, **88**(2): p. 253-261.

[72] **Nia, A. A. and Hamedani, J. H.** (2010). Comparative analysis of energy absorption and deformations of thin walled tubes with various section geometries. Thin-Walled Structures, **48**(12): p. 946-954.

[73] **Kaya, N. and Ozturk, F.** (2010). Multi-objective crashworthiness design optimisation of thin-walled tubes. International journal of vehicle design, **52**(1): p. 54-63.

[74] **Guler, M. A., Cerit, M. E., Bayram, B., Gerceker, B. and Karakaya, E.** (2010). The effect of geometrical parameters on the energy absorption characteristics of thin-walled structures under axial impact loading. International Journal of Crashworthiness, **15**(4): p. 377-390.

[75] **Ahmad, Z., Thambiratnam, D. and Tan, A.** (2010). Dynamic energy absorption characteristics of foam-filled conical tubes under oblique impact loading. International Journal of Impact Engineering, 2010. **37**(5): p. 475-488.

[76] **Toksoy, A. and Güden, M.** (2010). Partial Al foam filling of commercial 1050H14 Al crash boxes: the effect of box column thickness and foam relative density on energy absorption. Thin-Walled Structures, **48**(7): p. 482-494.

[77] **Hou, S., Han, X., Sun, G., Long, S., Li, W. and Yang, X. and Li, Q.** (2011). Multiobjective optimization for tapered circular tubes. Thin-Walled Structures, **49**(7): p. 855-863.

[78] **Yin, H., Wen, G., Hou, S. and Chen, K.** (2011). Crushing analysis and multiobjective crashworthiness optimization of honeycomb-filled single and bitubular polygonal tubes. Materials & Design, **32**(8): p. 4449-4460.

[79] **Ghamarian, A. and Abadi, M. T.** (2011). Axial crushing analysis of end-capped circular tubes. Thin-Walled Structures, **49**(6): p. 743-752.

[80] **Durrenberger, L., Lemoine, X. and Molinari, A.** (2011). Effects of pre-strain and bake-hardening on the crash properties of a top-hat section. Journal of Materials Processing Technology, **211**(12): p. 1937-1947.

[81] **Ghamarian, A., Zarei, H. R. and Abadi, M. T.** (2011). Experimental and numerical crashworthiness investigation of empty and foam-filled end-capped conical tubes. Thin-Walled Structures, **49**(10): p. 1312-1319.

[82] **Toksoy, A. and Güden, M.** (2011). The optimisation of the energy absorption of partially Al foam-filled commercial 1050H14 and 6061T4 Al crash boxes. International Journal of Crashworthiness, **16**(1): p. 97-109.

[83] **Oshkovr, S., Eshkoor, R. A., Taher, S. T., Ariffin, A. K. and Azhari C. H**. (2012). Crashworthiness characteristics investigation of silk/epoxy composite square tubes. Composite Structures, **94**(8): p. 2337-2342.

[84] **Qureshi, O.M. and Bertocchi, E.** (2012). Crash behavior of thin-Walled box beams with complex sinusoidal relief patterns. Thin-Walled Structures, **53**: p. 217-223.

[85] **Tang, Z., Liu, S. and Zhang, Z.** (2012). Energy absorption properties of non-convex multi-corner thin-walled columns. Thin-Walled Structures, **51**: p. 112-120.

[86] **Boria, S. and Belingardi, G.** (2012). Numerical investigation of energy absorbers in composite materials for automotive applications. International Journal of Crashworthiness, **17**(4): p. 345-356.

[87] **Zhang, Y., Sun, G., Li, G., Luo, Z. and Li, Q.** (2012). Optimization of foam-filled bitubal structures for crashworthiness criteria. Materials & Design, **38**: p. 99-109.

[88] **Qureshi, O.M. and Bertocchi, E.** (2013). Crash performance of notch triggers and variable frequency progressive-triggers on patterned box beams during axial impacts. Thin-Walled Structures, **63**: p. 98-105.

[89] **Kim, H.C., Shin, D. K., Lee, J. J. and Kwon J. B.** (2014). Crashworthiness of aluminum/CFRP square hollow section beam under axial impact loading for crash box application. Composite Structures, **112**: p. 1-10.

[90] **Yamashita, M., Kenmotsu, H. and Hattori, T**. (2013). Dynamic crush behavior of adhesive-bonded aluminum tubular structure—Experiment and numerical simulation. Thin-Walled Structures, **69**: p. 45-53.

[91] **Ma, J.** (2011). Thin-walled tubes with pre-folded origami patterns as energy absorption devices, University of Oxford.

[92] **Kiani, M., Shiozaki, H. and Motoyama, K.** (2013). Using experimental data to improve crash modeling for composite materials, in Composite Materials and Joining Technologies for Composites, Volume 7. Springer. p. 215-226.

[93] **Marzbanrad, J. and Keshavarzi, A.** (2014). A Numerical and experimental study on the crash behavior of the extruded aluminum crash box with elastic support. Latin American Journal of Solids and Structures, **11**(8): p. 1329-1348.

[94] **Ahmad, M., Ismail, K. and Mat, F.** (2013). Convergence of Finite Element Model for Crushing of a Conical Thin-walled Tube. Procedia Engineering, **53**: p. 586-593.

[95] **Lee, S. J., Lee, H. A., Yi, S., Kim, D. S., Yang., H. W. and Par, G. J.** (2012). Design flow for the crash box in a vehicle to maximize energy absorption. Proceedings of the Institution of Mechanical Engineers, Part D: Journal of automobile engineering.

[96] **Yang, S. and Qi, C**. (2013). Multiobjective optimization for empty and foam-filled square columns under oblique impact loading. International Journal of Impact Engineering, **54**: p. 177-191.

[97] **Yan-jie. L., Chun-yan, X., Lin, D. and Chun-hua, L.** (2013). Influence of Material on Automotive Crash-Box Crashworthiness Subjected to Low Velocity Impact. in Advanced Materials Research. Trans Tech Publ.

[98] **Andrei, C. V.** (2013). Crashing Behaviour Analysis of TWB Thin-Walled Structures with Various Cross-Sections. Applied Mechanics and Materials, **371**: p. 715-720.

[99] **Andrei, C. V.** (2013). Crashing Behaviour Analysis of TWB Tubular Structures with Different Cross-Sections. Advanced Materials Research, **814**: p. 159-164.

[100] **Chiu, Y. S. and S. T. Jenq.** (2014). Crushing behavior of metallic thin-wall tubes with triggering mechanisms due to quasi-static axial compression. Journal of the Chinese Institute of Engineers, **37**(4): p. 469-478.

[101] **Darvizeh, A., Darvizeh, M., Ansari, R. and Meshkinzar A.** (2013). Effect of low density, low strength polyurethane foam on the energy absorption characteristics of circumferentially grooved thick-walled circular tubes. Thin-Walled Structures, **71**: p. 81-90.

[102] **Sato, K., Inazumi T., Yoshitake, A. and Liu, S. D.** (2013). Effect of material properties of advanced high strength steels on bending crash performance of hat-shaped structure. International Journal of Impact Engineering, **54**: p. 1-10.

[103] **Eshkoor, R., Oshkovr, S. A., Sulong, A. B., Zulkifli, R., Ariffin A. K.,** et al. (2013). Effect of trigger configuration on the crashworthiness characteristics of natural silk epoxy composite tubes. Composites Part B: Engineering, 2013. **55**: p. 5-10.

[104] **Käfer, B., Bheemineni, V. K., Lammer, H., Kotnik, M. and Riemelmoser F. O.** (2013). Effects of Position and Cut Crushing Behavior Experimental and Simulation. World Academy of Science, Engineering and Technology International Journal of Mechanical, Industrial Science and Engineering.

[105] **Gunawan, L., Jusuf, A., Dirgantara, A. Putra, I. S.** (2013). Experimental study of foam filled aluminum columns under axial impact loading. Journal of KONES.

[106] **Yan-jie L., Lin, D., Qing-fen, L. and Dan, W.** (2013). Finite Element Analysis and Shape Optimization of Aluminum Alloy Automobile Energy-Absorbing Components. in Applied Mechanics and Materials. Trans Tech Publ.

[107] **Oshkovr, S. A., Taher, S. T., Oshkour, A. A., Ariffin, A. K. and Azhari, C. H.** (2013). Finite element modelling of axially crushed silk/epoxy composite square tubes. Composite Structures, 2013. **95**: p. 411-418.

[108] **Yin, H., Wen, G., Hou, S. and Qing, Q.** (2013). Multiobjective crashworthiness optimization of functionally lateral graded foam-filled tubes. Materials & Design, **44**: p. 414-428.

[109] **Dirgantara, T., Gunawan, L., Putra, I. S., Sitompul, S. A. and Jusuf, A.** (2013). Numerical and Experimental Impact Analysis of square crash box structure with holes. Applied Mechanics and Materials, **393**: p. 447-452.

[110] **Qaiser, Z., Qureshi, O. M., Awan, K. A. and Ahmed, H.** (2013). Numerical investigation of usage of patterned collapsible energy absorbers in steering column of an automotive vehicle. in Aerospace Science & Engineering (ICASE), 2013 International Conference on. IEEE.

[111] **Costas, M., Díaz, J., Romera, L. E., Hernández, S. and Tielas, A.** (2013). Static and dynamic axial crushing analysis of car frontal impact hybrid absorbers. International Journal of Impact Engineering, **62**: p. 166-181.

[112] **Trimiño, L. F. and Cronin, D. S.** (2014). Non-direct similitude technique applied to the dynamic axial impact of bonded crush tubes. International Journal of Impact Engineering, **64**: p. 39-52.

[113] **Xiao, M., Yi-shan, P. and Yong-hui, X.** (2014). Study on Application of the Mine Anti-Impact and Energy-Absorption Device. in Applied Mechanics and Materials. Trans Tech Publ.

[114] **Mohammadiha, O. and Beheshti, H.** (2014). Optimization of functionally graded foam-filled conical tubes under axial impact loading. Journal of Mechanical Science and Technology, **28**(5): p. 1741-1752.

[115] **Ma, J. and You, Z.** (2014). Energy absorption of thin-walled square tubes with a prefolded origami pattern—part I: geometry and numerical simulation. Journal of Applied Mechanics, **81**(1): p. 011003.

[116] **Nguyen, V. S., Wen, G., Yin, H. and Van, T. P.** (2014). Optimisation design of reinforced S-shaped frame structure under axial dynamic loading. International Journal of Crashworthiness, **19**(4): p. 385-393.

[117] **Zhang, X. and Zhang. H.** (2013). Energy absorption of multi-cell stub columns under axial compression. Thin-Walled Structures, **68**: p. 156-163.

[118] **Sun, G., Xu, F., Li, G. and Li, Q.** (2014). Crashing analysis and multiobjective optimization for thin-walled structures with functionally graded thickness. International Journal of Impact Engineering, **64**: p. 62-74.

[119] **Qi, C. and Yang, S.** (2014). Crashworthiness and lightweight optimisation of thin-walled conical tubes subjectedto an oblique impact. International Journal of Crashworthiness, **19**(4): p. 334-351.

[120] **Yin, H., Wen, G., Liu, Z. and Qing Q.** (2014). Crashworthiness optimization design for foam-filled multi-cell thin-walled structures. Thin-Walled Structures, **75**: p. 8-17.

[121] **Arifin, A. and Othman, A.** (2014). Crush Force Efficiency of Composite Square Profile under Off-Axis Loading. Key Engineering Materials, **594**: p. 711-714.

[122] **Yan, L., Chouw, N. and Jayaraman, K.** (2014). Effect of triggering and polyurethane foam-filler on axial crushing of natural flax/epoxy composite tubes. Materials & Design, **56**: p. 528-541.

[123] **Simhachalam, B., Srinivas, K. and Rao, C. L.** (2014). Energy absorption characteristics of aluminium alloy AA7XXX and AA6061 tubes subjected to static and dynamic axial load. International Journal of Crashworthiness, **19**(2): p. 139-152.

[124] **Shojaeefard, M. H., Najibi, A. and Anbarloei, M.** (2014). Experimental and numerical crashworthiness investigation of combined circular and square sections. Journal of Mechanical Science and Technology, **28**(3): p. 999-1006.

[125] **Xu, F., Sun, G., Li, G. and Li, Q.** (2014). Experimental study on crashworthiness of tailor-welded blank (TWB) thin-walled high-strength steel (HSS) tubular structures. Thin-Walled Structures, **74**: p. 12-27.

[126] **Ciubotariu, V. A.** (2014). Finite Element Modeling of Crashing Behavior Concerning Rectangular Multi-Layered Thin-Walled Structures. Journal of Engineering Studies & Research, **20**(1).

[127] **Qureshi, O. M., Bertocchi, E., Qaiser, Z. and Awan, K. A.** (2014). Frequency embedded box beam crash absorbers under oblique impacts. Thin-Walled Structures, **75**: p. 1-7.

[128] **Marzbanrad, J., Keshavarzi, A. and Aboutalebi, F. H.** (2014). Influence of elastic and plastic support on the energy absorption of the extruded aluminium tube using ductile failure criterion. International Journal of Crashworthiness, **19**(2): p. 172-181.

[129] **Jie, L. and Lin, D.** (2014). Influence of Material Properties on Automobile Energy-Absorbing Components Crashworthiness. Open Mechanical Engineering Journal, **8**: p. 113-116.

[130] **Bussadori, B., Schuffenhauer, K. and Scattina, A.** (2014). Modelling of CFRP crushing structures in explicit crash analysis. Composites Part B: Engineering, **60**: p. 725-735.

[131] **Yin, H., Wen, G., Fang, H., Qing, Q, Kong, X., Xiao, J. and Liu, Z.** (2014). Multiobjective crashworthiness optimization design of functionally graded foam-filled tapered tube based on dynamic ensemble metamodel. Materials & Design, **55**: p. 747-757.

APPENDICES

APPENDIX A: Information of articles on crash boxes

Table A1: Information of articles on crash boxes

Paper Year	software											Speed		Geometry							Material			Configuration			
	LS-DYNA	ADINA	PAM-CRASH	ABAQUS	ANSYS	other	Explicit	Implicit	Experimental	Theoretical	Mass (kg)	Quasi static (m/s)	Dynamic (m/s)	Circular	Square	Rectangular	Hexagonal	Other	Length (mm)	Thickness (mm)	Steel	Aluminum	Composite	Empty	Foam-filled	Singular	Multi-cell
1986 [4]									x	x	136	x	x	x	x				23.3-300.3	0.87-1.65	x			x		x	
1993 [21]				x					x			1.67E-4		x	x				100	1.6	MS	x		x	x	x	
1996 [13]									x	x		1.67E-4		x					12.7-127	2.3-5.7			x	x		x	
1997 [22]						MARC K6.2		x	x		7.92		1.4 2.8 3.7		x				100	1.0		A6063		x		x	
1997 [5]									x	x	210	1.0E-4 1.0E-3	12.14	x	x				20-1800	0.96-1.56	MS			x		x	
1989 [23]									x	x		1.67E-4			x				124.7-133.5	0.74-1.52	x			x		x	
1999 [14]	x						x		x		10-100	x	15.0		x				310	1.8-2.5		A6060-T4 A6060-T6		x		x	
1998 [24]			x						x	x	394		5.0		x				250	1.9	MS			x		x	
2000 [11]				x			x		x		0.2-335		4-180	x					38.1-152.4	0.91-6.35		A6061-T6		x		x	
2000 [25]									x	x		6.67E-4			x				800	1.76 1.90 2.46		A6060			x	x	

Table A1: Information of articles on crash boxes (cont.)

Paper Year	software											Speed		Geometry							Material			Configuration			
	LS-DYNA	ADINA	PAM-CRASH	ABAQUS	ANSYS	other	Explicit	Implicit	Experimental	Theoretical	Mass (kg)	Quasi static (m/s)	Dynamic (m/s)	Circular	Square	Rectangular	Hexagonal	Other	Length (mm)	Thickness (mm)	Steel	Aluminum	Composite	Empty	Foam-filled	Singular	Multi-cell
2000 [26]									x			2.1E-4			x				150	5.0			x	x		x	
2000 [27]									x			2.0E-4				x			350 657	2.0		HS5754		x	x	x	x
2000 [28]									x	x		5.5E-4 8.33E-4	12.6- 24.2		x				295	1.43 2.46		AA6060		x	x	x	
2001 [7]				x			x				0.0352 0.103		17.5-80	x					106.68	1.0- 1.65	x	x		x		x	
2001 [29]			x						x			2.0E-4			x				675	2.0		HS5754		x	x	x	
2002 [30]									x		200	x	5.7 13.33		x				80-300	1.2-1.6	HSS			x		x	
2002 [31]						Optivar					500		13.9	x					400	1.15- 1.30	fep06			x		x	
2002 [15]			x				x			x	600		13.4112	x	x				400	1.0, 2.0		A6063-T7		x		x	x
2002 [32]			x				x			x			2.0		x				330 490	0.3 3.0		A6060-T4		x	x	x	
2003 [33]									x			1.17E-4			x				50 100 125	2.63 3.51 4.39			CFRP	x		x	

Table A1: Information of articles on crash boxes (cont.)

Paper Year	software											Speed		Geometry							Material			Configuration			
	LS-DYNA	ADINA	PAM-CRASH	ABAQUS	ANSYS	other	Explicit	Implicit	Experimental	Theoretical	Mass (kg)	Quasi static (m/s)	Dynamic (m/s)	Circular	Square	Rectangular	Hexagonal	Other	Length (mm)	Thickness (mm)	Steel	Aluminum	Composite	Empty	Foam-filled	Singular	Multi-cell
2003 [34]				x						x	2.4		60		x				300	2.0		x					
2003 [2]	x						x		x		100		10	x	x		x	x	200	1.0-3.0		A6063		x		x	
2003 [35]	x						x		x			5.0E-5		x					245	1.47- 1.51		A6060-T4		x	x	x	
2003 [36]	x						x		x			2.7E-4			x				199	2.0-4.5		A6060-T4 A6060-T6		x		x	
2004 [37]	x						x		x	x	211	x	<16		x						HSS MS			x		x	
2004 [38]	x						x		x		1400	2.5E-3	13 20		x				400- 1920	2- 4.5		A6060-T6		x		x	
2004 [39]									x			1.6E-4	5.4		x				50 100 125	2.64 3.51 4.39			CFRP	x		x	
2004 [34]				x			x		x				14.84- 98.27	x	x				146	1.14		A6063		x		x	
2004 [40]	x						x		x			1.38E-4			x				199	1.77		A6060-T4 A6060-T6		x	x	x	
2004 [41]	x			x			x			x	80 90	x	<30			x			300	1.5 2.0 2.5	MS			x		x	

Table A1: Information of articles on crash boxes (cont.)

Paper Year	software											Speed		Geometry							Material			Configuration			
	LS-DYNA	ADINA	PAM-CRASH	ABAQUS	ANSYS	other	Explicit	Implicit	Experimental	Theoretical	Mass (kg)	Quasi static (m/s)	Dynamic (m/s)	Circular	Square	Rectangular	Hexagonal	Other	Length (mm)	Thickness (mm)	Steel	Aluminum	Composite	Empty	Foam-filled	Singular	Multi-cell
2004 [42]									x			2.5E-4						x	165	5.0			x	x		x	
2004 [43]	x						x		x			x			x				300	2.0 2.5 3.0		A6061-T4		x	x	x	
2005 [44]	X						X		x		82		18			x				3.0 3.5			FRC		x		x
2005 [45]				x			x					x				x			300	1.5 2.0 2.5	MS			x		x	
2005 [46]									x			2.5E-4		x				x	150				x		x	x	
2005 [47]	x						x		x	x		8.3E-5			x				200	1.5	MS			x	x	x	
2005 [48]									x			4.17E-5 1.6E-3		x					40	0.22, 0.29		x		x	x		
2006 [49]									x			4.1E-5			x				240- 645	1.40- 1.59		x		x		x	
2006 [50]				x			x		x			x	1.49 -3.33			x			100 200	1.0 2.0		A6063-T6		x		x	
2006 [51]			x				x		x		35 0		16			x			300	1.335		TRIP800		x		x	

Table A1: Information of articles on crash boxes (cont.)

Paper Year	software											Speed		Geometry							Material			Configuration			
	LS-DYNA	ADINA	PAM-CRASH	ABAQUS	ANSYS	other	Explicit	Implicit	Experimental	Theoretical	Mass (kg)	Quasi static (m/s)	Dynamic (m/s)	Circular	Square	Rectangular	Hexagonal	Other	Length (mm)	Thickness (mm)	Steel	Aluminum	Composite	Empty	Foam-filled	Singular	Multi-cell
2006 [52]									x			4.16E-5		x	x				27	2.5-3.0		x		x	x		x
2006 [53]			x		x		x		x			1.6E-3		x					40	0.23-0.29		x		x	x	x	
2006 [54]	x						x			x			10		x				150	0.6		A6060 T4		x			x
2007 [55]				x					x	x		1.2E-3		x					200	3.5	MS			x		x	
2007 [56]	x						x		x		92		12.5		x		x		150 91	2 2.4 2.7		x	woven fiber polyamid	x		x	
2007 [57]	x						x				250		1					x	127	1.52	x					x	
2007 [58]									x			1.0E-3		x	x				27	0.53 0.85 1.32		hybrid Al-Comp.	CFRP	x	x	x	
2007 [59]	x						x					x			x				120	1.2		A6060		x		x	
2008 [16]			x		x	x						4.16E-5			x		x		25 35	2.5		x		x	x	x	x
2008 [60]	x						x			x	500		10		x				400	1.4-3		A6061-T4		x		x	x

Table A1: Information of articles on crash boxes (cont.)

Paper Year	software											Speed		Geometry							Material			Configuration			
	LS-DYNA	ADINA	PAM-CRASH	ABAQUS	ANSYS	other	Explicit	Implicit	Experimental	Theoretical	Mass (kg)	Quasi static (m/s)	Dynamic (m/s)	Circular	Square	Rectangular	Hexagonal	Other	Length (mm)	Thickness (mm)	Steel	Aluminum	Composite	Empty	Foam-filled	Singular	Multi-cell
2008 [61]	x						x		x		128		12.5		x				550	2.0 3.0 4.0		6060		x	x		
2008 [62]				x			x		x			10E-4 10E-1	16			x			300- 500	3	MS			x		x	
2008 [63]	x						x		x		154		7-10		x				270	2		6060		x	x	x	
2008 [64]	x						x		x		28		2 4		x				70- 100	0.5 0.7 0.9	MS	x		x		x	
2008 [65]	x						x						10				x		150	0.5- 1.5		A6060		x			x
2008 [66]	x						x		x		154	x	5.1- 9.2	x	x	x			240	2		A6060		x			x
2008 [67]							x		x	x	90 560	x	15		x				300	1.5	MS			x	x		
2009 [9]	x						x				600		20		x				200	2.5		A6060		x		x	
2009 [68]									x		200	x	13 10		x	x			300	1	DC02			x		x	
2009 [69]	x						x				500		10		x				400	1.4- 3.0		A6060		x	x	x	

Table A1: Information of articles on crash boxes (cont.)

Paper Year	software											Speed		Geometry							Material			Configuration			
	LS-DYNA	ADINA	PAM-CRASH	ABAQUS	ANSYS	other	Explicit	Implicit	Experimental	Theoretical	Mass (kg)	Quasi static (m/s)	Dynamic (m/s)	Circular	Square	Rectangular	Hexagonal	Other	Length (mm)	Thickness (mm)	Steel	Aluminum	Composite	Empty	Foam-filled	Singular	Multi-cell
2009 [70]	x						x						10		x				130	1.2	HSS of SPRC40R			x		x	
2009 [71]	x						x					3.3E-5			x				250 100	3.0			GFRP	x	x		
2010 [72]	x						x		x			1.6E-3		x	x	x	x	x	100	1.0 1.5		A3003 H12		x		x	
2010 [73]	x						x		x		360		16	x	x	x	x	x	250	1.5	DP600			x		x	
2010 [74]	x										60 90		9 15	x	x		x		180	0.5- 2.5	MS			x		x	
2010 [6]	x						x					1.0E-1		x					250	1.0- 2.53	x			x		x	
2010 [8]	x						x		x		1400 600		13 20		x				638- 1920	2-4		A6060		x		x	
2010 [75]	x						x		x				15	x					200-300	1.5 2.0 2.5		x		x	x	x	
2010 [76]	x						x		x			8.3E-5 8.3E-3	5.5		x				120	2.0 2.5 3.0		1050H4 Al sheet alloy		x	x		
2011 [77]	x						x				250		10	x					200	2.2		A6061- T4		x	x	x	

Table A1: Information of articles on crash boxes (cont.)

Paper Year	software											Speed		Geometry							Material			Configuration			
	LS-DYNA	ADINA	PAM-CRASH	ABAQUS	ANSYS	other	Explicit	Implicit	Experimental	Theoretical	Mass (kg)	Quasi static (m/s)	Dynamic (m/s)	Circular	Square	Rectangular	Hexagonal	Other	Length (mm)	Thickness (mm)	Steel	Aluminum	Composite	Empty	Foam-filled	Singular	Multi-cell
2011 [78]	x						x			x	100		10		x		x	x	50	0.6- 1.4		AA6060 T4		x	x	x	x
2011 [79]				x			x		x			x	20 10	x					98.5 97.5	0.99 0.97		x			x	x	
2011 [3]									x			x		x	x		x	x	100	1.0 2.0			Synolit e 1408-		x	x	
2011 [80]			x				x		x		350		16			x			300	1.34 1.59	DP600			x		x	
2011 [81]				x			x		x			1.6667e-4		x					97.3 97.4 97.5	0.84- 1.0		x		x	x	x	
2011 [82]	x						x		x			x			x				120	2.0 2.5 3.0		1050H1 4- A061T4		x	x	x	
2012 [83]									x						x				50 80 120	1.7 3.4 4.2			silk/epo xy	x		x	
2012 [10]	x	x					x		x		600	x	5 -15		x				310	1.17- 1.20	HSS			x	x	x	
2012 [84]						x	x			x	500		15.6						1200	1.7		AL6260 T6		x		x	
2012 [85]	x						x		x				10		x				150	0.5- 3.0		AA6060 T4		x			x

Table A1: Information of articles on crash boxes (cont.)

Paper Year	software											Speed		Geometry							Material			Configuration			
	LS-DYNA	ADINA	PAM-CRASH	ABAQUS	ANSYS	other	Explicit	Implicit	Experimental	Theoretical	Mass (kg)	Quasi static (m/s)	Dynamic (m/s)	Circular	Square	Rectangular	Hexagonal	Other	Length (mm)	Thickness (mm)	Steel	Aluminum	Composite	Empty	Foam-filled	Singular	Multi-cell
2012 [86]	x						x		x		294		4	x	x				200 300	1.5 2.0 2.5			CFRP	x	x		
2012 [87]	x						x		x		400		15		x				250	2.0		A6063-T6		x	x	x	x
2013 [88]						x	x		x		500		15.60		x				1200	1.7		A6260-T6		x	x		
2013 [89]									x		250		4.44		x				250	1.94- 2.72			Al/CF RP	x	x		
2013 [90]	x						x		x		29		10		x				220	1.0		A1050-H24 A5052-H34		x		x	
2013 [91]				x			x					x	20					x	776.8	2.0	x	x		x		x	
2013 [92]	x						x				68.8 5		9.30	x					50 220	3.0			x	x		x	
2013 [93]				x			x		x		150		5 5.5 7		x				300	2.0		A6063 T4		x		x	
2013 [94]	x						x						6.94	x					75.1	0.8		A6061-T6		x		x	
2013 [95]	x						x						4.16	x	x			x	125 150 200	0.8 1.2 1.6	x			x		x	

Table A1: Information of articles on crash boxes (cont.)

Paper Year	software											Speed		Geometry							Material			Configuration			
	LS-DYNA	ADINA	PAM-CRASH	ABAQUS	ANSYS	other	Explicit	Implicit	Experimental	Theoretical	Mass (kg)	Quasi static (m/s)	Dynamic (m/s)	Circular	Square	Rectangular	Hexagonal	Other	Length (mm)	Thickness (mm)	Steel	Aluminum	Composite	Empty	Foam-filled	Singular	Multi-cell
2013 [96]	x						x		x				10		x				200	1.4 1.2 3.0		A6063 T6		x	x	x	
2013 [97]	x						x		x		1000	1.2E-3		x					160	1.65		A7075		x		x	
2013 [98]	x						x		x		110		6.5	x		x	x		200	0.7 0.85	x			x		x	
2013 [99]	x						x		x			2.0E-3			x			x	250	0.7	x			x		x	
2013 [100]	x						x		x			1.6E-4			x				200	1.00 3.15		A6060-T4		x		x	
2013 [101]									x			1.6E-4		x					144	1.0- 2.0	x			x	x	x	
2013 [102]									x			1.6E-4						x	320-470	1.0- 2.0	IF, DP, TRIP			x		x	
2013 [103]									x			3.3E-4			x				50	1.7			x	x		x	
2013 [104]	x						x		x			1.6E-4		x					100 200	1.5		A6060		x		x	
2013 [105]						x	x		x				6.10- 7.95		x				180	1.15 1.3		A6063 T1			x	x	

Table A1: Information of articles on crash boxes (cont.)

Paper Year	software										Mass (kg)	Speed		Geometry							Material			Configuration			
	LS-DYNA	ADINA	PAM-CRASH	ABAQUS	ANSYS	other	Explicit	Implicit	Experimental	Theoretical		Quasi static (m/s)	Dynamic (m/s)	Circular	Square	Rectangular	Hexagonal	Other	Length (mm)	Thickness (mm)	Steel	Aluminum	Composite	Empty	Foam-filled	Singular	Multi-cell
[2013 [106]	x						x		x		1000	1.2E-3							160	1.65		A7075		x		x	
2013 [107]						MSC Dytran	x		x			x			x				50 80 120	1.7 3.4 4.2			silk/epoxy	x		x	
2013 [108]	x						x				600		15		x				240	2.0		A6060 T4		x	x	x	
2013 [109]						x	x		x		45.5		4.36 - 4.40		x				180	1.15		A6063–T1		x		x	
2013 [110]	x						x						15.67	x					600			Al6260-T6		x		x	
2013 [111]				x			x		x		700		6.7			x				0.87-2.44	x			x	x	x	
2014 [19]	x						x		x		128		4.4		x				550	0.6-2.0		AlMg0.5 F22			x	x	
2014 [112]	x						x		x		600		5						410	1.2	DP800			x		x	
2014 [113]						x			x	x		x	5		x				180	6.0				x		x	
2014 [114]	x						x				60		20	x					200	1.5-2.5		x			x	x	

Table A1: Information of articles on crash boxes (cont.)

Paper Year	software											Speed		Geometry							Material			Configuration			
	LS-DYNA	ADINA	PAM-CRASH	ABAQUS	ANSYS	other	Explicit	Implicit	Experimental	Theoretical	Mass (kg)	Quasi static (m/s)	Dynamic (m/s)	Circular	Square	Rectangular	Hexagonal	Other	Length (mm)	Thickness (mm)	Steel	Aluminum	Composite	Empty	Foam-filled	Singular	Multi-cell
2014 [115]				x			x			x		x	20						17.2-40	1.0		x		x		x	
2014 [116]	x						x		x		600		15						780	2.0- 4.0		A6060-T4		x		x	
2014 [117]	x						x		x	x		5.0E-4		x					120	1.2		A6061		x		x	x
2014 [118]	x						x		x		600		5-15						310	1.2	DP800			x		x	
2014 [119]	x						x		x				10	x					200	1.2- 2.8		A6060-T5		x	x	x	
2014 [120]	x						x				600		15		x				200	0.8 1.0 1.2		A6060T4			x	x	x
2014 [121]									x			x			x				120	1.6		x	x	x		x	
2014 [122]									x			1.6E-4		x					96 129	2.4			FFRP - D64	x	x	x	
2014 [123]	x						x	x	x		60	x	7 10 15	x					135	1.4	DP800	A7005 A7003 A6061					
2014 [124]				x			x		x			5.0E-1		x	x				588	2.0				x		x	

Table A1: Information of articles on crash boxes (cont.)

Paper Year	software											Speed		Geometry							Material			Configuration			
	LS-DYNA	ADINA	PAM-CRASH	ABAQUS	ANSYS	other	Explicit	Implicit	Experimental	Theoretical	Mass (kg)	Quasi static (m/s)	Dynamic (m/s)	Circular	Square	Rectangular	Hexagonal	Other	Length (mm)	Thickness (mm)	Steel	Aluminum	Composite	Empty	Foam-filled	Singular	Multi-cell
2014 [125]									x			8.3E-5			x				100	1.0 1.5			DP600 DP800	x		x	
2014 [126]	x						x		x				6.5			x			250	0.7			SPE-220BH				
2014 [127]							x			x	500		15.56		x				600	1.7		AL6260-T6		x		x	
2014 [128]				x			x		x		125		10	x					300	2.0		EN AW-7108 T6		x		x	
2014 [129]	x						x				1000	1.2E-3							140	1.65	x	x		x		x	
2014 [130]			x				x		x			3.3E-4			x				150	2.08			CFRP	x		x	
2014 [131]	x						x		x		600		15	x					240	2.0		A6060 T4			x	x	

CURRICULUM VITAE

Name and Surname: Fatih Usta

Place and Date of Birth: Ordu 1986

E-Mail: ustaf@itu.edu.tr

EDUCATION:

B.Sc.:2013, ITU, Faculty of Aeronautics and Astronautics, Aeronautical Engineering

PUBLICATIONS, PRESENTATIONS AND PATENTS ON THE THESIS:

- Usta F., Eren Z., Turkmen H.S., Kazancı Z., Mecitoglu Z., 2015. Numerical Investigation of Stepped Concentric Crash Tubes Subjected to Axial Impact: The Effects of Number of Tubes. *International Congress* – RAST June 16-19, 2015 Istanbul, Turkey